TAMPEREEN TEKNILLINEN YLIOPISTO
TAMPERE UNIVERSITY OF TECHNOLOGY

CRISTINA ALLUÉ HOYOS

APPLICABILITY OF COMSOL MULTIPHYSICS TO COMBINED HEAT, AIR AND MOISTURE TRANSFER MODELLING IN BUILDING ENVELOPES

Master of Science Thesis

Examiner: Prof. Juha Vinha
Examiner and topic approved by the Faculty Council of the Faculty of Business and Built Environment on 7th May 2014.

ABSTRACT

TAMPERE UNIVERSITY OF TECHNOLOGY
Master's Degree Programme in Civil Engineering
ALLUÉ HOYOS, CRISTINA: Applicability of Comsol Multiphysics to combined heat, air and moisture transfer modelling in building envelopes.
Master of Science Thesis, 90 pages.
November 2014
Major: Structural Design
Examiner: Prof. Juha Vinha.
Keywords: Comsol Multiphysics, diffusion and convection simulations.

The intention of this project is to analyse the applicability of the programme Comsol Multiphysics for the study of different physics in building envelopes regarding the laboratory tests and other program, WUFI, in order to check its reliability. The laboratory tests and the WUFI's simulations were performed within the framework of a previous project carried out at the Civil Engineering Department at Tampere Universiy of Technology.

Two different types of simulations have been performed to accomplish the purpose: only diffusion and the combination of diffusion and convection. Ten structures have been used in the diffusion simulations and another different one has been chosen for the second simulation. All the structures used are building envelopes made of different construction materials such as gypsum board, spruce plywood, fiberglass, rock wool or flax insulation among others.

Several Comsol's modules have been tried before finding the correct ones, the "Free and Porous Media Flow" interface within the "Fluid Flow" module for the air transfer and the "Coefficient form PDE" interface within the "Mathematics" module for the coupled heat and moisture transfer.

The results of Comsol are more similar the laboratory results than the WUFI's results are in general. However, the results are not enough satisfactory which means that the differential equations are not enough even applied with Comsol whose numerical techniques are better. Those equations contain simplifications that can be the reason of the lack of accuracy, such as the Fickian transport.

PREFACE

This master thesis is the result of a year of hard work and growth as a student and as an engineer at the Civil Engineering Department at the Tampere University of Technology. I would like to thank my head supervisor, Juha Vinha, for allowing me to take part in this research, providing me the topic, the facilities and the research data. Also, I am grateful to the co-supervisors, Anssi Laukkarinen and Petteri Huttunen, for their guidance, support, knowledge and advices during this process.

Furthermore, several persons have helped me to write this thesis. Firstly, I would like to thank all my colleagues and friends at TUT for their daily listening, support, advices, and their constant encouragement along this project.

I am also grateful to my family and friends who have supported and encouraged me to go ahead not only this last year but along all these five years. And finally, I would like to specially thank Carlos for being there day after day.

Tampere, 22.10.2014

Cristina Allué Hoyos

TABLE OF CONTENTS

NOTATIONS

THEORETICAL PARAMETERS

Greek upper case letters

Φ	Heat flow	J
Ψ	Dissipation energy per unit of time	J

Greek lower case letters

β_p	Surface coefficient of water vapour transfer	m/s
δ_p	Vapour diffusion permeablility	kg/(m·s·Pa)
ϵ	Porosity	-
ϑ	Temperature	^oC
κ	Permeability	m^2
μ	Dynamic viscosity	kg/m·s
μ	Water vapour diffusion resistance factor	-
ξ	Moisture capacity	kg/m^3
ρ	Density	kg/m^3
λ	Thermal conductivity	W/(m·K)

Roman upper case letters

A	Area	m^2
C_p	Specific heat capacity at constant pressure	$J/m^3·K$
D_w	Moisture diffusion coefficient	m^2/s
H	Enthalpy	J
M_w	Mean molar mass of water	kg/mol
P	Total pressure	Pa
R	Ideal gas constant	J/(mol·K)
RH	Relative humidity	- ; %
R_a	Air flow rate	m^3/s
Q	Heat	J
T	Absolute temperature	K
U	Latent energy	J
W	Labour	J

i

Roman lower case letter

c	Specific heat capacity	J/(kg·K)
g	Vapour flux density	kg/(m^2·s)
h	Height	m
h_c	Convective surface heat transfer coefficient	W/(m^2·K)
p	Partial pressure	Pa
q	Heat flux	W/m^2
t	Time	s
u	Velocity	m/s
v	Vapour content of pore air	kg/m^3
w	Water content	kg/m^3

OPERATORS

$$\nabla = \left(\frac{\partial}{\partial x}, \frac{\partial}{\partial y}, \frac{\partial}{\partial z}\right) \quad \text{Gradient operator}$$

$$\nabla^2 = \frac{\partial^2}{\partial x^2} + \frac{\partial^2}{\partial y^2} + \frac{\partial^2}{\partial z^2} \quad \text{Lagrange operator}$$

1. INTRODUCTION

A common goal around the world in building sector is to reduce energy consumption. Heat losses through building envelope constitute a substantial portion of yearly energy consumption of buildings especially in the colder climates. Moreover, the reduction of the heat loss thanks to the insulation layers has a beneficial effect on the moisture's behavior in the building envelopes. For this reason, the research about the heat, air and moisture transfer through building envelopes becomes essential.

The purpose of the thesis is to analyse the accuracy of Comsol Multiphysics compared to the laboratory test and the WUFI's simulations when the transference of heat, air and moisture through an envelope is modelled. The structures and laboratory results used in this thesis belongs to a survey performed by a group of researchers at Civil Engineering Department. The survey consists of the simulation of different environmental conditions at both sides of a wall which is sited inside a chamber. There are several sensors located inside the wall in different positions so that the temperature and relative humidity are measured.

The first chapter develops the theoretical principles of heat, air and moisture transfer as well as the coupled moisture and heat transfer. It introduces the basic knowledge related to the survey; the main definition, explanations and equations of heat and mass transport mechanisms and how they are applied in Comsol.

The next two chapters show the modelling process that has been carried out in Comsol. The difference between these two chapters is that the first chapter contains the Comsol modelling of ten structures where the transfer mechanism is only diffusion while the next chapter includes one structure where the transfer mechanisms are diffusion and convection. The modelling process at both chapters includes the structure description, the physics configuration, the meshing and the study configuration. After the modelling, the results are shown as well as their comparisons with the laboratory and WUFI's results.

Finally, the discussion about the different results, the possible causes of mistake and the conclusions are presented. The comparisons have shown that even Comsol has better numerical techniques than WUFI, the equations which are the same in both programs are not enough and there are significant differences with the laboratory results.

2. THEORETICAL PRINCIPLES

2.1 Heat transfer

Energy can be exchanged between systems and also the environment through heat and work. The potential which defines the heat quality is the temperature: when the temperature increases, the quality increases as well and in turn the energy is higher. Therefore, one way to define heat transfer is the transmission of energy from one body or substance to another due to a temperature difference between both of them. (Hens 2007).

The importance of heat transfer in building physics resides in the need to understand and predict the heat transfer behaviour through the walls in order to decrease the energy consumption. (Hens 2007).

There is a general physical law (Hens 2007) which links the heat flow rate q with the temperature T, the conservation of energy:

$$\mathrm{d}\Phi + \mathrm{d}\Psi = \mathrm{d}U + \mathrm{d}W \tag{2.1}$$

- dΦ: heat flow between that infinitesimal volume and its environment.
- dΨ: dissipation energy per unit of time.
- d*U:* change of the integral energy per unit of time.
- d*W:* labour between the system and the environment per unit of time. This labour can be expressed as:

$$dW = Pd(dV) = P\,d^2V \tag{2.2}$$

where P is the pressure. When the pressure is constant (isobaric process), the law of conservation of energy can be expressed as:

$$d(U + PdV) = dQ + dE \tag{2.3}$$

where the term ($U + P$ dV) stands for the enthalpy (H) in the system dV and its derivative can be replaced by [$\partial(\rho\ C_p\ T)/\ \partial$t] d$V$, being ρ the density of the material and C_p representing the specific heat capacity at constant pressure. If the symbol dΨ is expressed as Φ′ dV, taking Φ′ as the dissipation per unit of time and unit of volume and the heat flow (dΦ) is replaced by –(div **q**) dV, the equation (2.1) becomes:

$$\left[\nabla \cdot \mathbf{q} + \mathbf{\Phi}' + \frac{\partial(\rho\, C_p\, T)}{\partial t}\right] \mathrm{d}V = 0 \tag{2.4}$$

Due to the little difference in solid and liquids between the specific heat capacity at constant pressure (C_p) and the specific heat capacity in other conditions, there is a simplification and it is called specific heat capacity whose symbol is c [J/(kg·K)]. Finally, the relation between the heat flow rate and the temperature in an infinitesimal volume (dV) is expressed: (Hens 2007).

$$\nabla \cdot q = -\frac{\partial(\rho\, c\, T)}{\partial t} - \Phi' \tag{2.5}$$

2.1.1 Conduction

Conduction is the process where the energy is transmitted due to the collision of vibration atoms and the movement of free electrons collectively, without a displacement of the molecules (Hagentoft 2001). This process can occur between solids which are in contact and are at different temperature or between points within the same solid which are at a different temperature. The transmission by conduction is also possible in liquids and gases and when the contact is between solids at one side and liquids or gases at the other side. Moreover, the directionality of this mode is always from the higher temperature to the lower temperature and it needs a medium. (Hens 2007).

The relation between heat flow and temperature due to conduction is established by the Fourier's first law (Hens 2007):

$$\boldsymbol{q} = -\lambda \nabla T \tag{2.6}$$

The formula indicates that the heat flow rate (**q** [W/m^2]) at a point in a substance is moving in the direction of decreasing temperature ergo in the opposite direction of the gradient. The thermal conductivity is a proportionality factor specific for each material and dependent on moisture and temperature conditions whose symbol is λ [W/(m·K)].

The negative symbol states the opposition between the heat flow rate and the temperature gradient, because as mentioned earlier, heat always streams from points at high temperature to others at low temperatures. (Hens 2007).

The temperature field can be calculated through an equation which comes from the combination of the energy balance (2.3) and his first law (2.4) (Hens 2007):

$$\nabla \cdot (\lambda \nabla T) = \frac{\partial(\rho c T)}{\partial t} - \Phi' \tag{2.7}$$

The equation simplifies if both the thermal conductivity and the specific heat capacity are constant, and it becomes in the second law of Fourier (Hens 2007):

$$\nabla^2 T = \left(\frac{\rho c}{\lambda}\right)\frac{\partial T}{\partial t} - \frac{\Phi'}{\lambda} \tag{2.8}$$

2.1.2 Convection

Convection means the movement of molecule groups at a different temperature within a fluid, which in building physics is typically air or sometimes water. This sort of heat transfer needs a medium and it cannot occur between two solids, it is necessary the presence of a fluid, due to the need of movement, so the transference is always between liquids and gases at one side and solids at the other. In liquid and gases, this process incorporates conduction. Depending on the cause of the movement, there are three kinds of convection: forced which is due to an external force, natural which is caused by different densities in the fluid or mixed which is due to both reasons. (Hens 2007).

The law which controls the convective heat transfer is the Newton's law of cooling from which the heat flow rate can be obtained (Hens 2007):

$$q_c = h_c(T_{fl} - T_s) \tag{2.9}$$

- h_c: convective surface heat coefficient [W/(m^{2}K)].
- T_{fl}: temperature in the fluid [K].
- T_s: temperature in the surface [K].

This equation is only used at the surfaces because the heat flux inside fluid flow is modelled by Navier-Stokes equations if the velocity filed is unknown or by the Fourier's second law (2.8) if the velocity field is known.

All the complexity of this mode resides in the coefficient since the equation is a linear relation between the heat flow rate and the difference of temperatures. In the convective mode there is also mass transfer whose flow comes from synthesizing the the mass conservation law and the law of conservation of momentum (vector equations), Navier-Stokes equation:

$$\nabla \cdot (\rho\, \mathbf{u}) = 0 \tag{2.10}$$

$$\frac{\mathrm{d}(\rho\, \mathbf{u})}{\mathrm{d}t} + \rho(\boldsymbol{u} \cdot \nabla)\boldsymbol{u} = \rho\, \mathbf{g} - \nabla P + \mu \nabla^2 \mathbf{u} \tag{2.11}$$

- **u**: velocity [m/s].
- μ: dynamic viscosity of fluid [kg/(ms)].
- (ρ **g**): the gravity force gradient.

The unknown terms in both equations are the velocity (u_x, u_y, u_z) and the pressure *P* (Hens 2007).

2.1.3 Radiation

The kind of radiation referred to heat transfer is the thermal radiation which consists of electromagnetic waves propagated because of the different temperature between bodies (Hens 2007). The total radiation at a certain point derives from the superposition of radiations of several wavelengths which can come from various directions (Hagentoft 2001). This is the only mode that does not need a medium to propagate, in fact, it is easier in vacuum and the physical laws followed by radiation are quite different from those of conduction and conviction. (Hens 2007).

The electromagnetic waves are defined by three magnitudes: its length λ [μm], velocity c [m/s] and frequency f [Hz] are related through this equation:

$$\lambda = \frac{c}{f} \tag{2.12}$$

Length values for thermal radiation are included in the range 0.1-100 μm which matches the emissions from a body at a range of temperatures between -100 ºC and 10 000 ºC. As mentioned before, this mode does not need a medium and it finds less difficulty in the vacuum which velocity is 299 792.5 km/s. (Hagentoft 2001).

After the radiation wave impacts a surface, it is divided into three parts: one of them is reflected, other is transmitted and the last one is absorbed by the body. The reflectivity (ρ), transmissivity (τ) and absorptivity (α) at a certain temperature *T* are defined by the equations:

$$\rho = \frac{q_{Rr}}{q_{Ri}} \tag{2.13}$$

$$\tau = \frac{q_{Rt}}{q_{Ri}} \tag{2.14}$$

$$\alpha = \frac{q_{Ra}}{q_{Ri}} \tag{2.15}$$

The conservation of energy states a relation between them only if they are emitted at the same temperature: $\alpha + \tau + \rho = 1$ (Hens 2007).

The transmissivity of most materials utilised in building physics is null ($\tau = 0$) because the layer which absorbs the radiation is highly thin. The glass makes an important exception as it transmits short wave radiation. (Hagentoft 2001).

2.2 Air transfer

The air flow through the building envelope has to be considered in heat and mass balances due to its influence on them. The transference of air which is intentional is called ventilation and if it is not then this noun is air leakages. This transference of air in buildings comes from the pressure differences and temperature differences, created by wind and fans, between the environment and the building or between two different sections of it. (Hagentoft 2001).

2.2.1 Air driving forces

The air flows can be consequence of three driving forces: wind (pressure differences), stack effect (temperature differences) and mechanical ventilation (fans) (Hagentoft 2001).

2.2.1.1 Wind pressure

The wind pressure occurs from the windward face of the building (where there is a positive pressure) to the leeward (where the pressure is negative) (Hagentoft 2001). The pressure difference over a building envelope can be caused by wind pressure, stack effects or a combination of both. For that reason, the pressure differences were applied in some of the laboratory experiments. The equation of the static pressure of the free wind in one point of the building comes from the application of Bernoulli's law in a case when the wind is horizontal, with a determined velocity *v* and next to an infinite obstacle:

$$P_w = C_p \frac{\rho_a \, v^2}{2} \tag{2.16}$$

where C_p is a coefficient called pressure factor whose function is correcting the equation in case the obstacle is finite instead of infinite. Its value depends on several factors:

- Wind direction.
- The aspects concerning the building such as the geometry, the surface roughness, the location and the specific spot of the façade.

Moreover, a negative value of the C_p coefficient accounts for wind suction on the envelope, depressurization whereas a positive value means overpressure (Hens 2007).

2.2.1.2 Stack effect

This effect in buildings is caused by difference of temperature between the environment and the interior of the building which in turn causes a vertical difference of pressures. There is a certain height where the pressure is the same at the interior and exterior sides of the building, *neutral pressure plane*. (Hagentoft 2001).

The combination of the decrease of pressure at a certain height **h** ($dP_a = -\rho_a g\, dh$) with the ideal gas law results on:

$$\frac{dP_a}{P_a} = -\frac{g\ dh}{R_a T} \tag{2.17}$$

The solution to this equation, when the temperature is constant, is called barometric equation and it gives the air pressure profile in vertical direction in a free air column:

$$P_a = P_{a0} \exp\left(-\frac{g\ h}{R_a T}\right) \tag{2.18}$$

Although the height is the variable which depends on the pressure, the temperature and composition produce pressure differences at the same height, thus stack appears. This difference of pressures at the same height is caused by temperature differences and it is relevant in the building applications. (Hens 2007).

2.2.1.3 Mechanical ventilation

This kind of air flow production is performed with fans; the value of the pressure difference can be positive if the flow moves from inside the building to the environment and negative in case the fan inserts air from outside to the interior (Hagentoft 2001).

2.2.2 Air transfer

The air flow needs to take into account three different equations depending on the media through which it goes: the Navier-Stokes equations, Darcy's law and Brinkman equation (COMSOL 2008). The Navier-Stokes equations have been mentioned before (2.11) describes a flow movement in free media. Darcy's law is used when the air flows through a porous material and its equation is (Bruneau & Mortazavi 2006):

$$\boldsymbol{u} = -\frac{\kappa}{\mu}\nabla P \tag{2.19}$$

- **u**: flow velocity [m/s]
- κ: permeability [m^2].
- μ: the dynamic viscosity [kg/m·s].
- P: the pressure [Pa].

The Brinkman equation expresses the transition between the two previous equations and it is used in porous materials. This equation determines the fluid flow in a porous media but only when the material porosity is near one (Bruneau & Mortazavi 2006). It follows from Brinkman's equation in stationary state but neglecting the inertia term because the flow moves with low velocity so the effect is insignificant (Shi & Wang 2007):

$$0 = -\nabla P + \frac{\mu}{\varepsilon_p}\nabla^2\boldsymbol{u} - \frac{\mu}{\kappa}\boldsymbol{u} - \rho\mathbf{g} \tag{2.20}$$

- P: pressure [Pa].
- μ: dynamic viscosity of fluid [kg/(m·s)].
- ε_p: porosity [-].
- **u:** flow velocity [m/s].
- κ: permeability [m^2].
- ρ: density of air [kg/m^3].
- **g**: gravitational acceleration vector = $[0;0;-9{,}81]^T$ m/s^2.

2.3 Moisture transfer

The moisture is the water present in a body or in the air and this water can be in any of its three states: solid (ice), liquid (water) or gas (vapour). There are several sources of moisture but this modelling will focus on the indoor and outdoor air humidity. (Hagentoft 2001).

The moisture in all of its forms may exists also in the buildings and its effect on them is not beneficial: the moisture degrades and destroys the natural and man-made materials. These situations usually come from a leakage or perforation in the wall, hence it is important the study of moisture behaviour inside perforated walls in order to prevent and avoid it. (Hagentoft 2001).

The parameter which relates the environment conditions with the moisture storage capacity of a building material is the relative humidity (RH). The relative humidity can be expressed as the rate between the humidity by volume or water vapour content in the air v (kg/m^3) and the maximum possible water vapour content in the air vs (kg/m^3).
This rate can be also set between other parameters such as the density or the pressure. The water vapour content in the air (v) contributes with the total air pressure with its partial pressure p_v (Pa). These parameters are linked by the General Gas Law (Hagentoft 2001):

$$p_v = \frac{R}{M_w} \cdot T \cdot v = 461.4 \cdot T \cdot v \tag{2.21}$$

- R: ideal gas constant (8.314 [J/(molK)]).
- M_w: mean molar mass of water (0.018 [kg/mol]).
- T: temperature [K].

Therefore, the relative humidity can be set with these three equations (Hagentoft 2001); (Hens 2007):

$$\boldsymbol{\varphi = \frac{v}{v_s}} \qquad \boldsymbol{\varphi = \frac{\rho_v}{\rho_{v,sat}}} \qquad \boldsymbol{\varphi = \frac{p_v}{p_{sat}}} \tag{2.22}$$

The saturation pressure can approximated with relatively accuracy following the next expression (Hens 2007):

$$p_{sat} = p_{c,sat} exp\left[2.3026\ \kappa \left(1 - \frac{T_c}{T}\right)\right] \tag{2.23}$$

- T_c: critical temperature of water, the temperature from which the only state of water is the vapour (T_c = 647.4 [K])
- $p_{c,sat}$: related saturation pressure ($p_{c,sat} = 217.5 \cdot 10^5$ [Pa]).
- κ: parameter which depends on temperature T [K]:

$$\kappa = 4.39553 - 6.2442\left(\frac{T}{1000}\right) + 9.953\left(\frac{T}{1000}\right)^2 - 5.151\left(\frac{T}{1000}\right)^3$$

The materials whose surface tends to capture the water vapour molecules are called hydrophilic (Straube 2006). Some building materials belongs to this group of materials and, in addition, they able to absorb water, increasing its water content: they are hygroscopic. These materials can absorb water until a certain amount and that state of saturation is called capillary saturation (Künzel 1995). The hygroscopic materials can be included in three levels of moisture storage depending on the increase of moisture environment conditions:

- Region A: this region is called the sorption moisture or hygroscopic region. The feature of this region is the accumulation of water by the air moisture sorption until an equilibrium state is reached (Krus 1996). The material relative humidity belongs to the range: from 0% to around 95%. The relation between the sorption and the relative humidity is represented in the sorption isotherm, as seen in figure 1, where it is possible to observe the S-shaped of hygroscopic materials and the hysteresis effect existing due to the difference between adsorption and desorption. (Künzel 1995).

- Region B: called the capillary water region. It is the intermediate between ranges A and B and it is defined by the states of equilibrium. After the 95% of relative humidity, the increase in the sorption isotherm is really sharply and it hinders the knowledge of the accurate relative humidity. In this region the capillary saturation is reached, i.e the maximum moisture content absorbed naturally without any force and under normal pressure. (Krus 1996).

- Region C: the supersaturated region can be only attained by lowering the condensation point or by artificial pressure or vacuum which remove the enclosed air from the pores (Krus 1996). The relative humidity value is 100% and there are not states of equilibrium, the processes are transient (Künzel 1995).

The figure 1 shows the behaviour between the moisture content and relative humidity at these three different regions in a hygroscopic porous material.

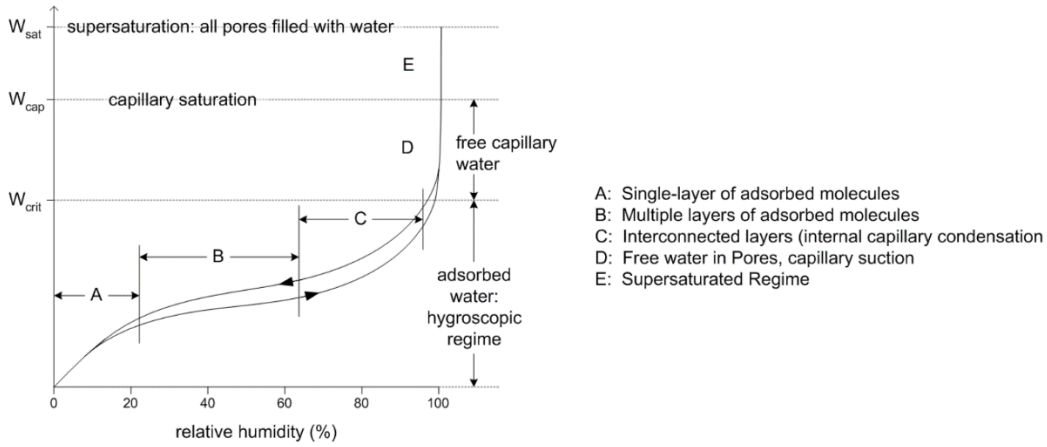

Figure 1: Diagram of the moisture storage regions of the hygroscopic materials. Modified from (Straube 2006).

In addition to the sorption isotherms, there are several expressions which can be used to define the rate between moisture storage and relative humidity. The most recommendable approximation, due to the problems of other expressions at 100% of relative humidity, is the following (Künzel 1995):

$$w = w_f \cdot \frac{(b-1)RH}{b - RH} \tag{2.24}$$

- RH: relative humidity [-].
- w: equilibrium water content [kg/m^3].
- w_f: free water saturation [kg/m^3].

The term **b** is an approximation factor whose value follows from the replacement of the values of water equilibrium content when the relative humidity is 80%. This factor must be always greater than one.

The moisture transfer can be performed by water vapour diffusion, surface diffusion or capillary conduction. The factors responsible for the moisture movement are the temperature and the relative humidity. In building components, the temperature is different inside and outside which causes a temperature gradient which in turn causes a difference of vapour pressure. The figure 2 shows the moisture transport mechanism and the relation with these two factors which have opposite directions (during winter). (Künzel 1995).

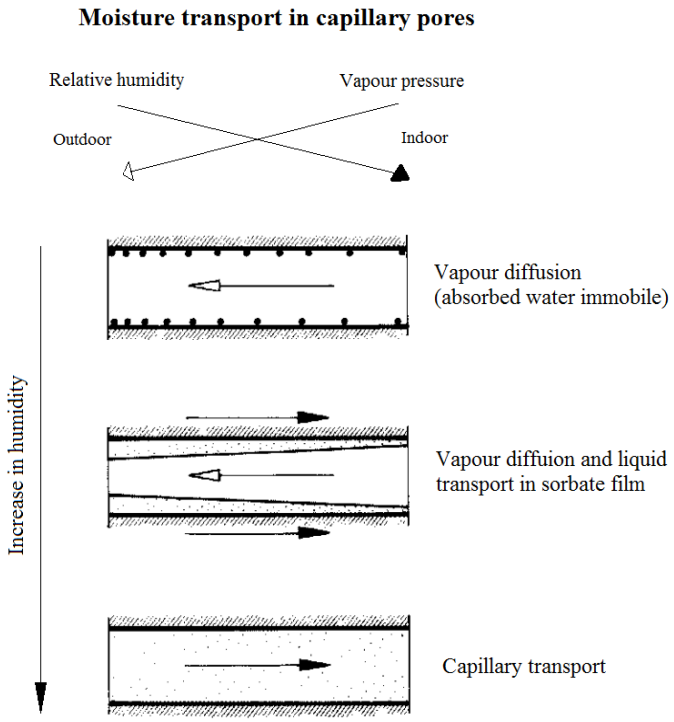

Figure 2: Moisture transport in porous hygroscopic building materials (Künzel 1995).

2.3.1 Water vapour diffusion

The diffusion of molecules in gas mixtures with several components is described by an equation composed by three terms according to the kinetic gas theory. These three diffusion potentials correspond to the mass fraction, temperature and total pressure. In one hand, the total pressure can be neglected when it is applied to the diffusion of moisture in the air in building physics context and in the other hand, if the temperature gradient diffusion is compared with the diffusion coming from mass fraction differences, it can be neglected as well. (Künzel 1995).

The mass fraction diffusion, known also as Fick's diffusion, can be expressed in terms of total pressure due to the relation established by General Gas Law between these two parameters. Hence, the diffusion of water vapour in air can be expressed through the following equation (Künzel 1995):

$$g_v = -\delta \nabla p \tag{2.25}$$

- g_v: the water vapour diffusion flux density [kg/(m^{2}s)].
- p: water vapour partial pressure [Pa].
- δ: water vapour diffusion coefficient in air [kg/(msPa)].

This last coefficient can be expressed as a function of the air pressure and the absolute temperature, according to DIN 52615 (Künzel 1995):

$$\delta = 2.0 \cdot 10^{-7} \frac{T^{0.81}}{P_L} \tag{2.26}$$

- T corresponds to the absolute temperature [K].
- P_L to the air pressure [Pa].

The diffusion of water vapour in porous materials depends on the size of the pores (Künzel 1995):

- *Pore radius < 5·10^{-9} m*: the transport mechanism is called effusion or Knudsen transport. It occurs when the molecules collide with each other with less frequency than they do with the pores.
- *Pore radius > 10^{-6} m:* the transport mechanism is the Fick's diffusion.
- *Pore radius between the previous sizes:* there is a mixed transport.

The problem related to the pores radius is simplified in building physics by introducing in the equation of Fick's diffusion a coefficient. It is called water vapour diffusion resistance factor and it is specific for each building material. The following equation, which establishes the diffusion in porous building materials, is only acceptable if the vapour pressure is lower than the 10% of total pressure because if it is greater, it will appear convection. (Künzel 1995).

$$g_v = -\frac{\delta}{\mu} \nabla p \tag{2.27}$$

where all the parameters are the same as in equation (2.25) unless the water vapour diffusion resistance factor μ (dimensionless).

2.3.2 Capillary conduction

The capillary conduction has water retention gradient equal to zero everywhere apart from the meniscus where there is infinite gradient. The meniscus changes its position in time when there is suction and that position can be calculated with the Hagen-Poiseuille law for cylindrical capillary (Künzel 1995):

$$s = \sqrt{\frac{\sigma r \cos\Theta}{2\eta} t} \tag{2.28}$$

- s: water penetration depth [m].
- r: capillary radius [m].
- σ: surface tension of the water [N/m].
- Θ: contact angle [°].
- η: the viscosity of the water [kg/(ms)].
- t: time of suction [s].

The above equation can be simplified: $s = B\sqrt{t}$, being B ($m/\sqrt{s}$) the water penetration coefficient. Also, the adsorbed amount of water m_w (kg/m^2) can be calculated from the previous formula (Krus 1996):

$$m_w = A\sqrt{t} \tag{2.29}$$

being A ($kg/m^2\sqrt{s}$) the water absorption coefficient. This equation allows calculating the amount of water adsorbed in the moment of the contact with water; however it does not allow establishing how the water is distributed or figuring out how the capillary equilibrium is. (Krus 1996).

The buildings materials have a gradient of water content because the pores, which are interconnected, have different sizes and that causes differences in capillary pressure and flow resistance. This gradient leads the capillary flux (Krus 1996):

$$g_w = -D_w \frac{dw}{dx} \tag{2.30}$$

- g_w : liquid transport flux density [$kg/(m^2s)$].
- D_w: liquid transport coefficient [m^2/s].
- w: water content [kg/m^3].

2.4 Coupled heat and moisture transfer

The thermal behaviour in dry conditions has already been established but in this study the moisture is included. Therefore, the heat and moisture balances have to be combined to obtain the heat and moisture transfer. Both balances include a convective transport term as the following:

$$\nabla \cdot (v\boldsymbol{u}) = (\nabla v) \cdot \boldsymbol{u} + v(\nabla \cdot \boldsymbol{u}) \tag{2.31}$$

- **u:** velocity vector [m/s].
- *v:* vapour content of pore air [kg/m^3].

As the flow is incompressible, the mass conservation (2.10) is applied and considering the density as a constant, the last term of the equation can be neglected. The vapour content is function of relative humidity, vapour saturation pressure and temperature according to the General Gas Law (2.21):

$$\nabla v = \nabla\left(\frac{p_v M_w}{RT}\right) = \nabla\left(\frac{RH \cdot p_{vsat} M_w}{RT}\right) \tag{2.32}$$

Hence, the gradient of the vapour content is expressed as:

$$\nabla v = \frac{p_{vsat} M_w}{RT}\nabla RH + \frac{RH \cdot M_w}{RT}\nabla p_{vsat} + \frac{RH \cdot p_{vsat} M_w}{R}\nabla\left(\frac{1}{T}\right)$$

A couple of simplification can be accomplished. First, the saturation pressure is a function of only the temperature so its derivative can be expressed as: $\mathrm{d}p_{vsat} = \frac{dp_{vsat}}{dT} \cdot dT$. Furthermore, the derivative is $\nabla\left(\frac{1}{T}\right) = -\frac{1}{T^2}\nabla T$ and this term is quite small compared with the others so it can be deleted. Finally, the convective transport term according to the previous equations is:

$$\nabla v = \frac{p_{vsat} M_w}{RT}\nabla RH + \frac{RH \cdot M_w}{RT} \cdot \frac{dp_{vsat}}{dT}\nabla T \tag{2.33}$$

The heat balance comes from the Fourier's second law (2.8) and if it is applied to this specific case, it results:

$$\left(\rho C_p + w C_{p,w}\right)\frac{dT}{dt} = \nabla \cdot (\lambda \nabla T) - \rho_{air} C_{p,air}\boldsymbol{u} \cdot \nabla T + S_h \tag{2.34}$$

- ρ: density of the material [kg/m^3].
- C_p: specific heat capacity at constant pressure of the material [J/(m^{3}K)].
- $C_{p,w}$: water specific heat capacity [J/(m^{3}K)].
- w: water content [kg/m^3].
- λ: thermal conductivity [W/(mK)].
- T: temperature [K].

There are two more terms. The first accounts for the heat convection, considering **u** as the velocity vector whose components are (u,v). The air density can be replaced by the atmosphere pressure (a constant: p_{atm} = 101325 Pa) divided by the specific gas constant of air (also a constant: R_{air} = 287.058 J/(kgK)) and the temperature, and the specific heat capacity is also a constant value so this term can be expressed as follows:

$$\rho_{air} C_{p,air} \boldsymbol{u} = \frac{p_{atm}}{R_{air} T} C_{p,air} \begin{bmatrix} u \\ v \end{bmatrix} = \frac{101325}{287.058 \cdot T} \cdot 1003.5 \begin{bmatrix} u \\ v \end{bmatrix}$$

The term S_h is a heat source which represents the interaction between the vapour diffusion and the phase change (Künzel 1995):

$$S_h = -H_v \nabla \cdot g_v \tag{2.35}$$

- H_v: latent heat of phase change [J/kg].
- g_v: vapour diffusion flux density [kg/(m^{2}s)], equation (2.25).

The pressure p, as seen in equation (2.22), is a product between the relative humidity and the saturation pressure which in turn depends on the temperature. Hence, the pressure term is derived as follows:

$$\nabla p = \nabla (RH \cdot p_{vsat}) = RH \nabla p_{vsat} + p_{vsat} \nabla RH = RH \frac{dp_{vsat}}{dT} \nabla \mathrm{T} + p_{vsat} \nabla RH$$

Therefore, the final expression of the equation (2.36) is the following:

$$S_h = H_v \nabla \frac{\delta}{\mu} RH \frac{dp_{vsat}}{dT} \nabla T + H_v \nabla \frac{\delta}{\mu} p_{vsat} \nabla RH \tag{2.36}$$

Moreover, the moisture balance is (Künzel 1995):

$$\frac{dw}{dt} = \frac{dw}{dRH} \cdot \frac{dRH}{dt} = -\nabla (g_v + g_w) - \nabla \cdot (v \boldsymbol{u}) = -\nabla \left(-\frac{\delta}{\mu} \nabla p - D_w \nabla w \right) - \nabla \cdot (v \boldsymbol{u}) \tag{2.37}$$

being w the water content and g_v, g_w the vapour diffusion flux density (2.25) and capillarity flux density (2.34). The gradient of the water content can be denoted like this:

$$\nabla w = \frac{dw}{dRH} \nabla RH = \xi \nabla RH$$

Therefore, taking into account the gradient of the water content and the convective term (2.37), the moisture balance (2.41) can be expressed as follows:

$$\xi \cdot \frac{dRH}{dt} = -\nabla\left(-\frac{\delta}{\mu} RH \frac{dp_{vsat}}{dT} \nabla T + p_{vsat} \nabla RH - D_w \xi \nabla RH\right) - \left(\frac{p_{vsat} M_w}{RT} \nabla RH + \frac{RH \cdot M_w}{RT} \cdot \frac{dp_{vsat}}{dT} \nabla T\right) \cdot \boldsymbol{u} \qquad (2.38)$$

3. DIFFUSION MODELLING IN COMSOL

The main purpose of this project is to analyse the accuracy of Comsol's simulations in heat, air and moisture transfer modelling. The first step to achieve this aim is the simulations of the moisture and heat diffusion by Comsol and the comparison of its results with the laboratory tests measurements and with WUFI's simulation results. WUFI is another simulation program which has been used to study the behaviour of heat, air and moisture transfer in a series of structures tested in the laboratory.

The structures included in the simulations have been chosen due to their discrepancies between computational (WUFI) and experimental results. By simulating these structures with Comsol (whose simulations had a computing mesh visibly much more dense than in in older WUFI simulations), it is possible to find out if those discrepancies were caused by insufficient numerical scheme.

The structures have been subjected only to heat and moisture transfer. The study of the next ten structures has been performed so that the pressure difference over them remained as close to zero as possible; hence the air transfer is not taken into account. Each one of the next structures has different sizes, materials and initial values.

3.1 Structures

The envelopes are composed by different materials, as it is possible to observe in the table 1. The structures used in the laboratory test were symmetric, as seen in figure 3, so in order to simplify the simulations they have been reduced and the model geometry is a quarter of the real wall, except for the last one which has been modelled as half of the real wall. The envelope layers remain invariable in every structure: the inner lining, the air or vapour barrier, the insulation, the sheathing and the inferior frame; the exception is again the last structure, which has the superior frame as well.

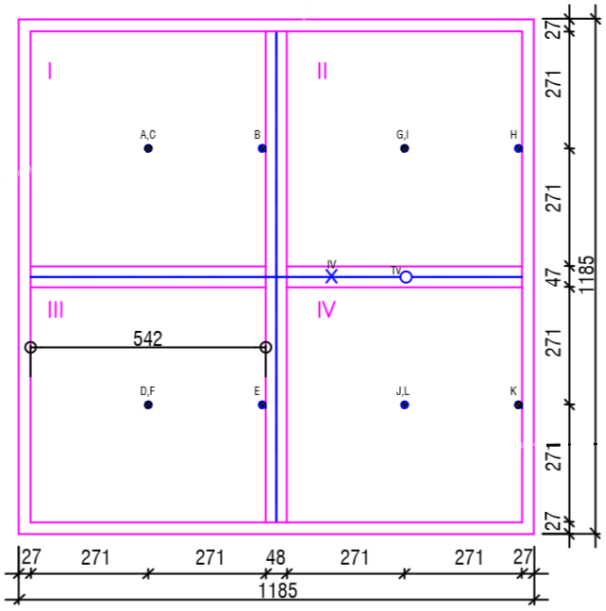

Figure 3: Front view of the structures. Picture from TUT's archives.

The side view of the ten structures which will be modelled can be observed in the figures from 4 to 13, which come from the TUT's archives.

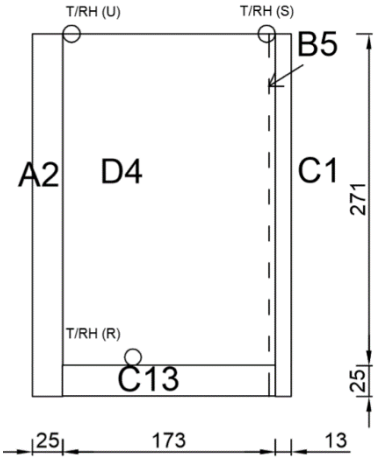

Figure 4: Structure 1.

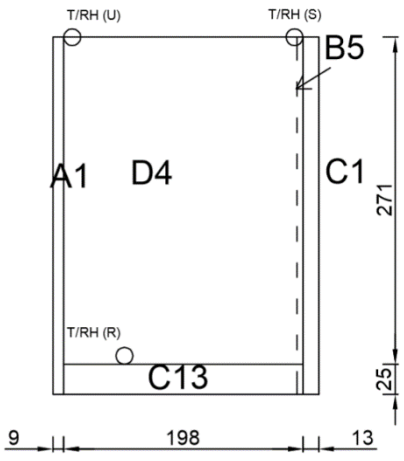

Figure 5: Structure 2.

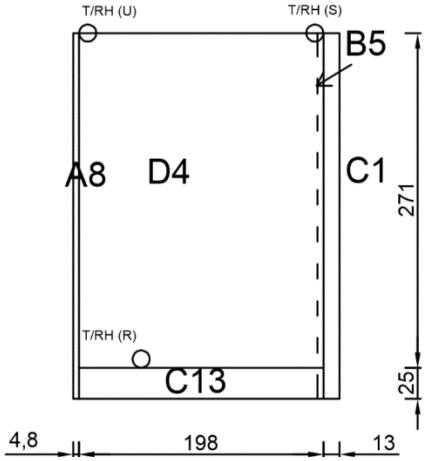

Figure 6: Structure 3.

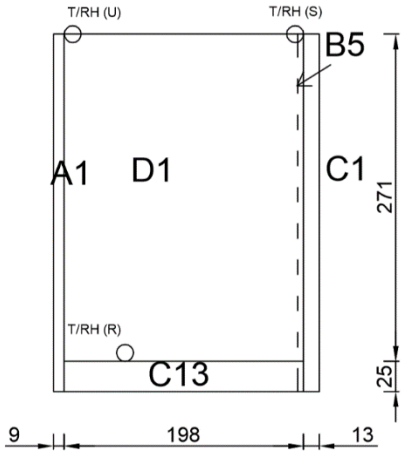

Figure 7: Structure 4.

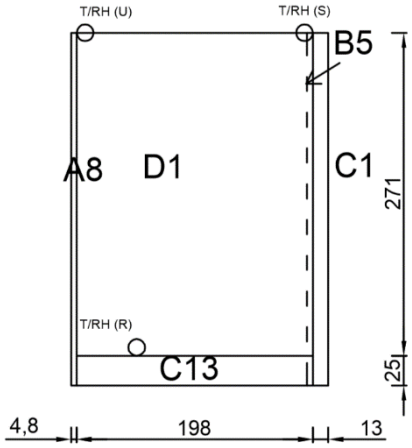

Figure 8: Structure 5.

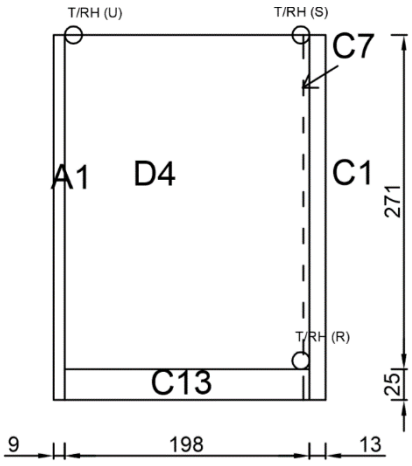

Figure 9: Structure 6.

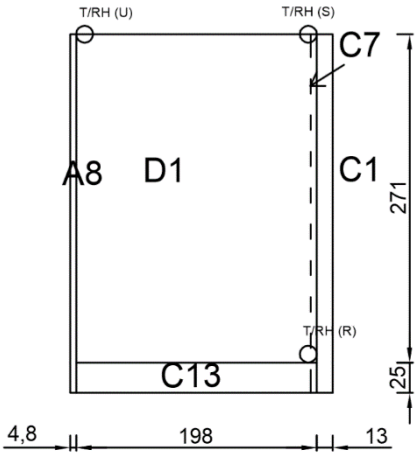

Figure 10: Structure 7.

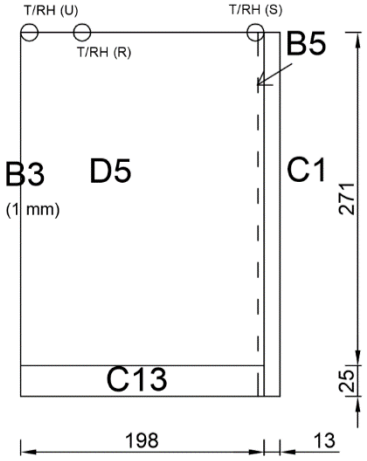

Figure 11: Structure 8.

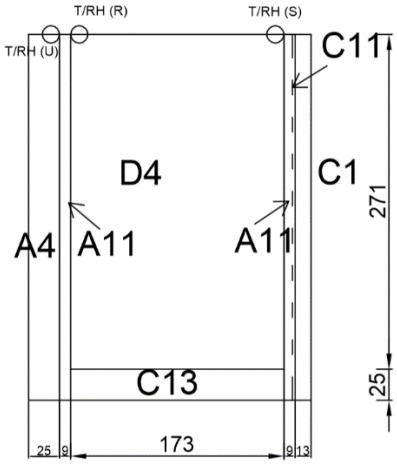

Figure 12: Structure 9.

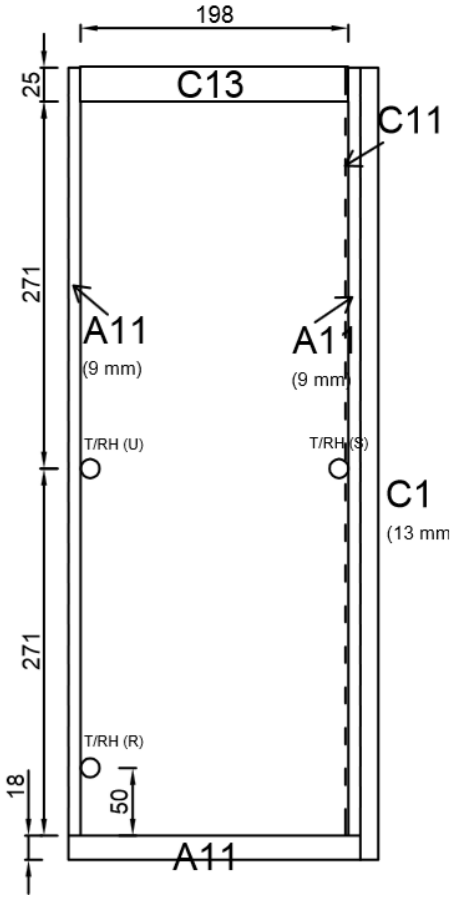

Figure 13: Structure 10.

The tables 2 and 3 show the properties of the different materials that will be needed in the modelling.

Table 1: Materials and sizes of the different structures and their layers.

		Structure 1	Structure 2	Structure 3	Structure 4	Structure 5	Structure 6	Structure 7	Structure 8	Structure 9	Structure 10
1) Inner lining	Material	Gypsum board									
	Size [mm]	296 x 13									585 x 13
2) Air/vapour barrier	Material	Bituminous paper					Plastic coated paper		Bituminous paper	Plywood + plastic foil	Plastic foil + plywood
	Size [mm]	296 x 1									585 x 13
3) Insulation	Material	Cellulose			Fiberglass		Cellulose	Fiberglass	Flax	Cellulose	Rock wool
	Size [mm]	271 x 172	271 x 197							271 x 173	542 x 197
4) Sheathing	Material	Wood fiberboard	Gypsum board	Wood hardboard	Gypsum board	Wood hardboard	Gypsum board	Wood hardboard	Windbreak protection	Fiberglass + plywood	Plywood
	Size [mm]	296 x 25	296 x 9	296 x 4.8	296 x 9	296 x 4.8	296 x 9	296 x 4.8	296 x 1	296 x (25+9)	567 x 9
5) Inferior frame	Material	Pine									Plywood
	Size [mm]	25 x 172	25 x 197							25 x 173	18 x 197
6) Superior frame	Material	-									Pine
	Size [mm]	-									25 x 197

Table 2: Materials properties.

	Materials	Density (ρ_p) [Kg/m^3]	Porosity (ϵ_p) [-]	Heat capacity dry ($C_{p,p}$) [J/m^3·K]	Water vapor diffusion resistance factor (μ) [-]	Thermal conductivity (λ) [W/(m·K)]	Thermal conductivity as a function of the relative humidity (λ(RH)) [W/(m·K)]				
							0	0.33	0.65	0.86	0.97
A1	Gypsum board	774	0.68	1100	7.9		0.19	0.19	0.19	0.2	0.21
A2	Wood fiberboard	280	0.85	1500	4.6		0.0485	0.0514	0.052	0.0553	0.0541
A4	Fiberglass sheathing	104	0.93	850	1.8		0.0312	0.031	0.0313	0.0311	0.0315
A8	Wood hardboard	1140	0.7	1500	79.5		0.11	0.11	0.12	0.13	0.14

	Materials	Density (ρ_p) [Kg/m^3]	Porosity (ϵ_p) [-]	Heat capacity dry ($C_{p,p}$) [J/m^3·K]	Water vapor diffusion resistance factor (μ) [-]	Thermal conductivity (λ) [W/(m·K)]	Thermal conductivity as a function of the relative humidity (λ(RH))) [W/(m·K)]				
							0	0.33	0.65	0.86	0.97
A11	Spruce plywood	394	0.65	1500	100		0.11	0.11	0.11	0.12	0.13
B3	Windbreak protection	232	0.6	1500	150	0.1					
B5	Bituminous paper	938	0.6	1500	100	0.1					
C1	Gypsum board	574	0.77	1100	6.9		0.19	0.19	0.19	0.2	0.21
C7	Plastic coated paper	940	0.3	2000	9640	0.1					
C11	Plastic film	950	0.01	2300	89000	0.1					
C13	Pine	532	0.78	2700	49		0.1	0.11	0.12	0.13	0.15
D1	Fiberglass	22	0.98	850	1.2		0.0348	0.0351	0.0351	0.0354	0.0353
D2	Rock wool	37	0.97	850	1.2		0.0337	0.0336	0.0336	0.0333	0.0337
D4	Cellulose	37	0.97	2000	1.3		0.0378	0.0382	0.0383	0.0394	0.0418
D5	Flax insulation	39	0.97	2000	1.4		0.0347	0.0359	0.0366	0.038	0.0405

Table 3: Sorption isotherm of each material.

	Materials	Sorption isotherm w(RH) [+23 °C] [kg/m3]										
		0	0.33	0.55	0.65	0.75	0.8	0.83	0.86	0.93	0.97	1
A1	Gypsum board	0	6.1	8.2	8.925	9.65	10.74375	11.4	13.44	18.2	23.8	500
A2	Wood fiberboard	0	12.3	20	24.1	28.2	35.7	40.2	47.58	64.8	74.8	140
A4	Fiberglass sheathing	0	0.8	0.9	0.965	1.03	1.43625	1.68	2.574	4.66	6.3	7
A8	Wood hardboard	0	69.9	88.2	125.45	162.7	194.5125	213.6	235.92	288	328	999
A11	Spruce plywood	0	22.9	31	43.2	55.4	67.525	74.8	86.47	113.7	126	590
B3	Windbreak protection	0	0.144040	0.354758	0.53555	0.855171	1.128853	1.3658428	1.6973125	3.4315231	7.1140443	28.288541
B5	Bituminous paper	0	0.144040	0.354758	0.53555	0.855171	1.128853	1.3658428	1.6973125	3.4315231	7.1140443	28.288541
C1	Gypsum board	0	4.6	6.1	6.65	7.2	7.95	8.4	9.93	13.5	17.7	371
C7	Plastic coated paper	0	0.072020	0.177379	0.26777	0.427585	0.564426	0.6829214	0.8486562	1.7157615	3.5570221	14.144270
C11	Plastic film	0	0.002400	0.005912	0.00892	0.014252	0.018814	0.0227640	0.0282885	0.0571920	0.1185674	0.4714756
C13	Pine	0	32.3	45	62.55	80.1	97.5375	108	126.36	169.2	185	866
D1	Fiberglass	0	0.45	0.54	0.66	0.78	0.9425	1.04	1.304	1.92	2.2	2.5
D2	Rock wool	0	0.15	0.23	0.33	0.43	0.53	0.59	0.62	0.69	0.8	0.9
D4	Cellulose	0	1.9	3.1	3.95	4.8	6.05	6.8	8.63	12.9	15.2	430
D5	Flax insulation	0	1.8	2.7	3.2	3.7	4.95	5.7	8.58	15.3	17.6	94

3.2 Heat and moisture transfer

The heat and moisture transfer are simulated together and this simulation is considerably difficult due to the nature of the transported substance. The moisture is not a material itself, since it cannot be considered neither water nor air and this fact hinders the model construction.

The "Mathematics" module represents the solution for this problem considering that it covers several types of partial differential equations (PDEs) and ordinary differential equations (ODEs). The proper interface among all is the PDE interface and within it, the preferable option is the "Coefficient form PDE". The reason is that coefficient form is easier than the general or the weak forms because the user has to input just the coefficients of equations (3.1). Due the nature of the module chosen, the moisture and heat transfer need to be calculated at the same time in this PDE coefficient.

The first step in order to perform the moisture transfer consists of setting the name of the field and the number and name of the variables. The field is called **u** by default and the variables in this transfer are two: the temperature (T) and the relative humidity (RH).

The default node is "Coefficient form PDE" as well and each material included in the geometry has one of these nodes because it is necessary to describe the physics equations for each material. The equation associated with this node is:

$$e_a \frac{\partial^2 \boldsymbol{u}}{\partial t^2} + d_a \frac{\partial \boldsymbol{u}}{\partial t} + \nabla \cdot (-c\nabla \mathbf{u} - \alpha \mathbf{u} + \gamma) + \beta \cdot \nabla \mathbf{u} + a\mathbf{u} = f \tag{3.1}$$

$$\boldsymbol{u} = [T, RH]^T$$

$$\nabla = \left[\frac{\partial}{\partial x}, \frac{\partial}{\partial y}, \frac{\partial}{\partial z}\right]$$

where **u** stands for the field vector which contains both variables, *t* is the time and the other symbols are the following coefficients:

- e_a : Mass Coefficient [s^2/m^2].
- d_a : Damping or Mass Coefficient [s^2/m^2].
- c : Diffusion Coefficient [-].
- α : Conservative Flux Convection Coefficient [1/m].
- β : Convection Coefficient [1/m].
- a : Absorption Coefficient [$1/m^2$].
- γ : Conservative Flux Source [1/m].
- f : Source Term [$1/m^2$].

This equation is formed depending of which ones of the coefficients are not zero in the equation that is being representing. In our case, the coefficients, which represent the energy and moisture balances, have to be input by hand. These balances involve the equations from (2.35) to (2.42) so according to them, the coefficients of equation (3.1) which have a non-zero value are the diffusion and damping or mass coefficients (c and d_a), leaving this equation:

$$d_a \frac{\partial \boldsymbol{u}}{\partial t} + \nabla \cdot (-c\nabla \boldsymbol{u}) = 0 \tag{3.2}$$

Taking into account that **u** is the field vector whose components are the temperature and the relative humidity, the two terms are:

$$\mathrm{d_a} \cdot \frac{d\boldsymbol{u}}{dt} = \begin{bmatrix} \mathrm{d_{aT}} & 0 \\ 0 & \mathrm{d_{ap}} \end{bmatrix} \cdot \begin{bmatrix} \dfrac{dT}{dt} \\ \dfrac{dRH}{dt} \end{bmatrix} = \begin{bmatrix} \rho C_p + cw & 0 \\ 0 & \xi \end{bmatrix} \cdot \begin{bmatrix} \dfrac{\mathrm{dT}}{\mathrm{dt}} \\ \dfrac{\mathrm{dRH}}{\mathrm{dt}} \end{bmatrix} \tag{3.3}$$

$$\nabla(-c\nabla \boldsymbol{u}) = -\nabla \begin{bmatrix} c_{T,T} & c_{T,RH} \\ c_{RH,T} & c_{RH,RH} \end{bmatrix} \cdot \begin{bmatrix} \nabla T \\ \nabla RH \end{bmatrix} = - \begin{bmatrix} \lambda + H_v \delta_p RH \cdot \dfrac{dp_{vsat}}{dT} & H_v \delta_p p_{vsat} \\ \delta_p RH \cdot \dfrac{dp_{vsat}}{dT} & \delta_p p_{vsat} \end{bmatrix} \cdot \nabla \begin{bmatrix} \nabla T \\ \nabla \mathrm{RH} \end{bmatrix} \tag{3.4}$$

where, the components of all the coefficients have been developed in the section 2.4. This equations have to be written at the corresponding coefficient in Comsol. Those coefficients together form the equation that Comsol uses to calculate the temperature and relative humidity throughout the wall.

Using the Mathematic module of Comsol, the vapour membranes were modelled by adding the "Weak Contribution" node, which is a pair definition, for RH and another for T. This node has an equivalent effect as the slit-boundary conditions, available as the "Thin thermally resistive layer" which belongs to the heat transfer module (COMSOL 2012). This node connects overlapping boundaries of different domains since Comsol does not assemble it automatically.

The default nodes concerning to boundary conditions are "Zero flux" and "Initial values". The "Initial values" node requires the initial value for T and RH and the initial time derivative of T and RH (∂T/∂t and ∂RH /∂t). These last two conditions are zero in this modelling. The number of this kind of nodes increases depending on the number of initial temperatures and relative humidities; in this case, the initial temperature is the same at every layer, T = 20 ºC, but the initial relative humidity is not the same, as the table 4 shows:

Table 4: Initial relatives humidites of every layer.

	RH [%]				
	1 Inner lining	3 Insulation	4 Sheathing	5 Inferior frame	6 Superior frame
Structure 1	70	78	78	70	-
Structure 2		75	86		
Structure 3		75	86		
Structure 4		86	86		
Structure 5		86	86		
Structure 6		81	65		
Structure 7		65	65		
Structure 8		86	86		
Structure 9		83	67		
Structure 10		55	55	55	70

The "Zero flux" node provides a lack of flow to the surface. The surfaces affected by this condition are the upper and lower surfaces. This boundary condition is governed by the following equation:

$$-\boldsymbol{n} \cdot (-c\nabla \mathbf{u} - \alpha \mathbf{u} + \gamma) = 0 \tag{3.5}$$

$$\boldsymbol{u} = [T, RH]^T$$

$$\nabla = \left[\frac{\partial}{\partial x}, \frac{\partial}{\partial y}, \frac{\partial}{\partial z}\right]$$

being **n** the outward unit normal vector on the domain boundary.

The default nodes become insufficient to describe all the boundary conditions, so two "Dirichlet Boundary Condition" nodes are added in order to set the conditions at the internal and external surfaces. The Dirichlet condition is used to assign a specific temperature and relative humidity value to the external surface by means of the next equation (COMSOL 2012):

$$\boldsymbol{u} = r \tag{3.6}$$

$$\boldsymbol{u} = [T, RH]^T$$

where *r* accounts for a vector whose components r_1 and r_2 contain the initial temperature and relative humidity. These values at both the internal and external surfaces change in function of time.

The values of temperature and relative humidity used as boundary conditions in those Dirichlet conditions are the surface values. The surface temperatures have been measured while the surface relative humidities have to be calculated through the norm DIN 4108-5 and the equations (2.21) and (2.22):

$$p_{vsat} = 288.68 \cdot \left(1.098 + \frac{\vartheta}{100}\right)^{8.02} \quad ; \quad p_v = RH \cdot p_{vsat} \quad ; \quad \nu = \frac{(p_v \cdot 0.018)}{8.314 \cdot (\vartheta + 273.15)}$$

$$p_{surf} = \frac{[\nu \cdot 80.314 \cdot (\vartheta_{surf} + 273.15)]}{0.018} \quad ; \quad p_{vsat,surf} = 288.68 \left(1.098 + \frac{\vartheta_{surf}}{100}\right)^{8.02}$$

$$RH_{surf} = \frac{p_{surf}}{p_{vsat,surf}}$$

- ϑ: the layer initial temperature, which has been previously established at 20ºC.
- RH: the relative humidity [-] which can be observed at table 4.
- ϑ_{surf} : the initial surface temperature, which have been measured and can be observed in the figures from 14-18 [ºC].

The surface temperatures and the surface relative humidities which have been previously calculated are represented in the next figures. The first structure has its own boundary conditions as well as the structure 8, as seen in figures 14 and 17. Otherwise, the structures 2-3-4-5, 6-7 and 9-10, respectively, share the temperature as well as the relative humidity, as can be seen in the figures 15, 16 and 18.

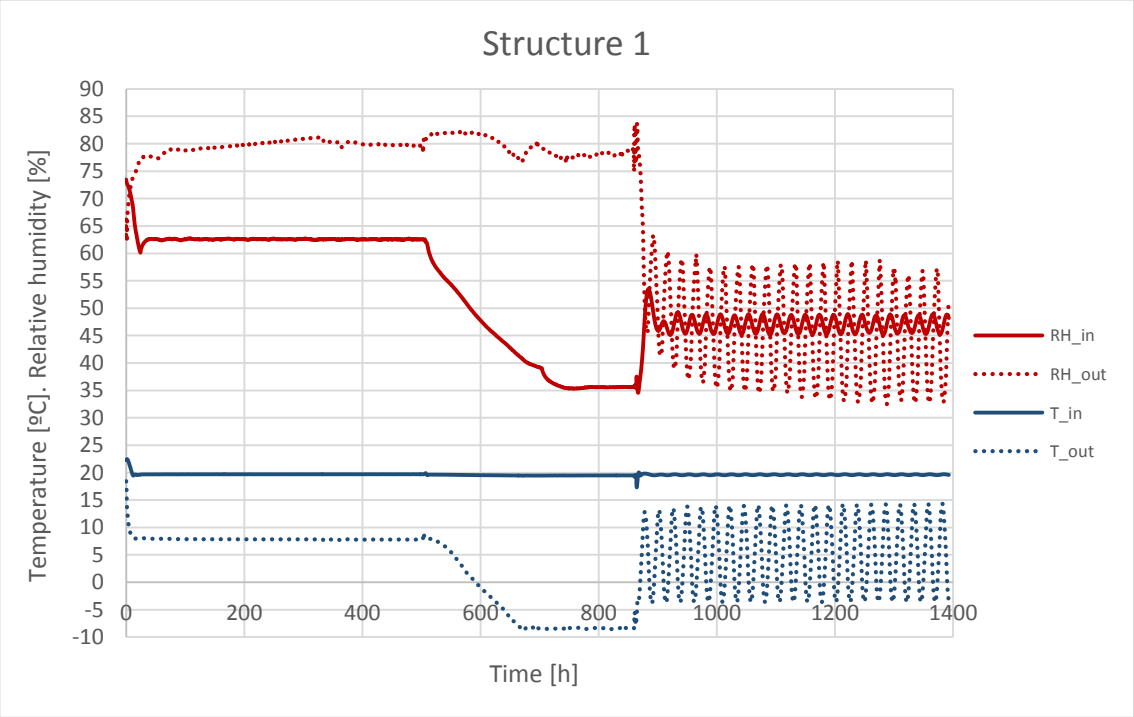

Figure 14: Boundary conditions of the structure 1.

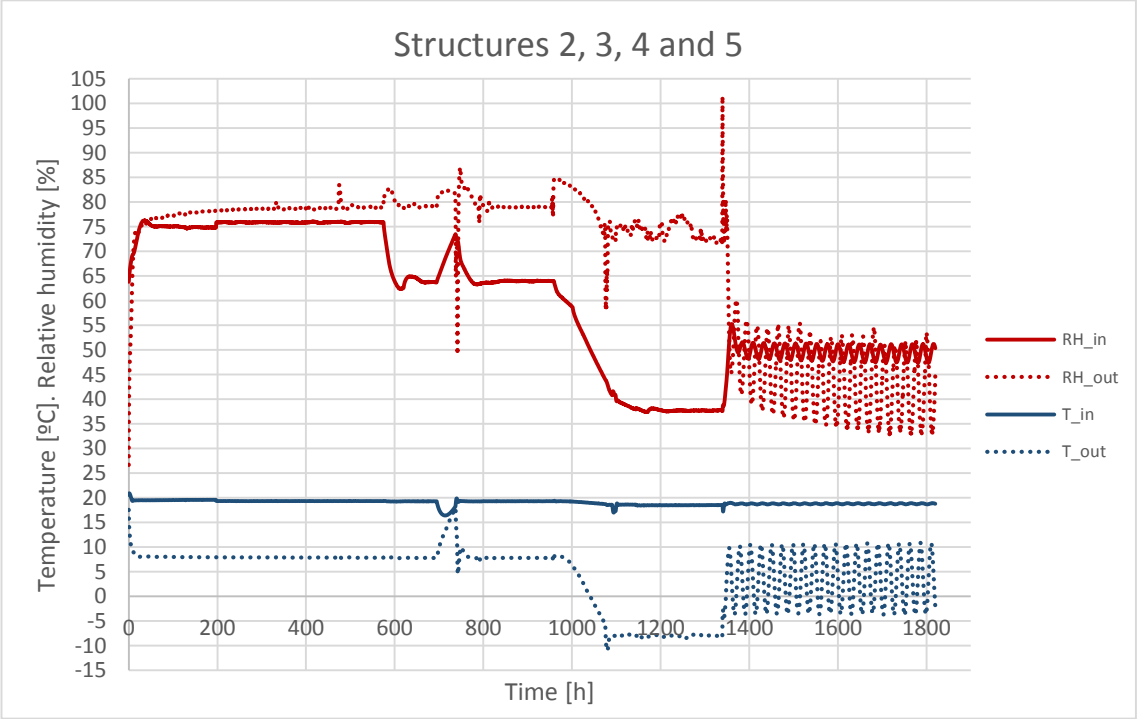

Figure 15: Boundary conditions of structures 2, 3, 4 and 5.

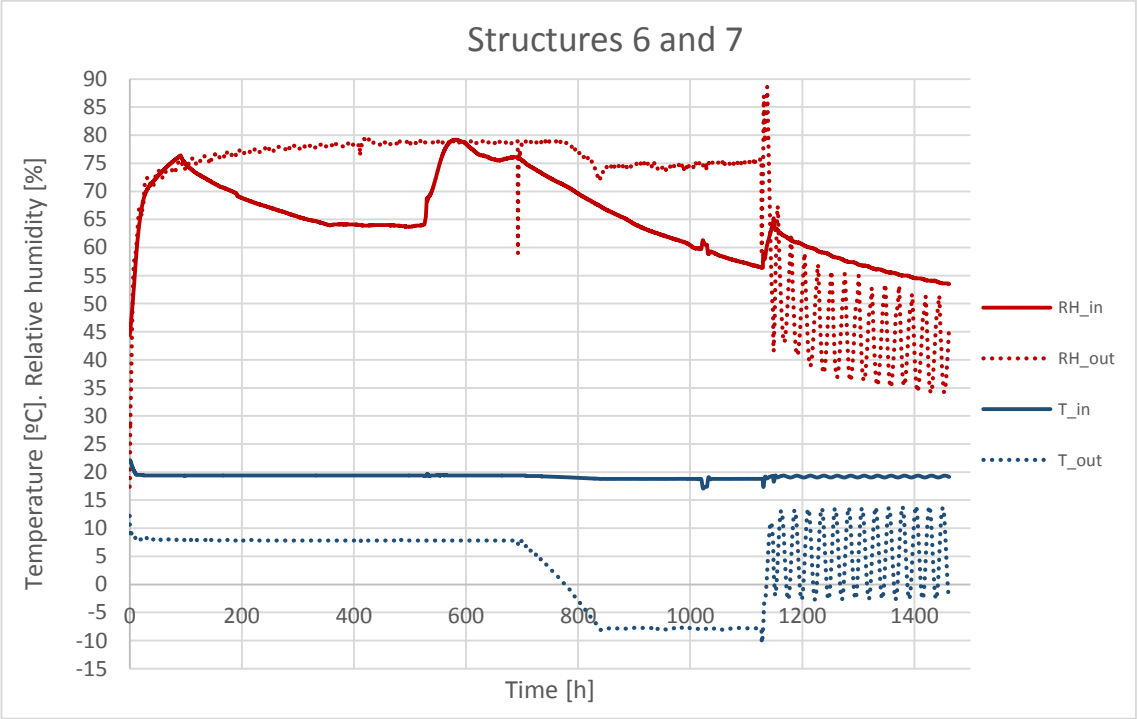

Figure 16: Boundary conditions of structures 6 and 7.

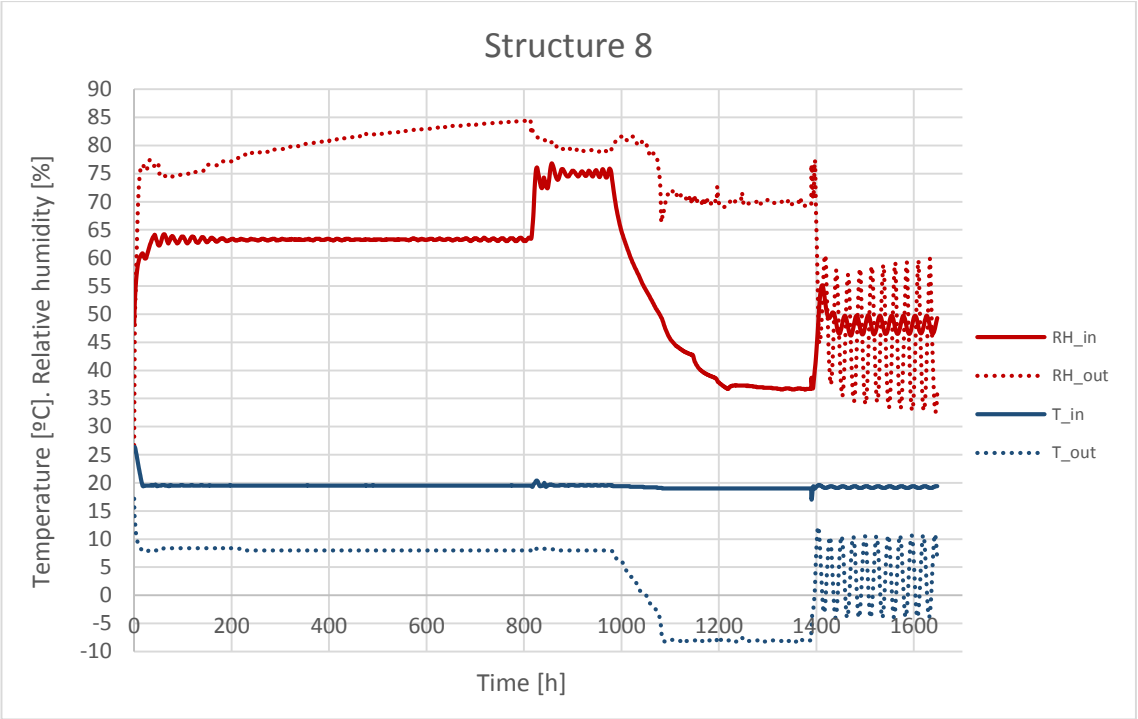

Figure 17: Boundary conditions of the structure number 8.

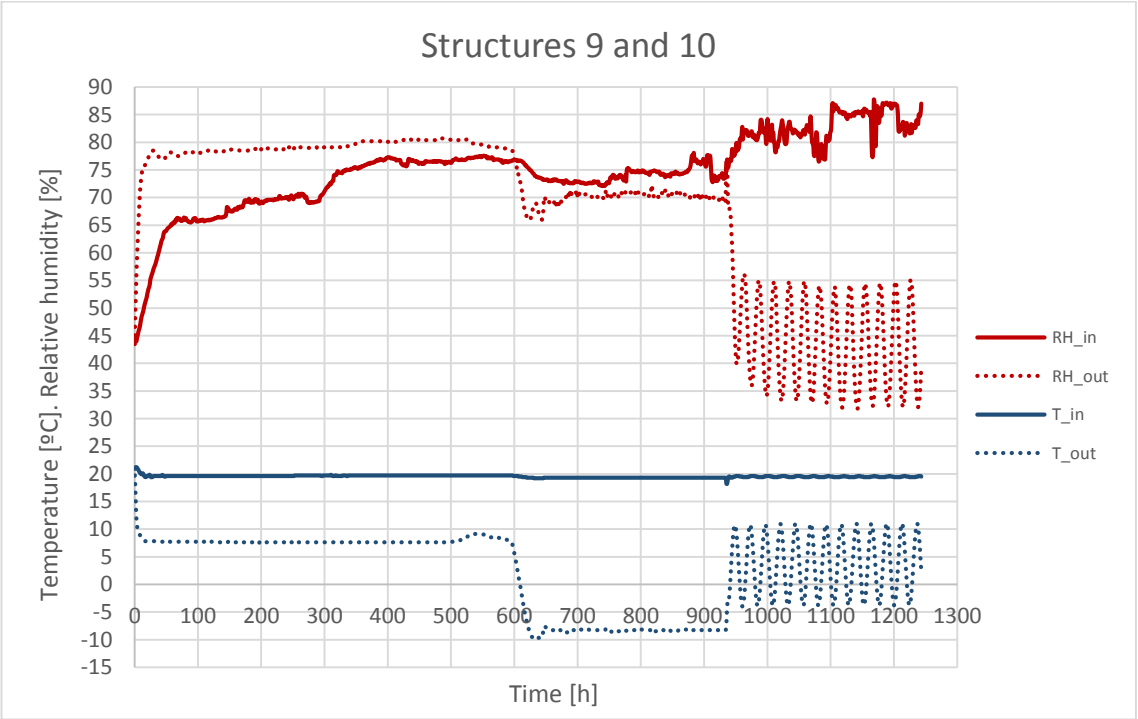

Figure 18: Boundary conditions of structures 9 and 10.

3.2.1 Mesh

The mesh has a great importance when performing the computation. A wrong choice of mesh can cause a mistake in the results due to a lack of accuracy or even an error in the computation. The meshes can be built or it is also possible to allow the program that it builds it which is the default option. The mesh for this interface has been built with the option "user-controlled meshing". The mesh used in every layer is the most common in 2D, called "Free triangular". It creates a triangular structured mesh and it is used one in each domain.

The number, size and distribution of the mesh elements can be modified according to the accuracy required. The size of the mesh, which goes from extremely fine to extremely coarse, has to be precisely chosen in each layer. It is necessary to specify if the model is related to general physics, fluid dynamics or plasma. This could seem a trivial detail but it helps to a better built of the mesh because the fluids need a finer mesh than the other two. Every layer has used the free triangular mesh and within it, the fluid dynamics option, but the mesh accuracy depends on the layer. The first layer of this geometry which has been meshed is the air or water barrier because it is the thinnest one so it needs the greatest accuracy (extremely fine). After that, lining boards mesh has been built (finer), then the exterior frame (fine) and finally the insulation layer (normal).

It is important the order in which the meshes are built; a layer mesh starts to be built from the nodes of the previous meshes. If the order is not the mentioned one, the mesh will be designed in the wrong way and this can cause an error in the simulation.

3.2.2 Study

This section contains the parameters related to the time control, the simulation time and the computation time. The selected kind of study is "Time-dependent" for moisture and heat coupled transfer because the moisture transfer develops over the time so its analysis must be done over the time as well.

The study interface in case of "Time dependent" node needs some changes to decrease at minimum possible the amount of errors. First of all, the range of time has to be established in the study settings window of the "Time dependent" node. In the simulation, the range of time goes from zero to the total number of hours (H) with an interval of 3600 seconds (0, 3600, H*3600). The simulation length is the time that the laboratory tests took and it depends on the structure, as can be observed in the table 5:

Table 5: Laboratory tests duration of the every structure.

	Str.1	Str.2	Str.3	Str.4	Str.5	Str.6	Str.7	Str.8	Str.9	Str.10
Time [h]	1393	1820	1820	1820	1820	1463	1463	1649	1244	1244

After establishing the range of time, within the "Solver configurations" node, in the "Time-Dependent Solver" section, the maximum step, which is a parameter of the Time stepping, should be modified according to the selected time range (3600 s).

Once the kind of study has been selected, the default nodes in the solver are "Direct" and "Fully coupled". The "Direct" option solves a system of linear equations using algorithms based on LU-decomposition. There is another solver option called "Iterative" which solves systems of linear equations as well, but by an iterative method, gradually. At the beginning, it starts with a guess, then it calculates an approximation and updates the solution vector in each step. Each one of those steps is a linear iteration. It uses a convergence criterion to decide if it is necessary to continue the process or the solution is as accurate that the final solution has been reached and the iteration is over. There is a maximum number of iterations which has been determined and in case that the solution is not accurate enough when this number of iterations is reach, the computation stops and the next error arises: "Error: Failed to find a solution. Returned solution is not converged". (COMSOL 2012).

The main reason that the chosen mode is "Iterative" is the memory. The direct solver can be more robust but the iterative solver takes up less memory which entails an important advantage in this model due to the great amount of calculations needed. Also, the number of iterations can be modified so it does not lead to any problems. The PDE module requires a great amount of time and memory; hence the best option in this module is iterative one due to the save of memory.

The other default node in the study section is the "Fully coupled" approach which is an algorithm to solve multiphysics finite element models in COMSOL. This kind of algorithm is based on the Newton-Raphson iterations. This method, as seen in figure 19, starts with an initial estimation of the solution and then a succession of approximations is built recursively through the formula (Palacios 2008):

$$x_{j+1} = x_j - \frac{f(x_j)}{f'(x_j)} \tag{3.7}$$

The "Fully coupled" approach treats all the couplings between the physics at the same time so the function f is the system containing the equations of the different physics. According the kind of calculations performed in this model, the "Fully coupled" approach

is used in the simulation of the fluid-flow module, even if there is another approach which is more memory-efficient.

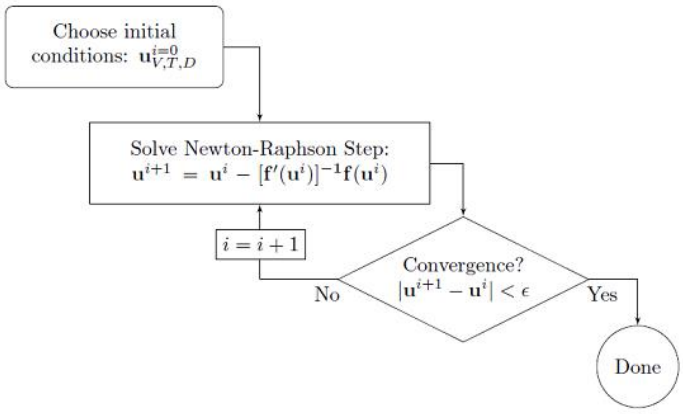

Figure 19: Algorithm of "Fully coupled" approach. (Frei 2013)

The "Segregated" mode will replace the "Fully coupled" one in the moisture transfer simulation. The "Segregated" approach is, like the "Fully coupled" one, an algorithm to solve multiphysics finite element models in COMSOL and it is also based in Newton-Raphson iterations. The "Fully coupled" cannot be used in this case because its compilation takes too much memory and it is too slow compared with the "Segregated". These two reasons lead to the change of approach.

The "Segregated" option has an individual treatment for each physic and it uses the results already obtained in the previous physic in order to help in the calculations of the next physic. The main advantage of this approach consists of the use of the optimal iterative solver in each linear substep: the solved problems in each step are smaller and in addition the solver is faster and it takes up less memory. This approach needs more iterations but the used memory is smaller.

The sequence of the "Segregate" algorithm, represented in figure 20, is the following: (Frei 2013)

I. Establish the initial conditions for every physic.
II. Start the counter of iterations number.
III. Solve for the first physic, using the previous step.
IV. Solve the second physic, using the results from the previous physic.
V. Repeat the solving of every physic until the convergence or until the iterations number is reached.

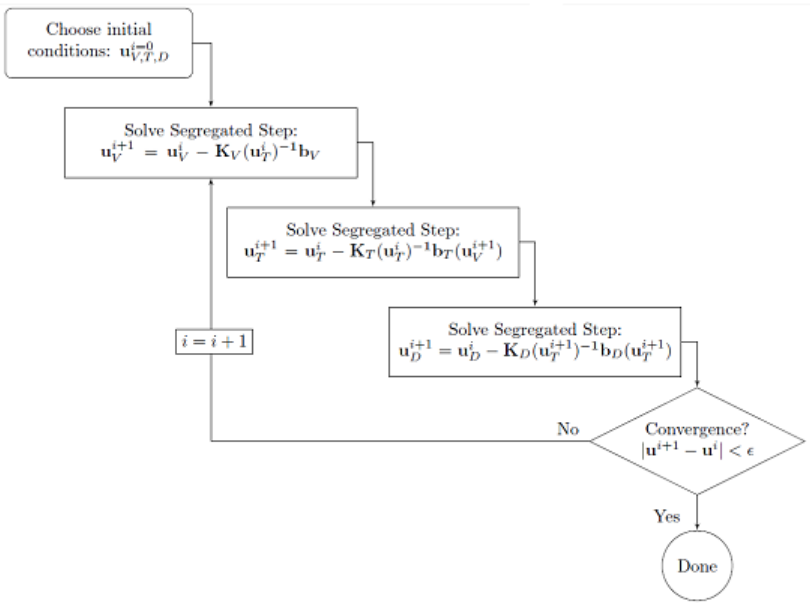

Figure 20: Algorithm of "Segregated" approach, in case of three physics. (Frei 2013)

There is just one "Segregated step" node by default in the segregated mode and this simulation has two variables, the temperature and the relative humidity, so one more segregated step node is added so that each step corresponds to a variable.

3.3 Results and comparison with the laboratory tests and WUFI's results

The results of the transferences of heat and moisture are gathered by measuring and recording the signal of changing temperature and relative humidity through three sensors placed at different points inside the structures, as seen in the figures 4-13. The sensors, called S, R and U measure the temperature and relative humidity throughout the whole test. Therefore, the same points have been chosen to extract the results from Comsol's simulations in order to compare them with the laboratory test. After obtaining the results, they are plotted along with the results from the laboratory and WUFI in the same graph.

The figures from 21 to 80 contain the graphs with the results of the ten structures at the different points. Therefore, there are six graphs of each structure which show the temperature and the relative humidity at points S, R and U. The point S is the inner sensor, the point U is the outer sensor and the point R is placed inside the insulation but it varies depending on the structures.

3.3.1 Results structure 1

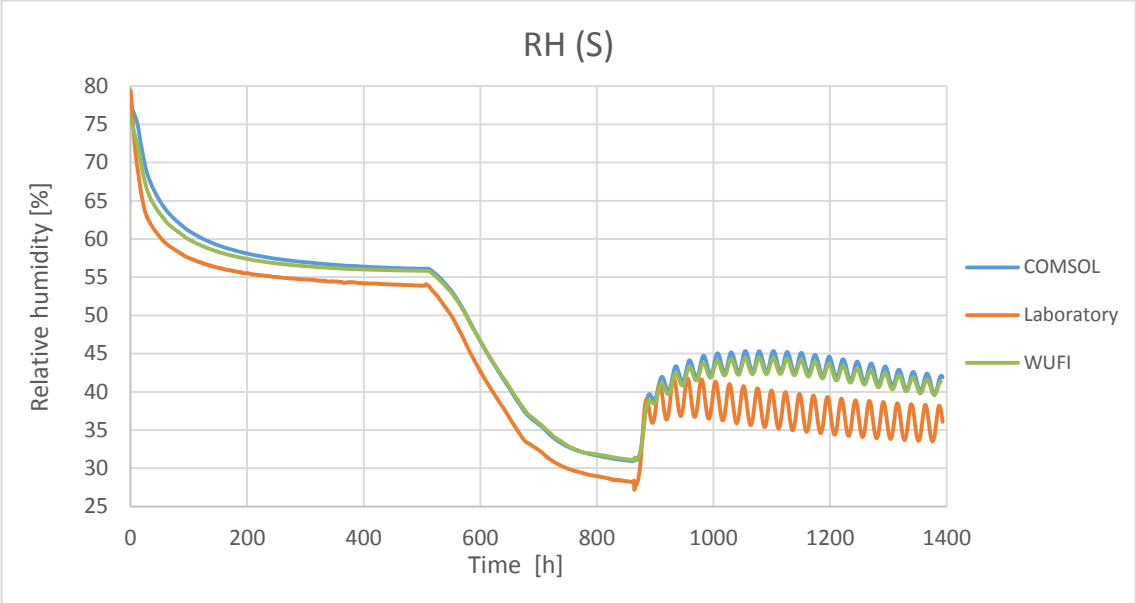

Figure 21: Comsol, WUFI and laboratory relative humidity at point S of the structure 1.

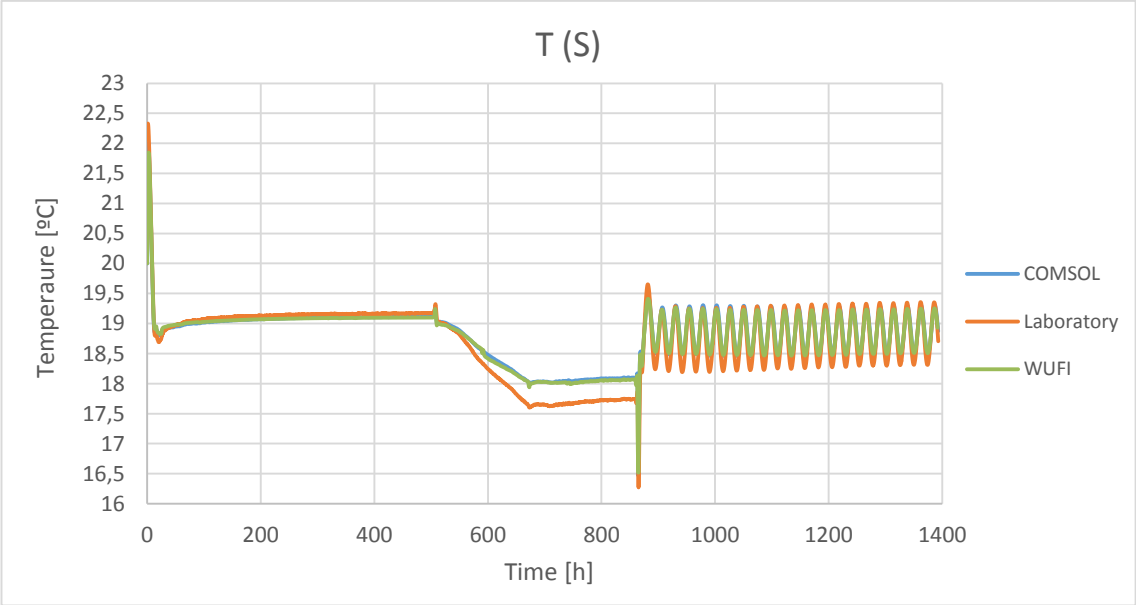

Figure 22: Comsol, WUFIi and laboratory temperature at point S of the structure 1.

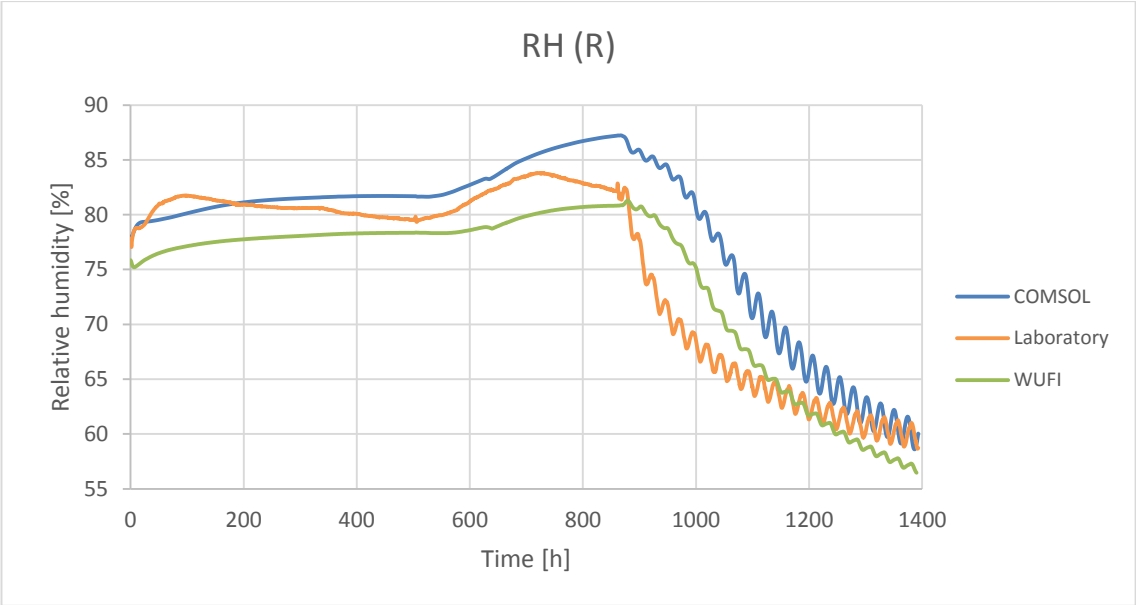

Figure 23: Comsol, WUFI and laboratory relative humidity at point R of the structure 1.

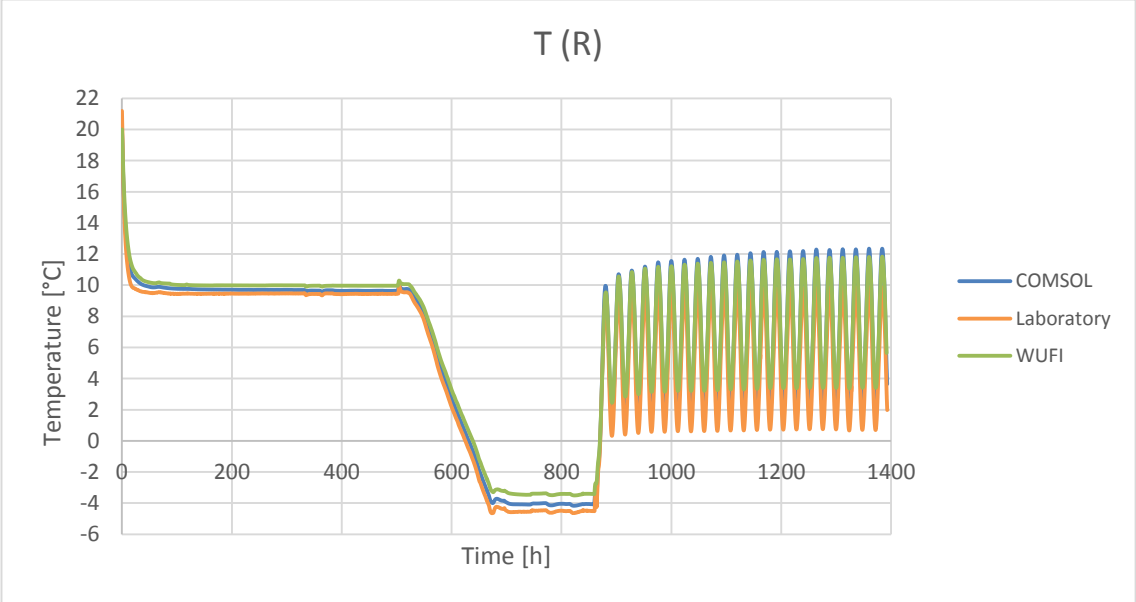

Figure 24: Comsol, WUFI and laboratory temperature at point R of the structure 1.

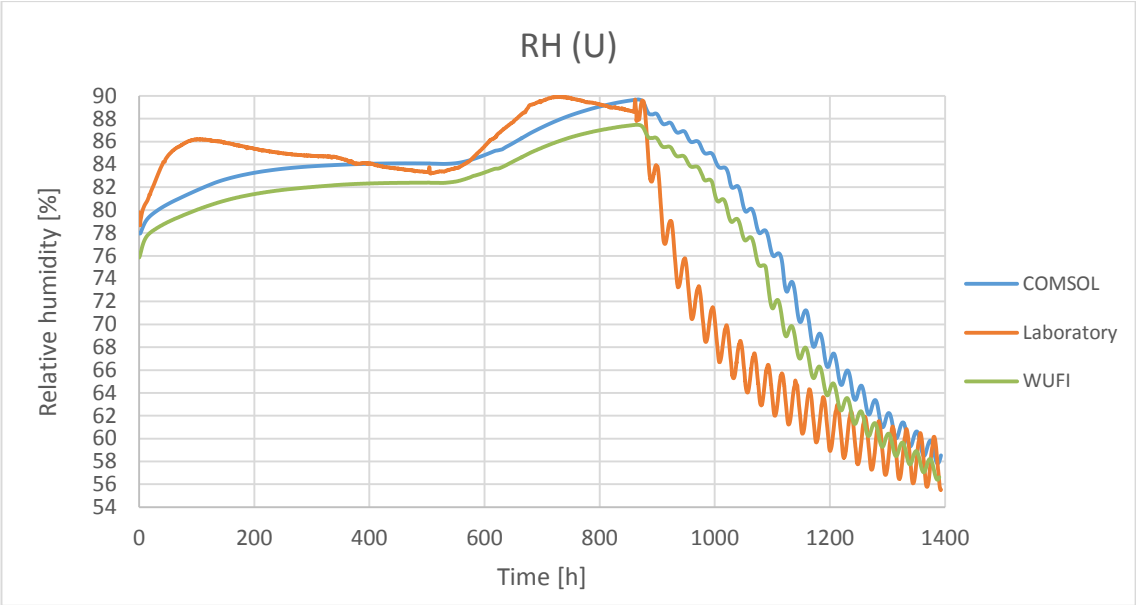

Figure 25: Comsol, WUFI and laboratory relative humidity at point U of the structure 1.

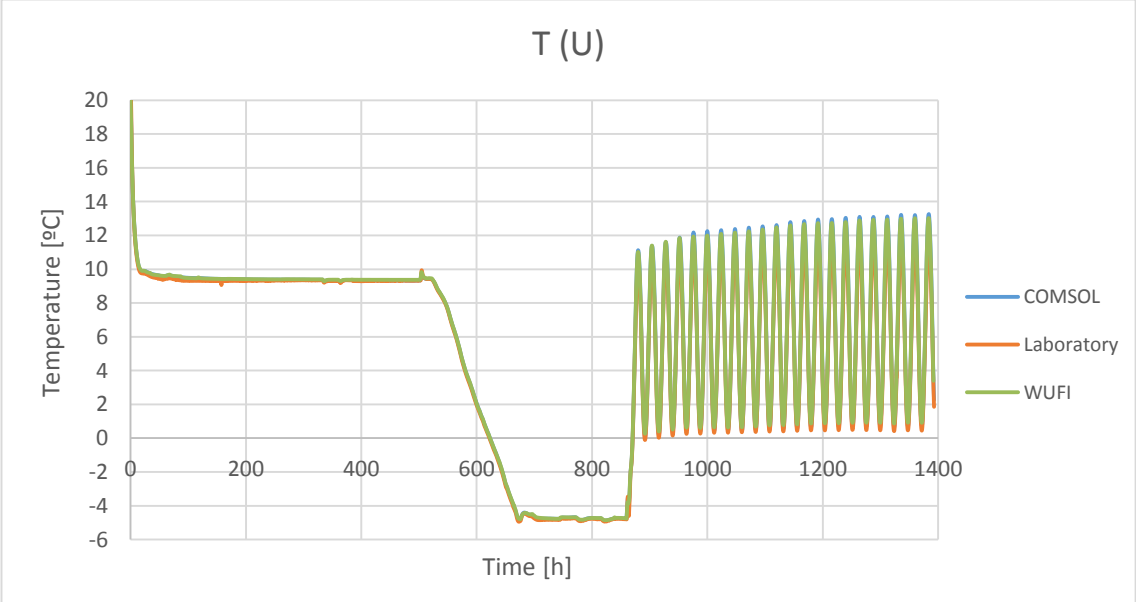

Figure 26: Comsol, WUFI and laboratory temperature at point U of the structure 1.

3.3.2 Results structure 2

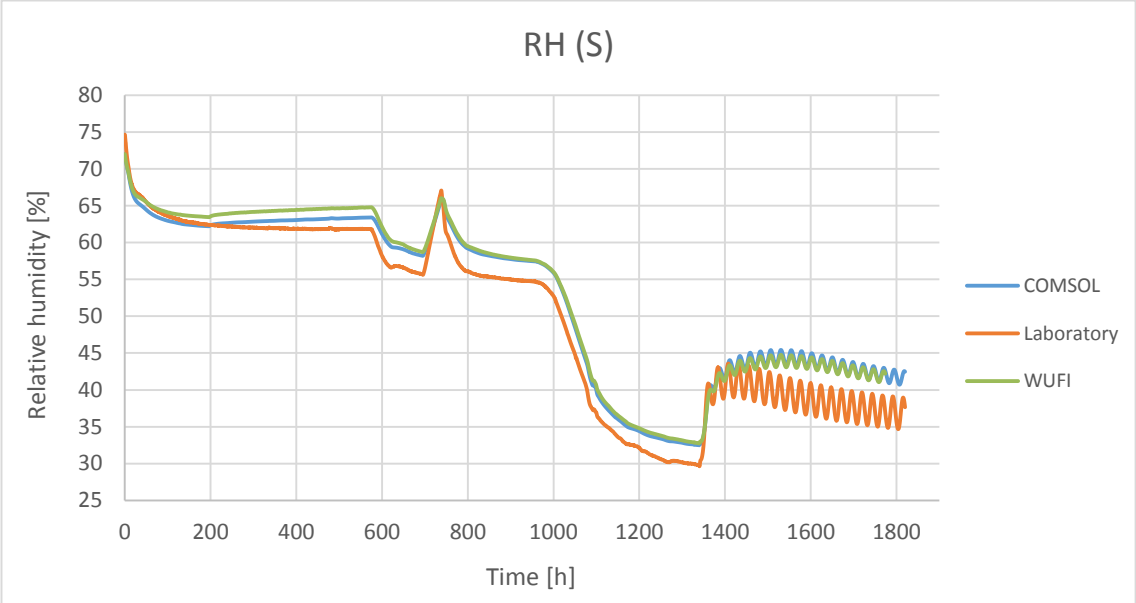

Figure 27: Comsol, WUFI and laboratory relative humidity at point S of the structure 2.

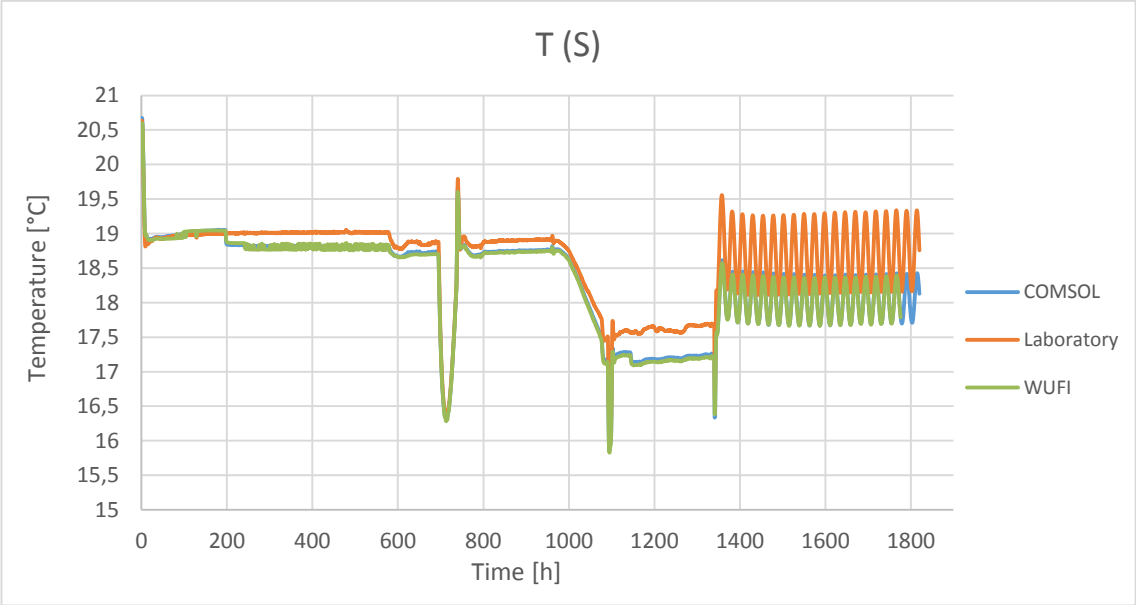

Figure 28: Comsol, WUFI and laboratory temperature at point S of the structure 2.

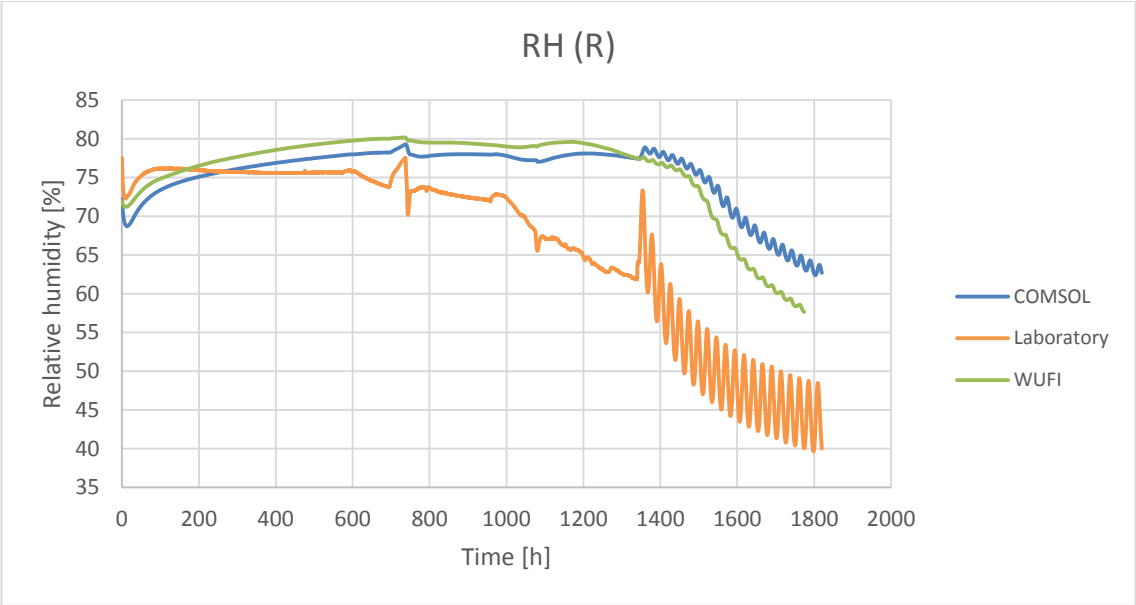

Figure 29: Comsol, WUFI and laboratory relative humidity at point R of the structure 2.

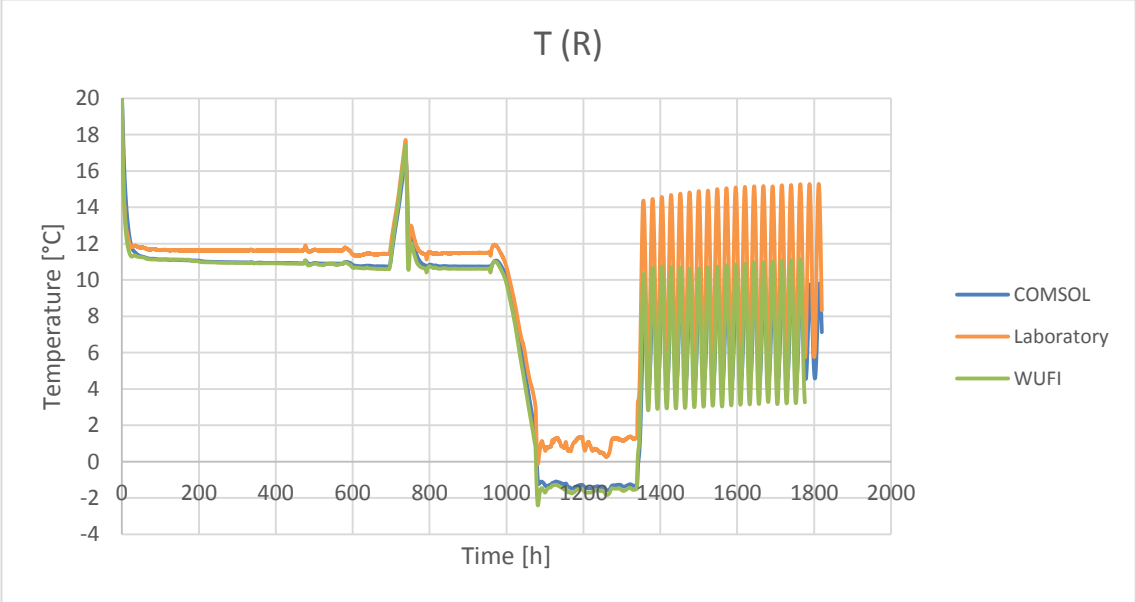

Figure 30: Comsol, WUFI and laboratory temperature at point R of the structure 2.

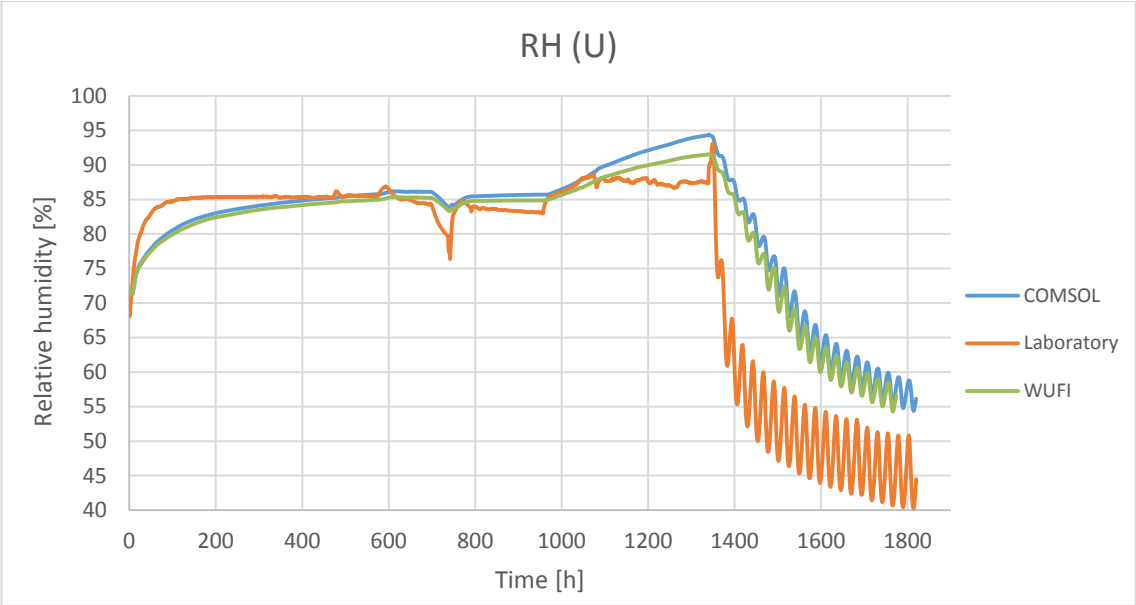

Figure 31: Comsol, WUFI and laboratory relative humidity at point U of the structure 2.

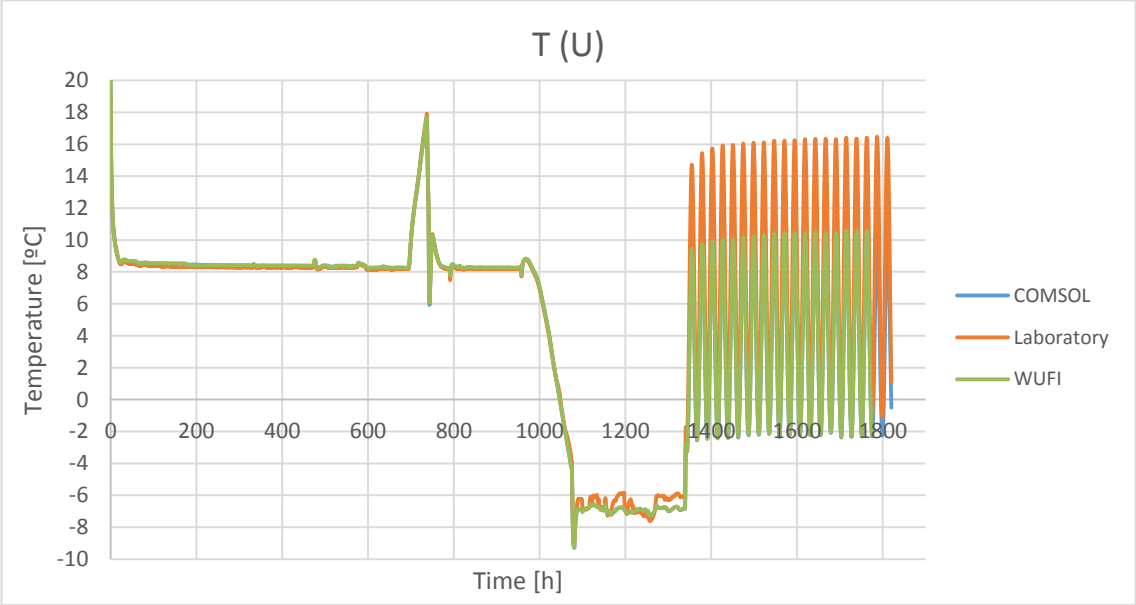

Figure 32: Comsol, WUFI and laboratory temperature at point U of the structure 2.

3.3.3 Results structure 3

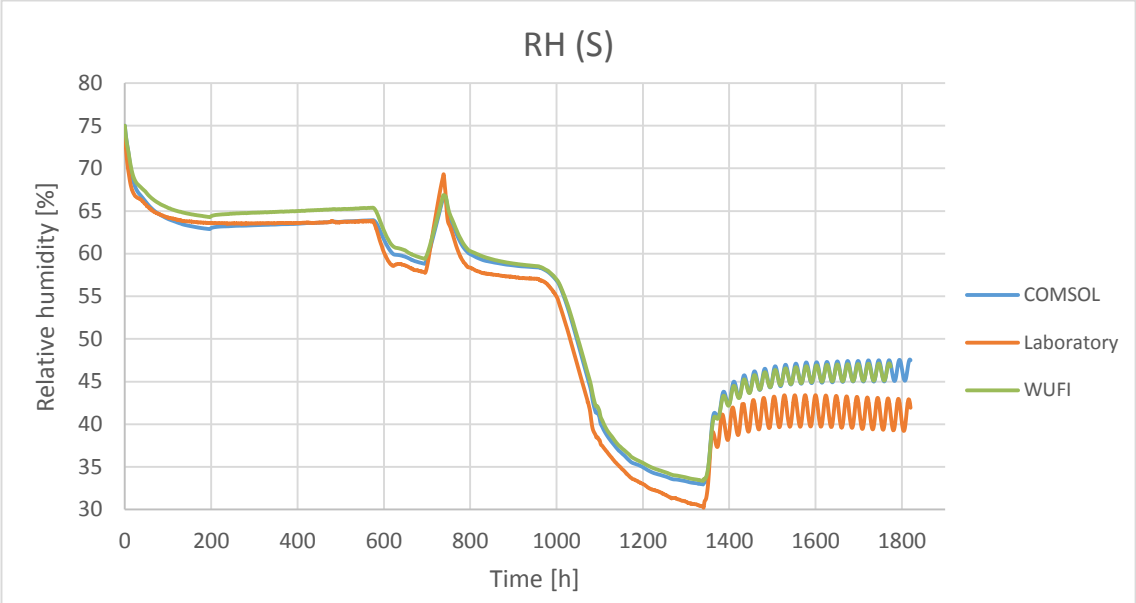

Figure 33: Comsol, WUFI and laboratory relative humidity at point S of the structure 3.

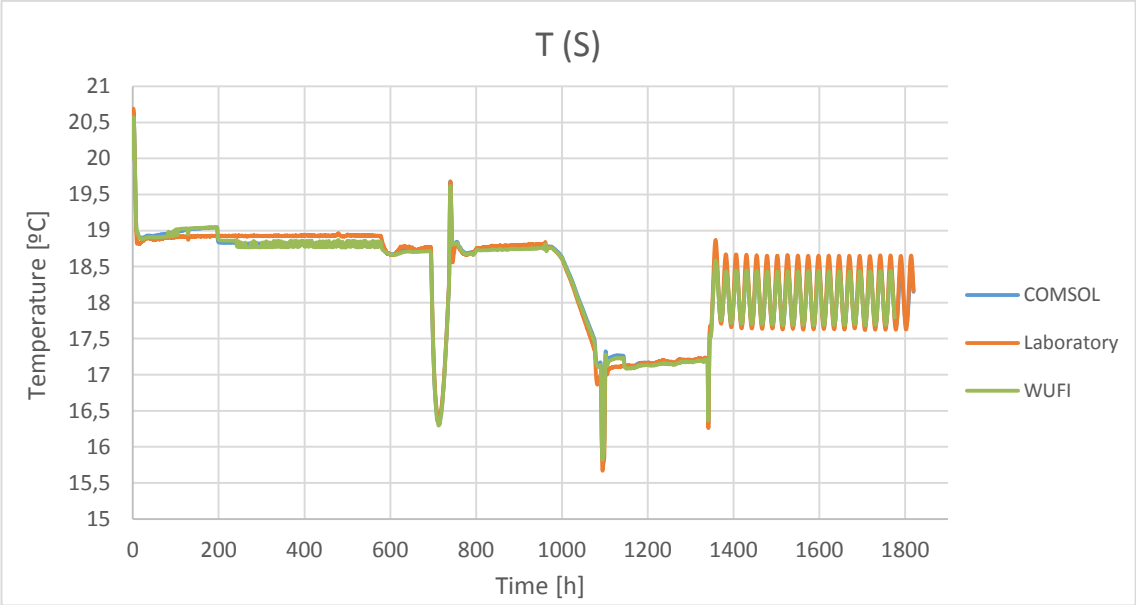

Figure 34: Comsol, WUFI and laboratory temperature at point U of the structure 3.

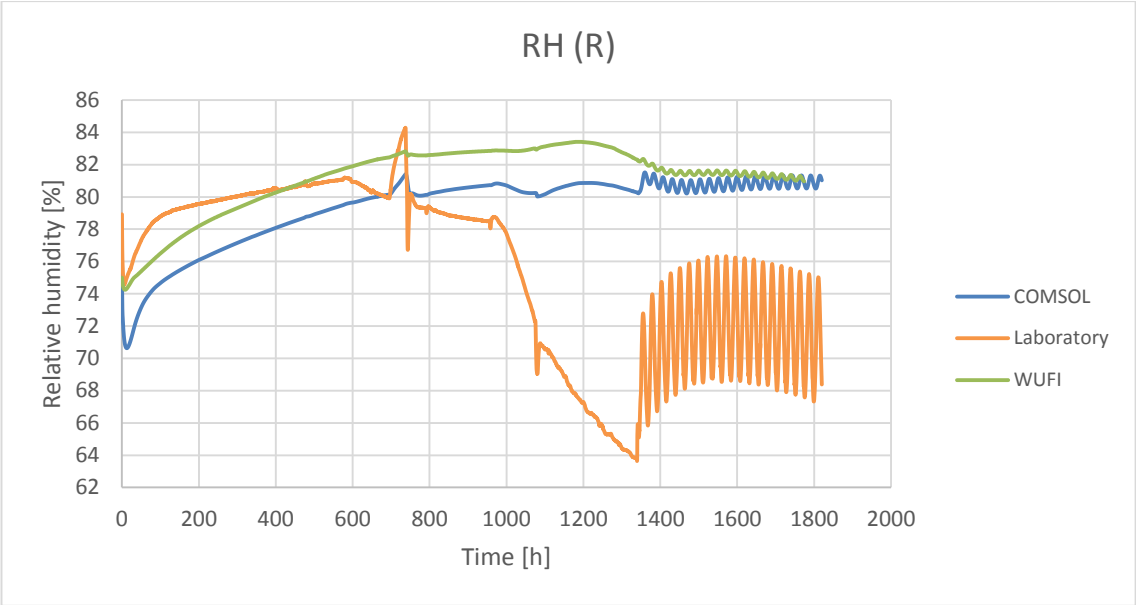

Figure 35: Comsol, WUFI and laboratory relative humidity at point R of the structure 3.

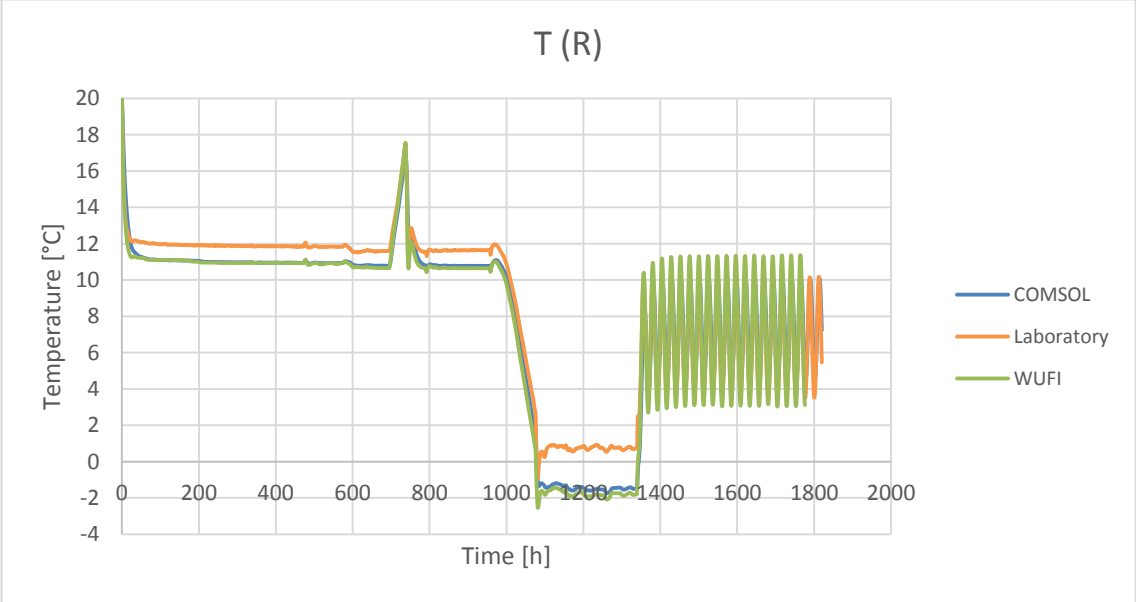

Figure 36: Comsol, WUFI and laboratory temperature at point R of the structure 3.

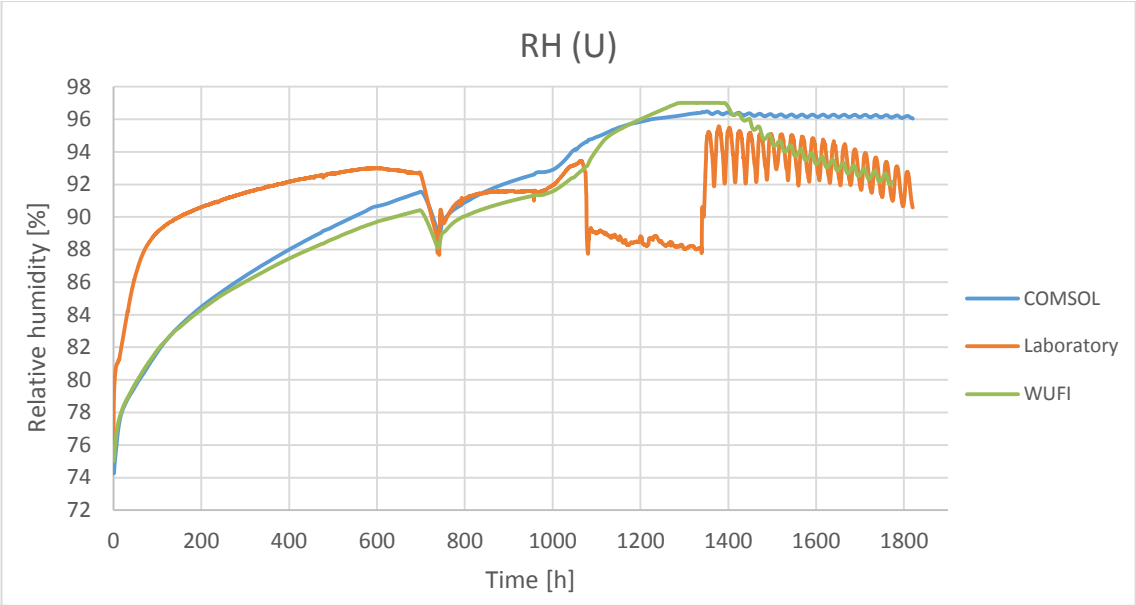

Figure 37: Comsol, WUFI and laboratory relative humidity at point U of the structure 3.

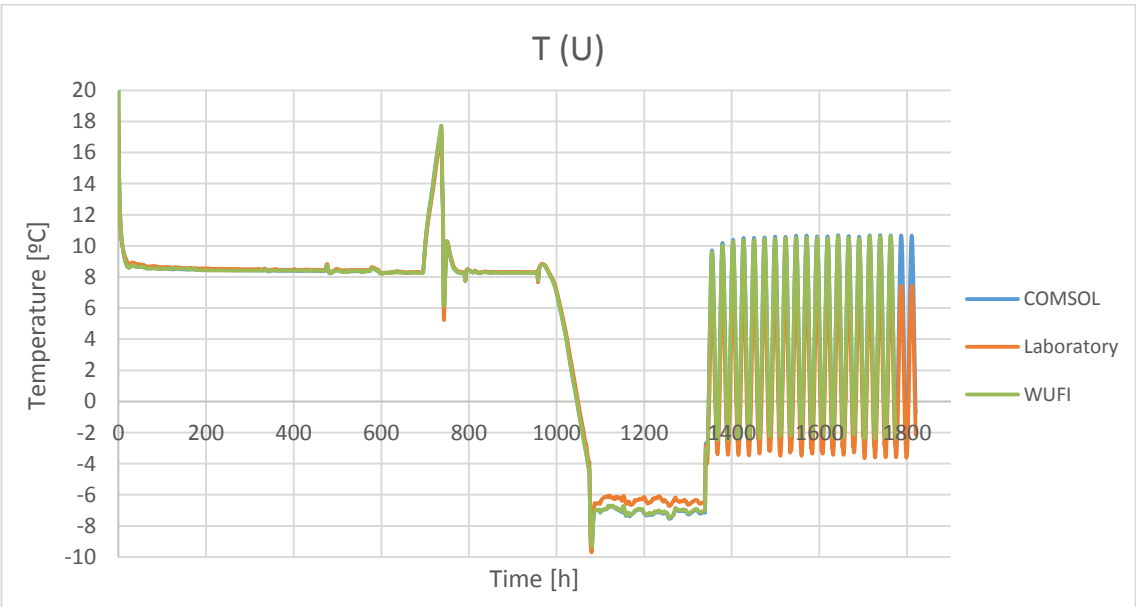

Figure 38: Comsol, WUFI and laboratory temperature at point U of the structure 3.

3.3.4 Results structure 4

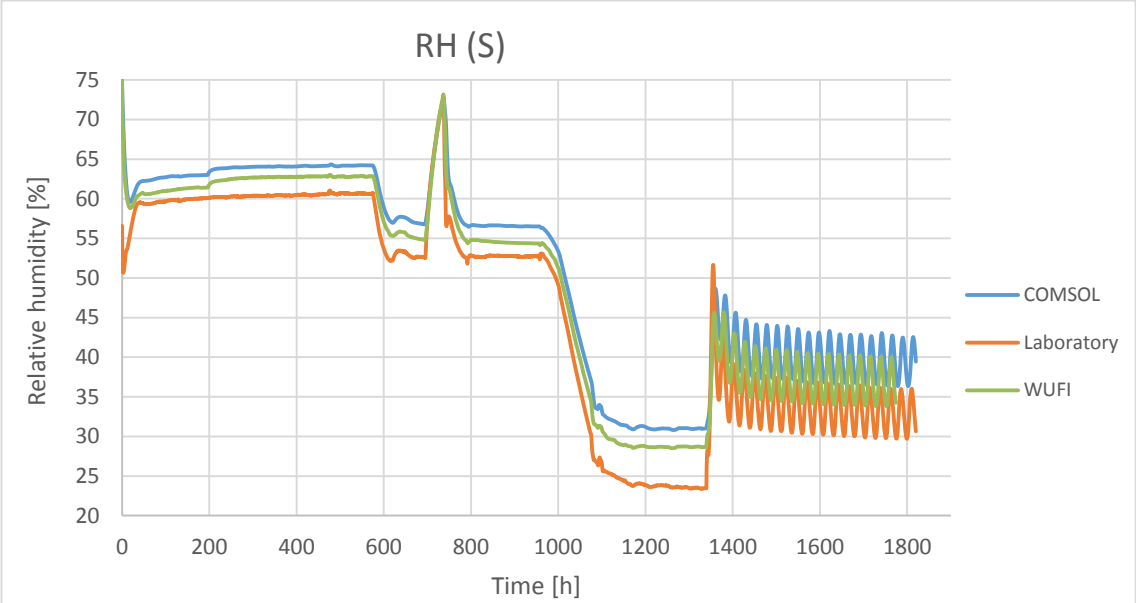

Figure 39: Comsol, WUFI and laboratory relative humidity at point S of the structure 4.

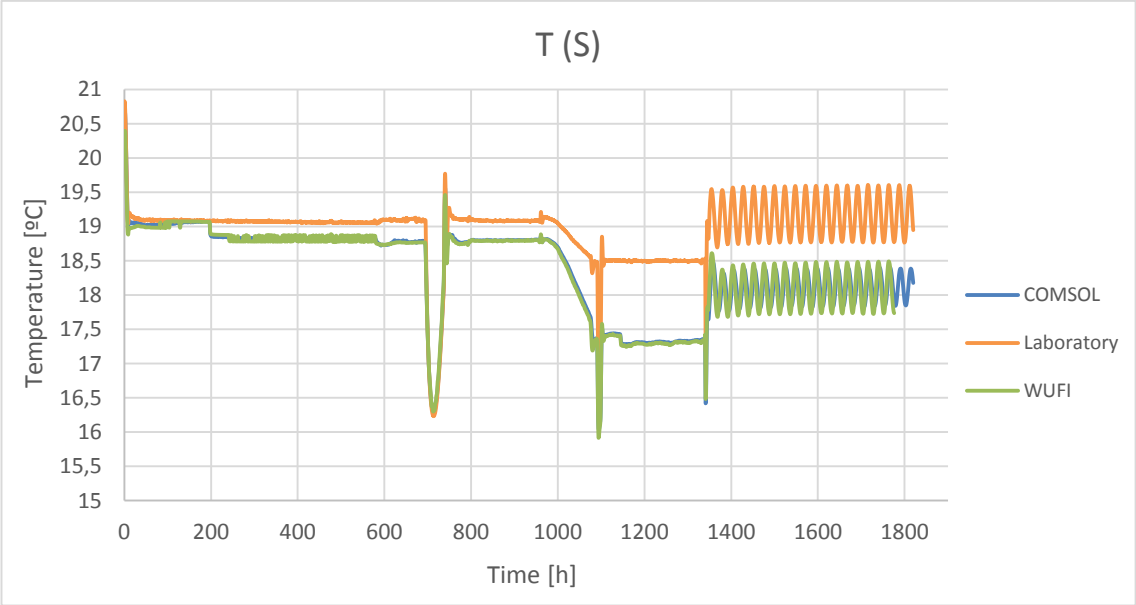

Figure 40: Comsol, WUFI and laboratory temperature at point S of the structure 4.

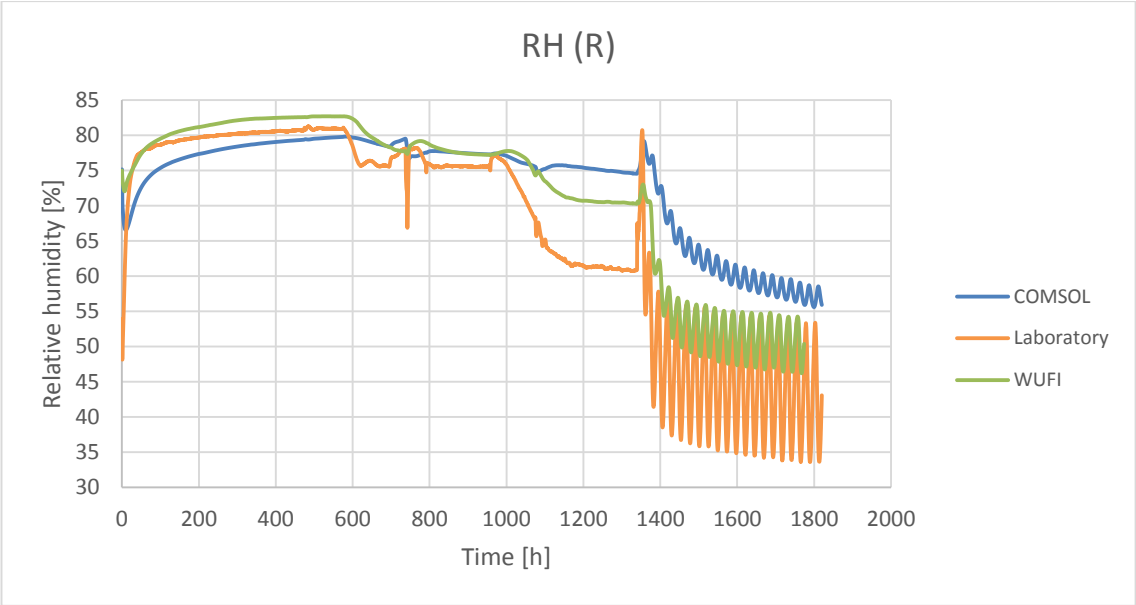

Figure 41: Comsol, WUFI and laboratory relative humidity at point R of the structure 4.

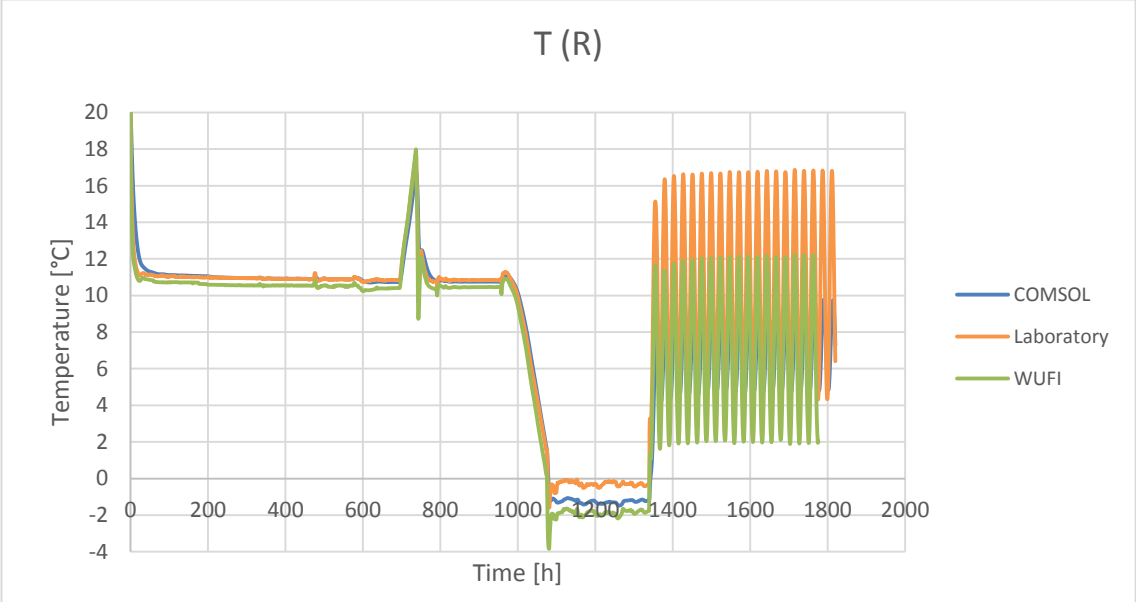

Figure 42: Comsol, WUFI and laboratory temperature at point R of the structure 4.

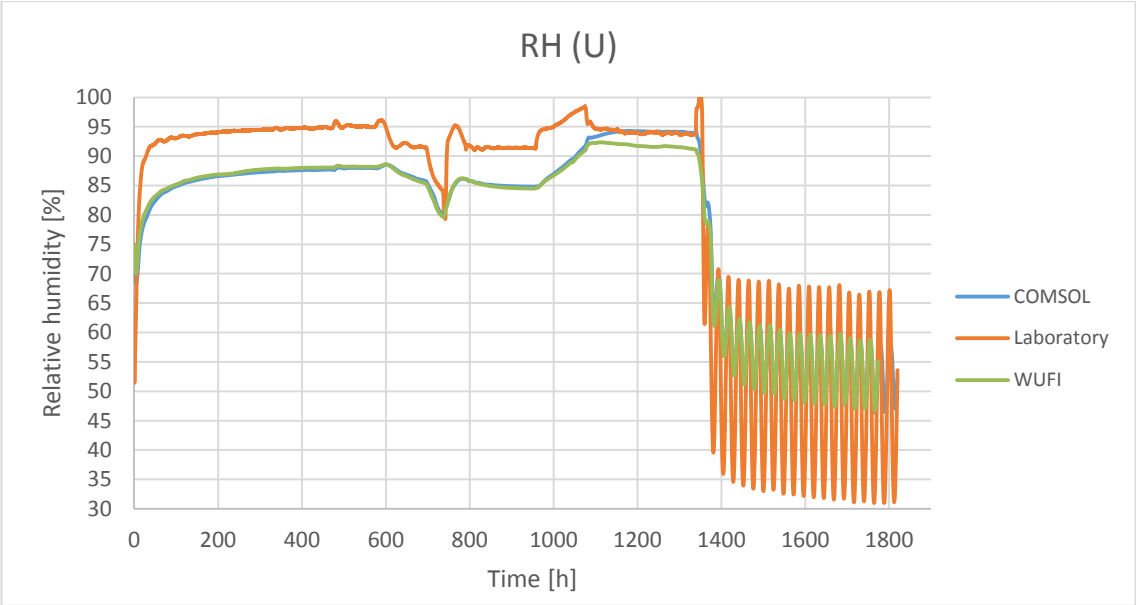

Figure 43: Comsol, WUFI and laboratory relative humidity at point U of the structure 4.

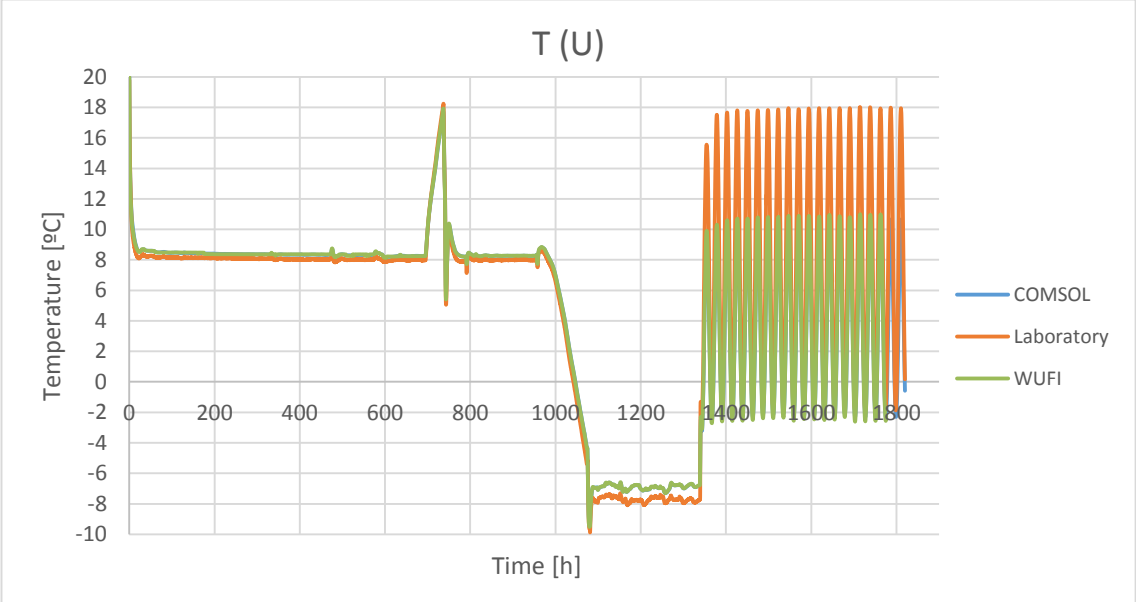

Figure 44: Comsol, WUFI and laboratory temperature at point U of the structure 4.

3.3.5 Results structure 5

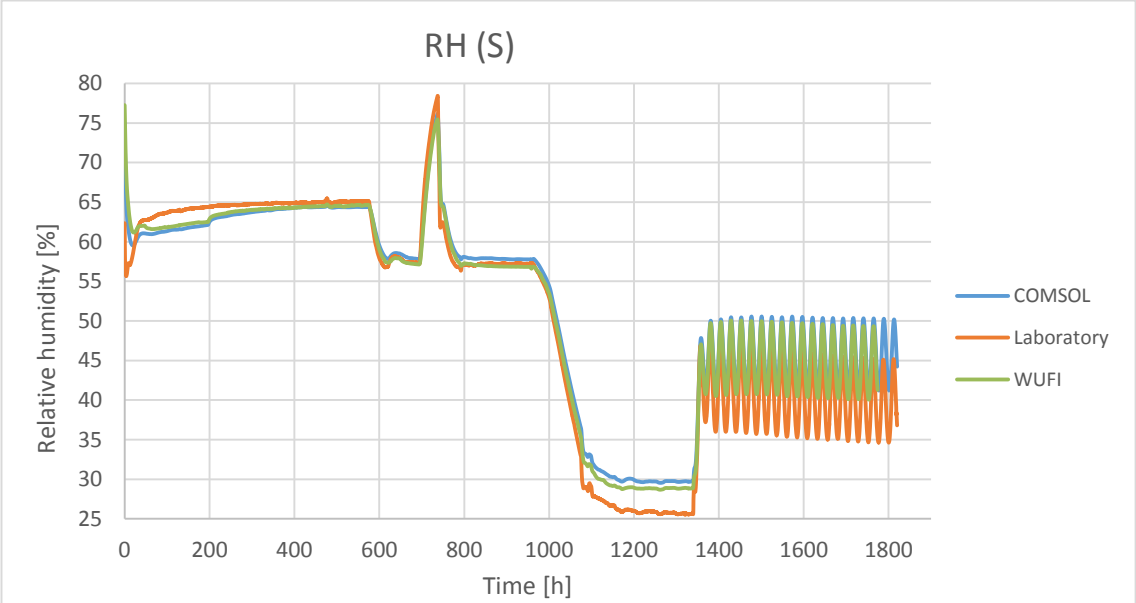

Figure 45: Comsol, WUFI and laboratory relative humidity at point S of the structure 5.

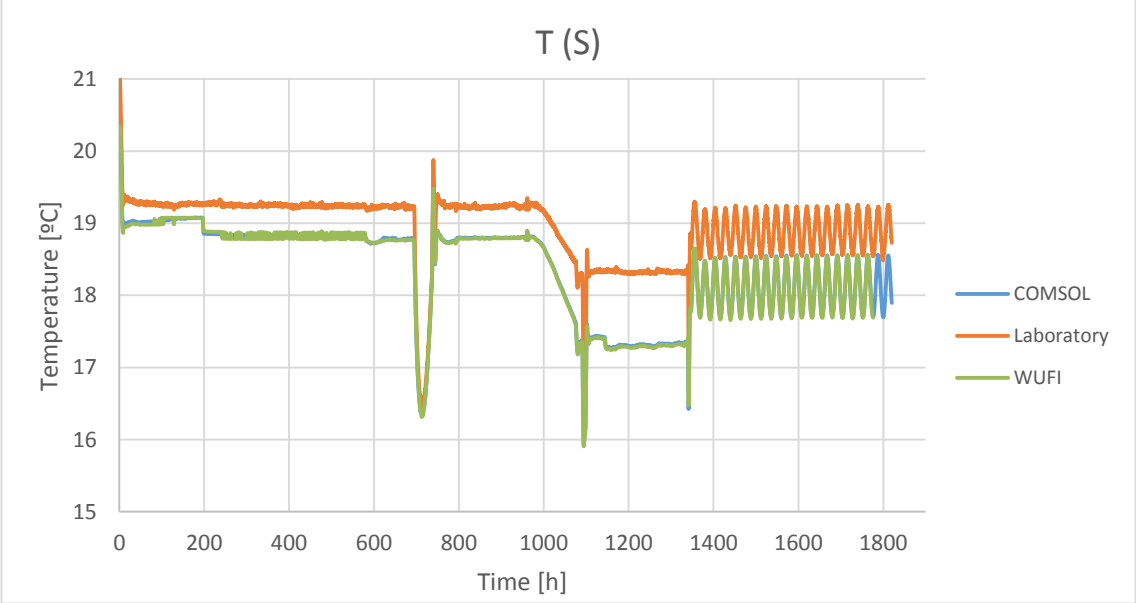

Figure 46: Comsol, WUFI and laboratory temperature at point S of the structure 5.

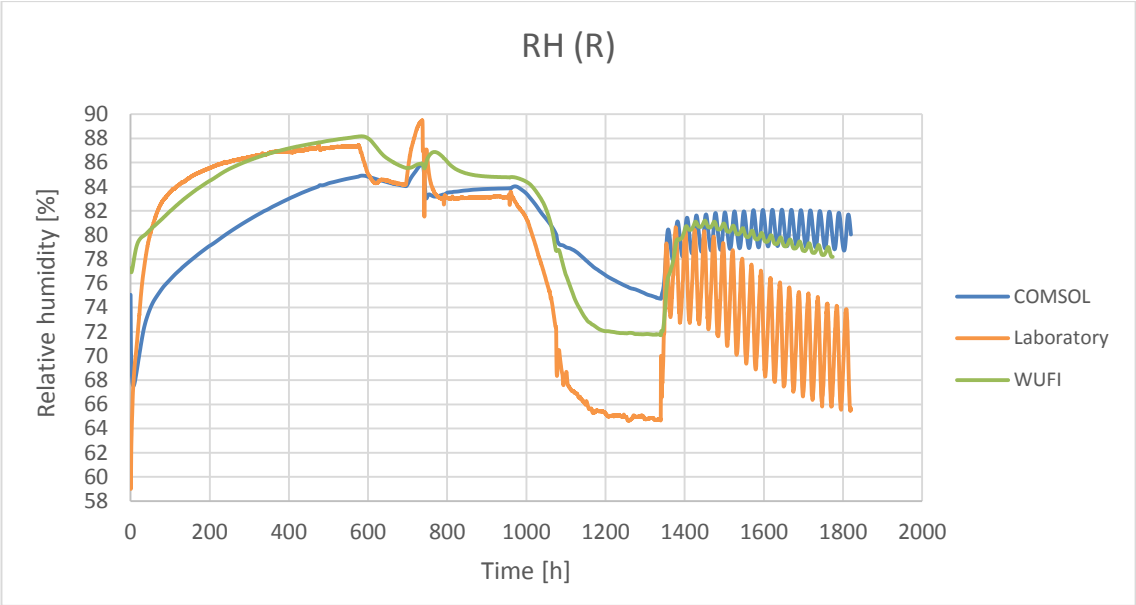

Figure 47: Comsol, WUFI and laboratory relative humidity at point R of the structure 5.

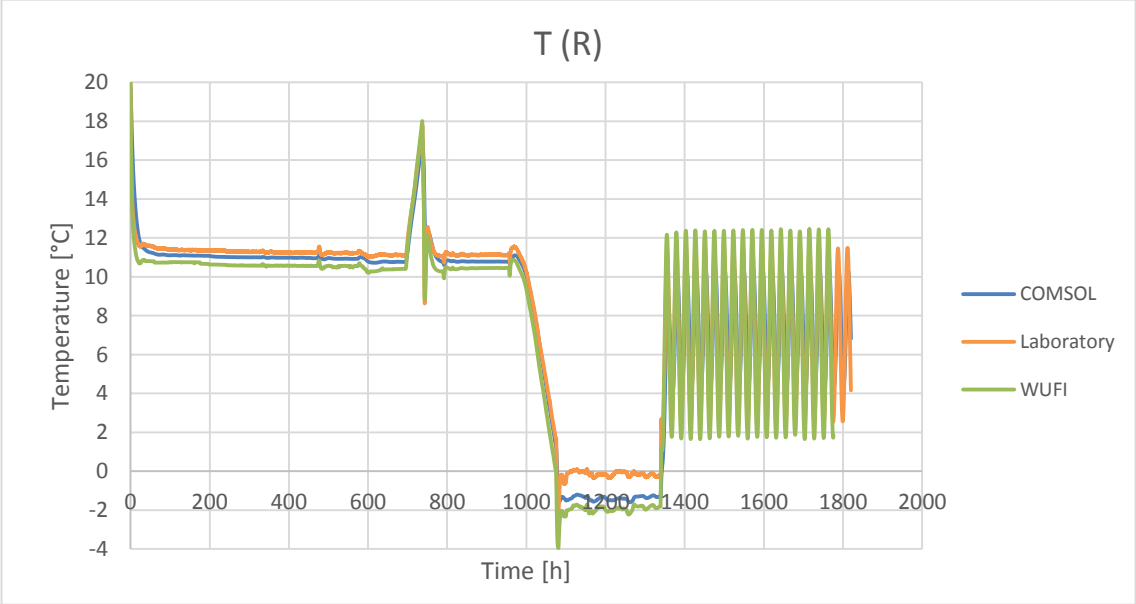

Figure 48: Comsol, WUFI and laboratory temperature at point R of the structure 5.

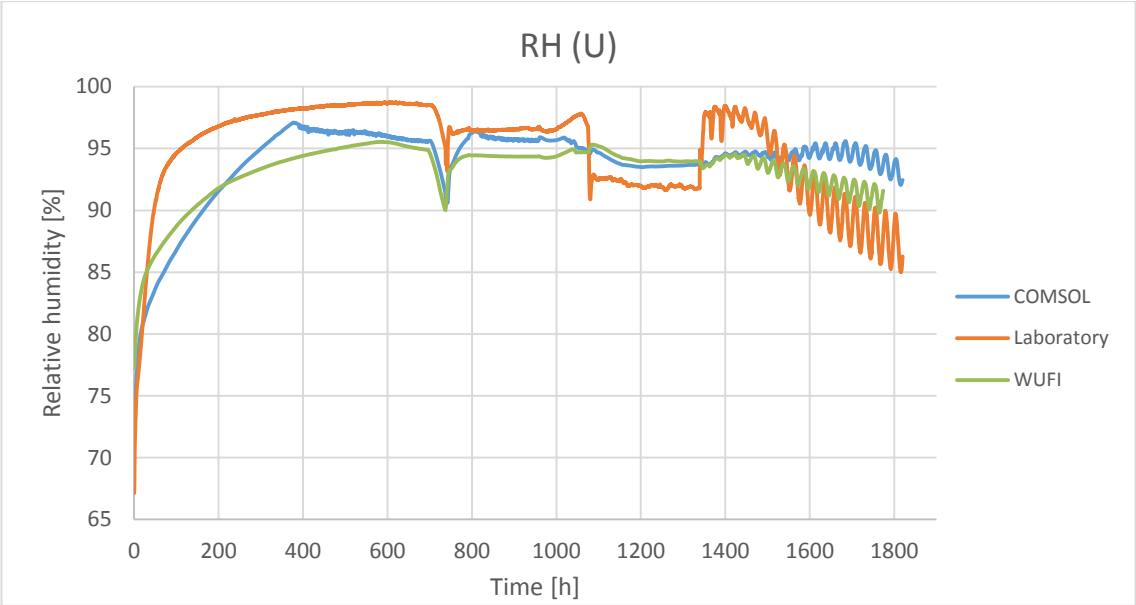

Figure 49: Comsol, WUFI and laboratory relative humidity at point U of the structure 5.

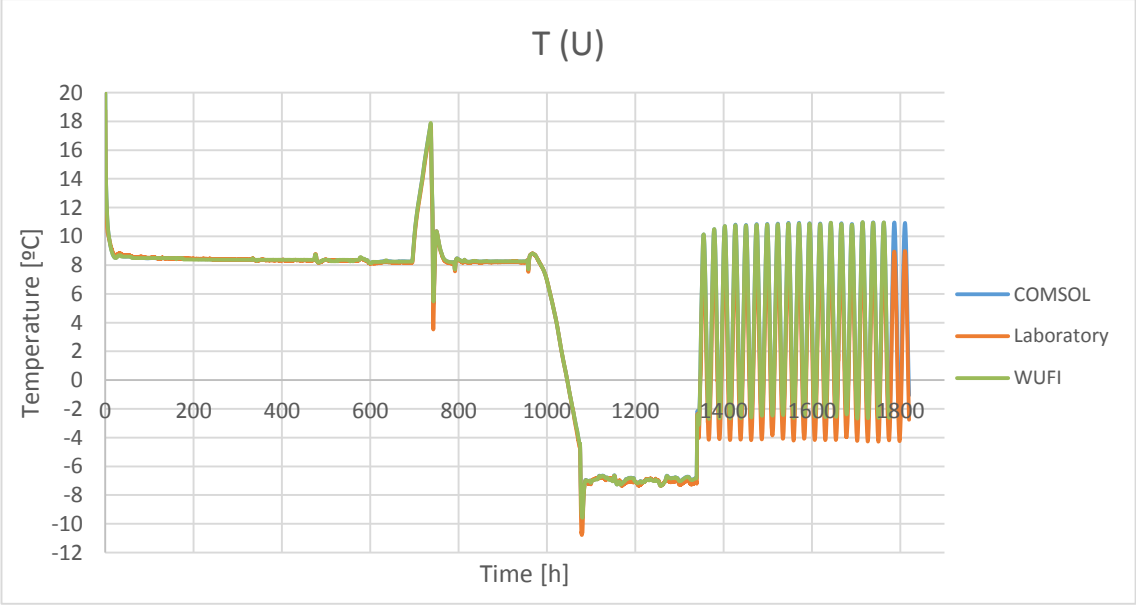

Figure 50: Comsol, WUFI and laboratory temperature at point U of the structure 5.

3.3.6 Results structure 6

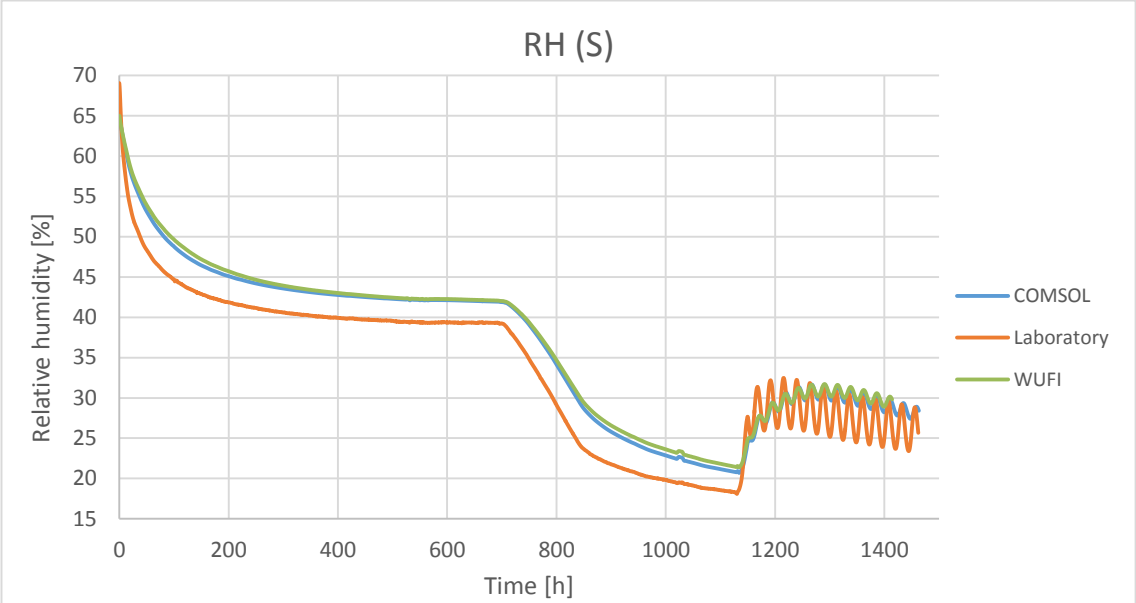

Figure 51: Comsol, WUFI and laboratory relative humidity at point S of the structure 6.

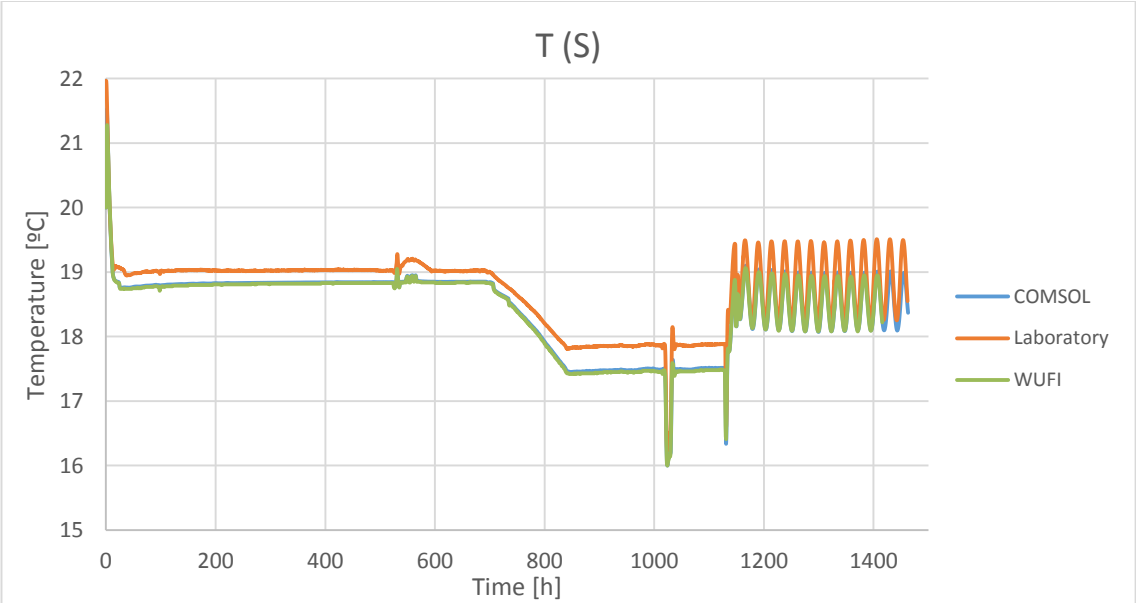

Figure 52: Comsol, WUFI and laboratory temperature at point S of the structure 6.

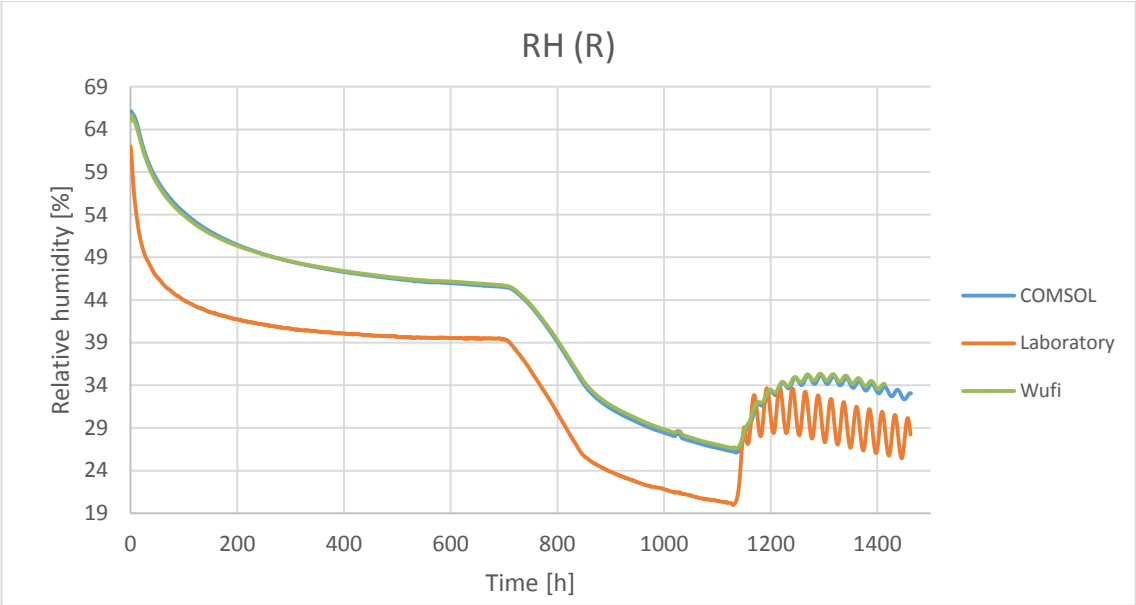

Figure 53: Comsol, WUFI and laboratory relative humidity at point R of the structure 6.

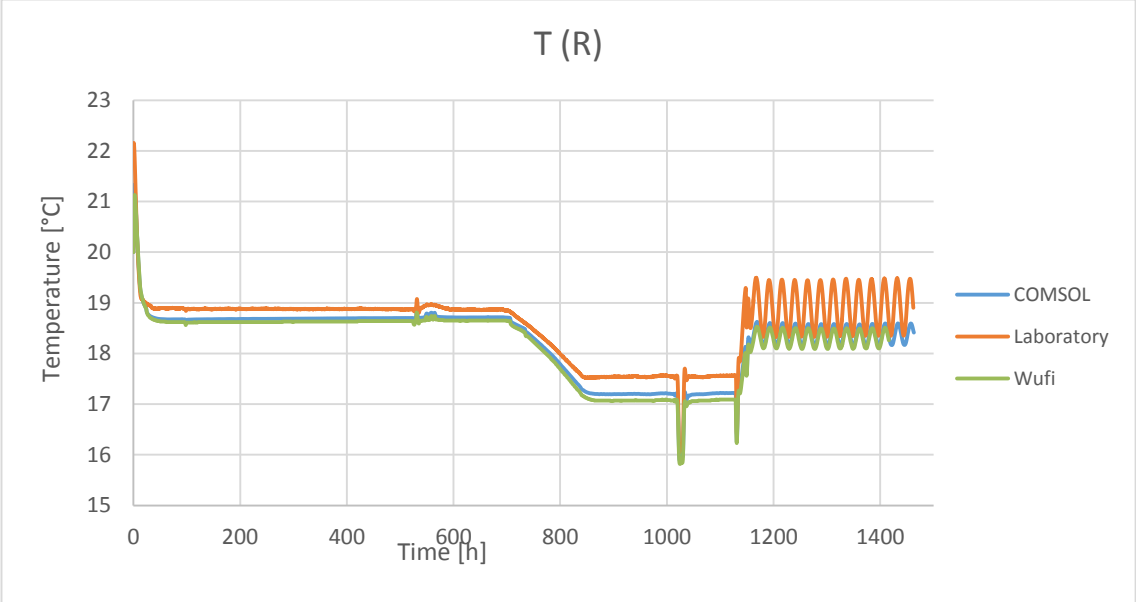

Figure 54: Comsol, WUFI and laboratory temperature at point R of the structure 6.

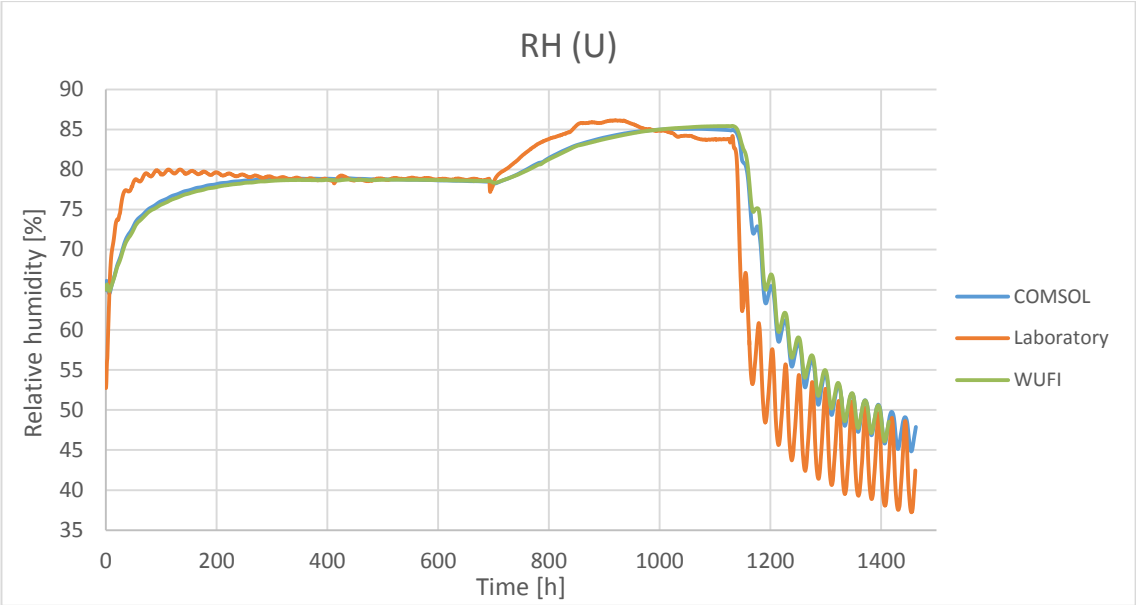

Figure 55: Comsol, WUFI and laboratory relative humidity at point U of the structure 6.

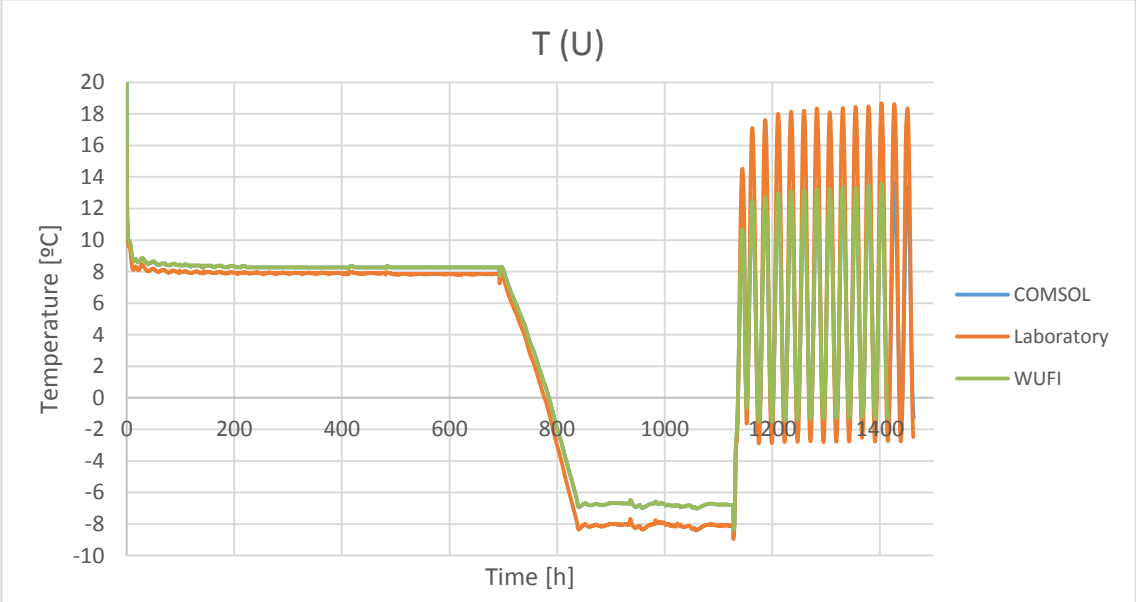

Figure 56: Comsol, WUFI and laboratory temperature at point U of the structure 6.

3.3.7 Results structure 7

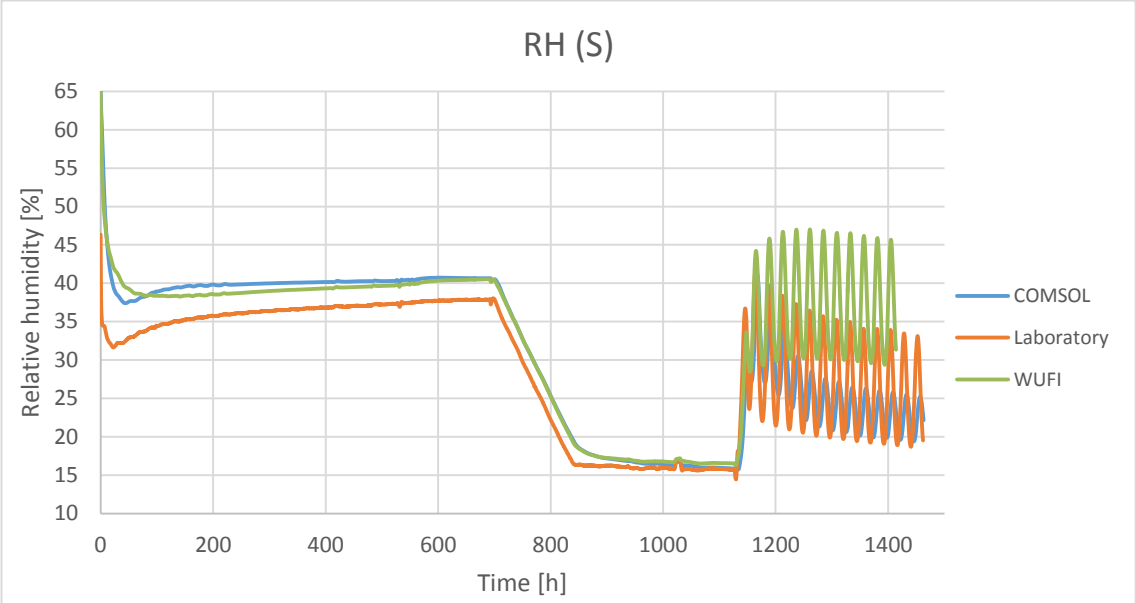

Figure 57: Comsol, WUFI and laboratory relative humidity at point S of the structure 7.

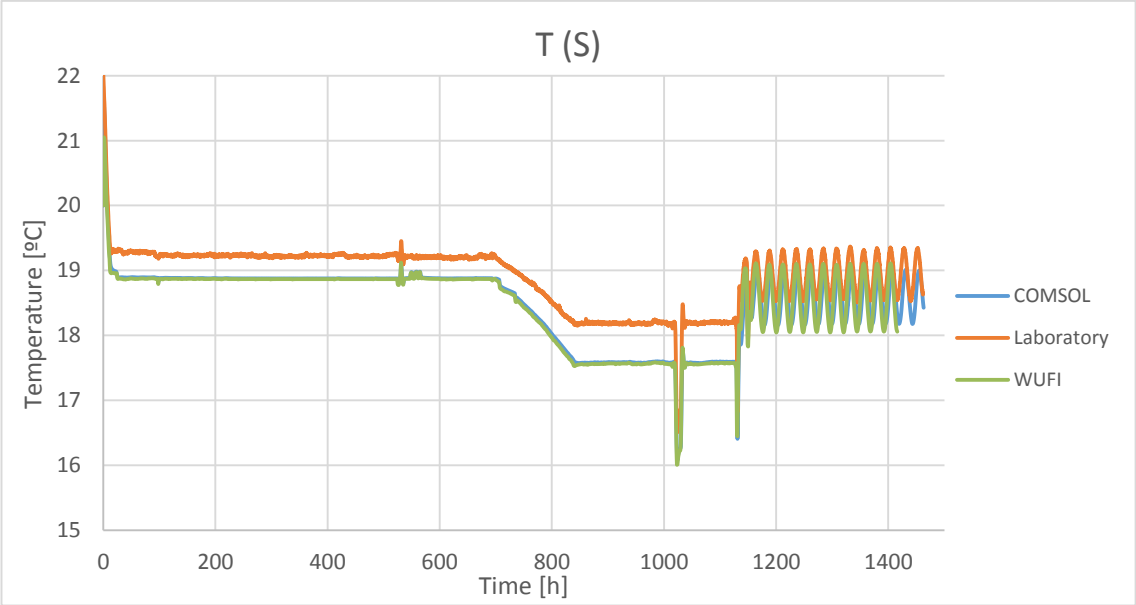

Figure 58: Comsol, WUFI and laboratory temperature at point S of the structure 7.

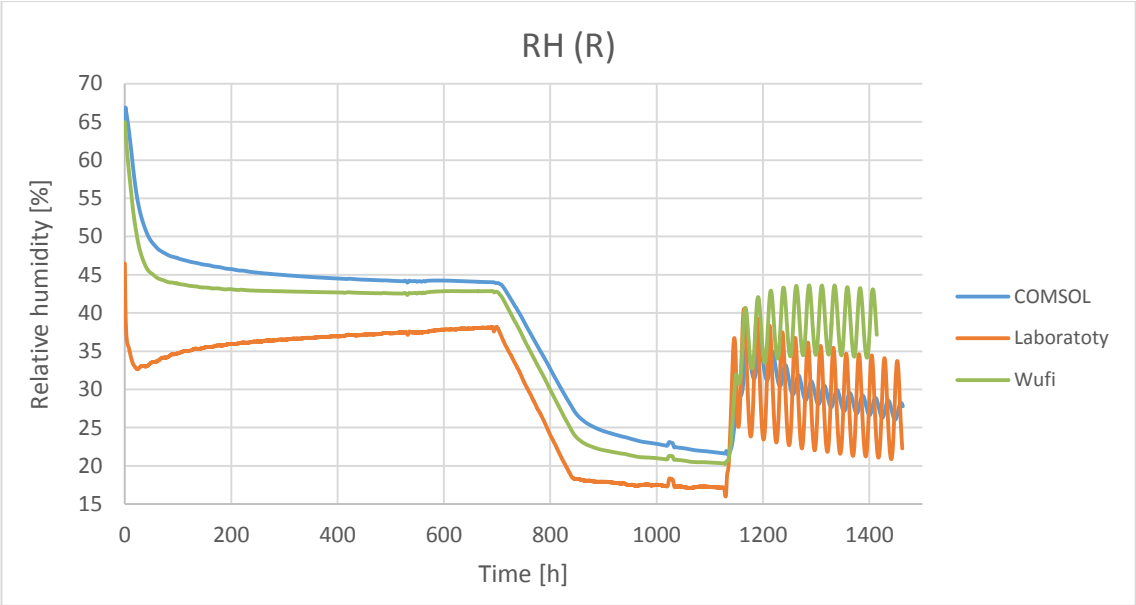

Figure 59: Comsol, WUFI and laboratory relative humidity at point R of the structure 7.

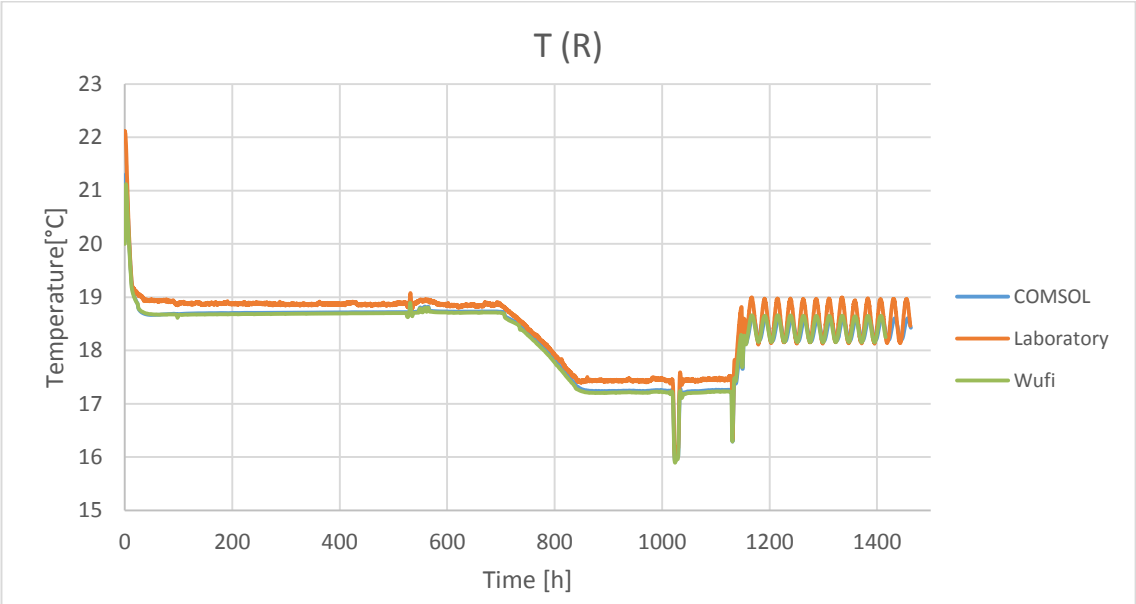

Figure 60: Comsol, WUFI and laboratory temperature at point R of the structure 7.

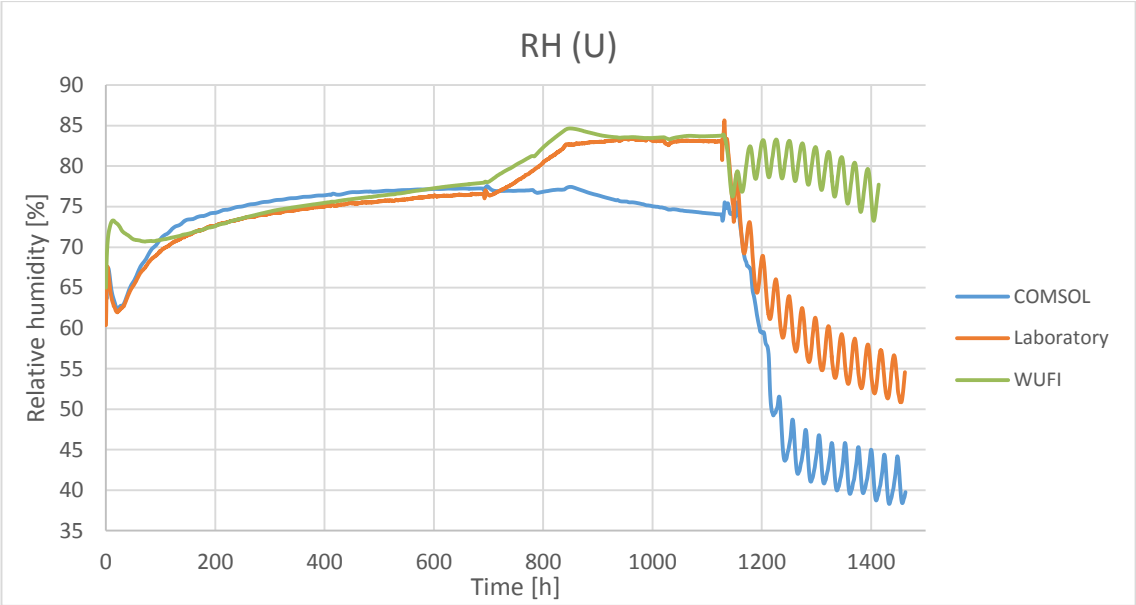

Figure 61: Comsol, WUFI and laboratory relative humidity at point U of the structure 7.

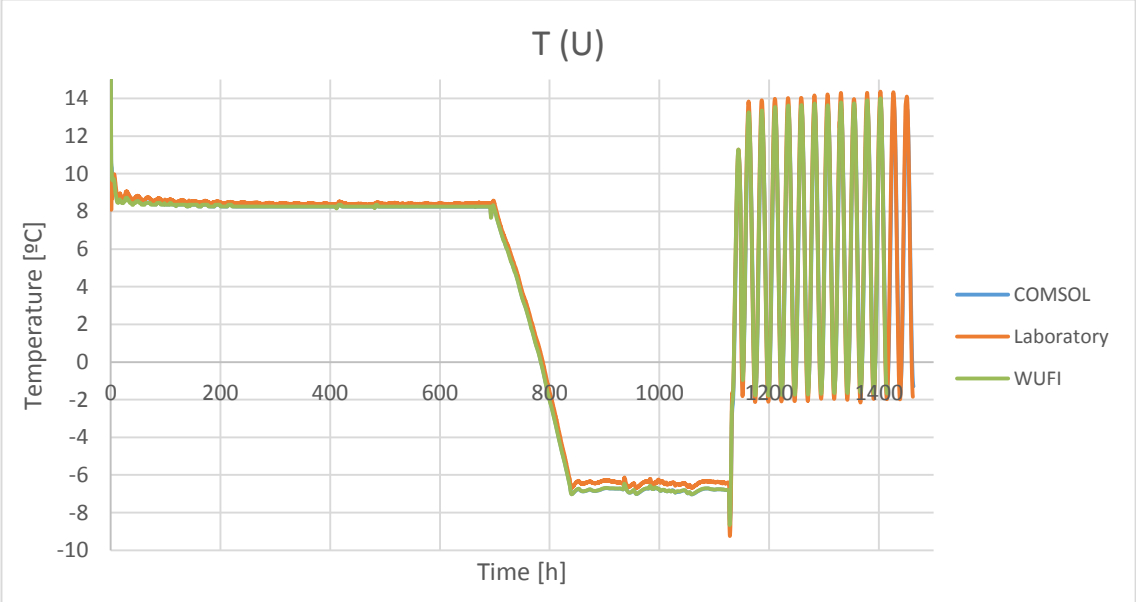

Figure 62: Comsol, WUFI and laboratory temperature at point U of the structure 7.

3.3.8 Results structure 8

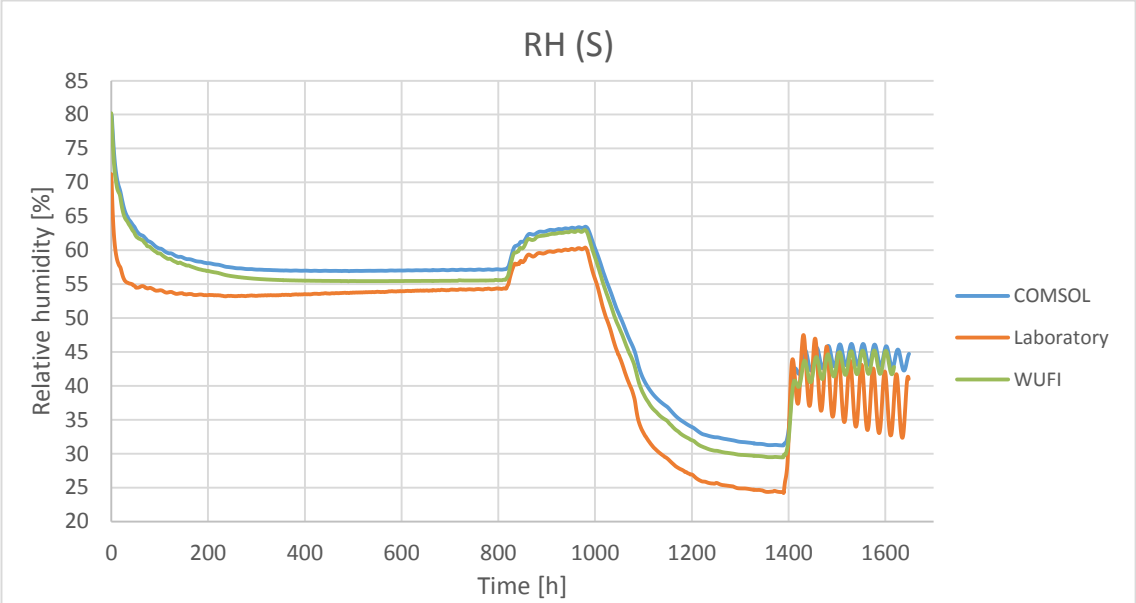

Figure 63: Comsol, WUFI and laboratory relative humidity at point S of the structure 8.

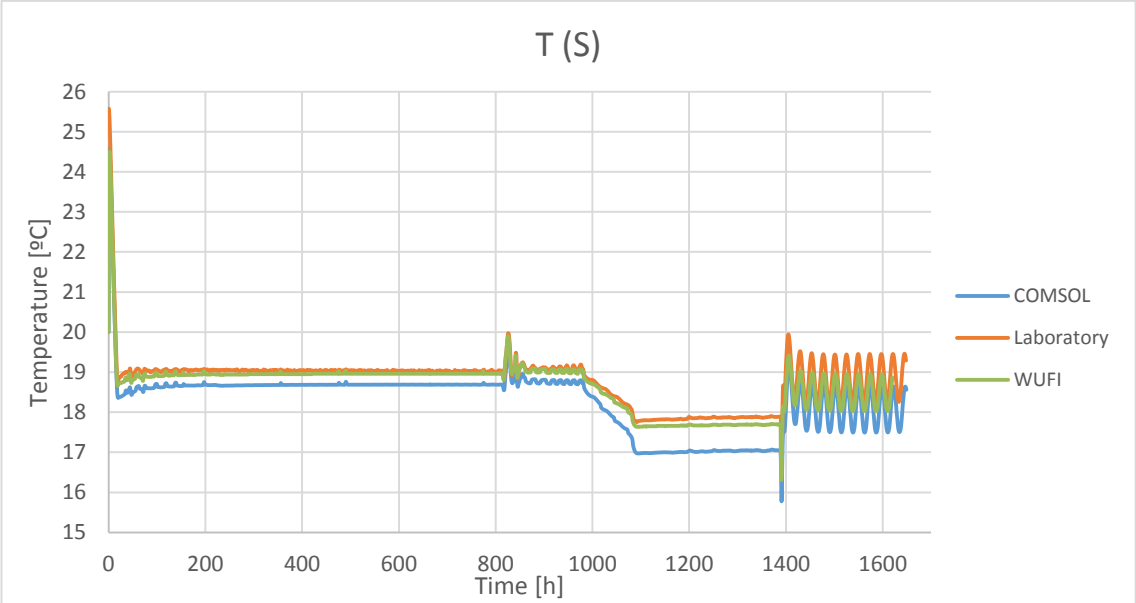

Figure 64: Comsol, WUFI and laboratory temperature at point S of the structure 8.

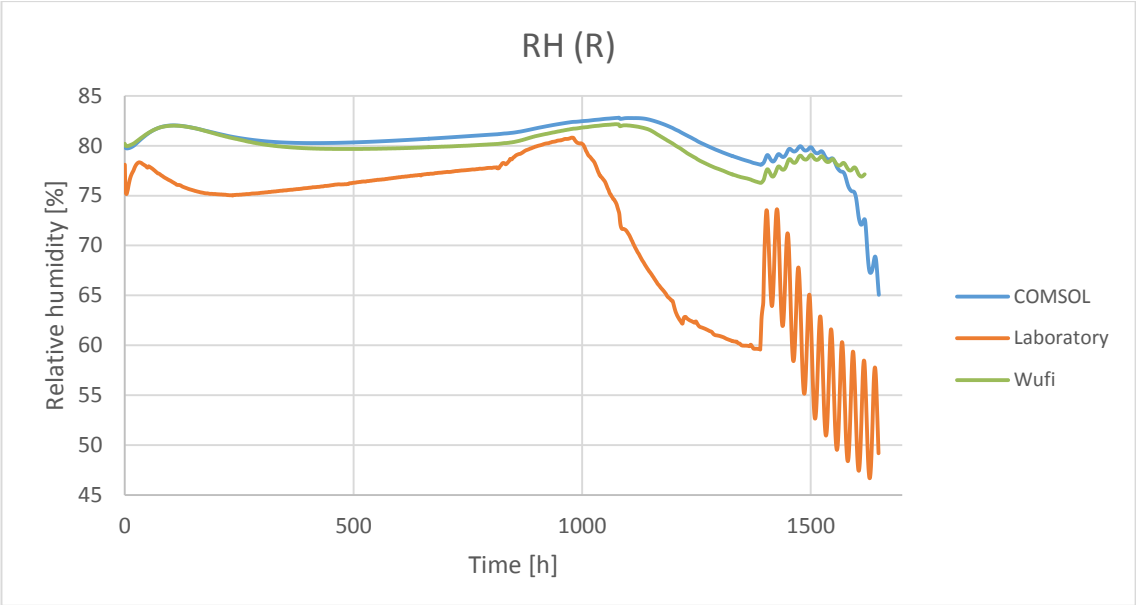

Figure 65: Comsol, WUFI and laboratory relative humidity at point R of the structure 8.

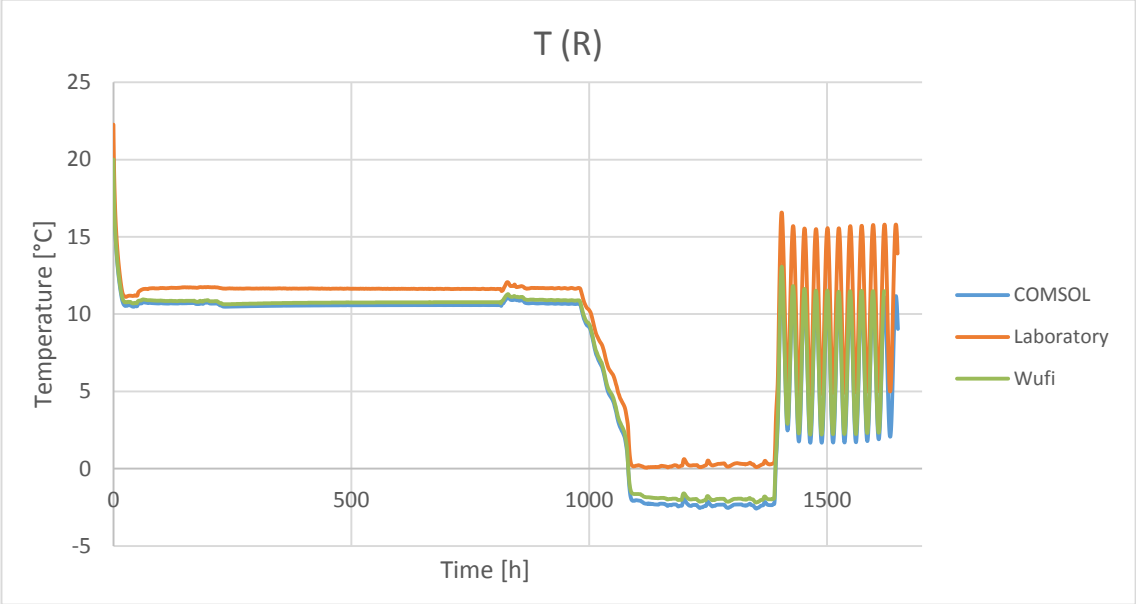

Figure 66: Comsol, WUFI and laboratory temperature at point R of the structure 8.

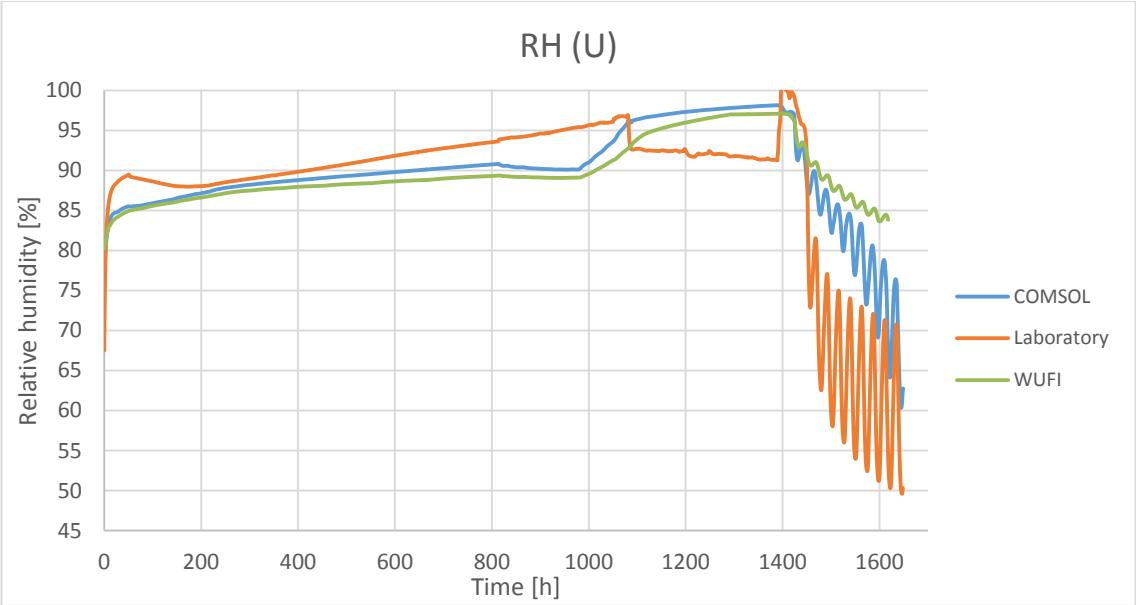

Figure 67: Comsol, WUFI and laboratory relative humidity at point U of the structure 8.

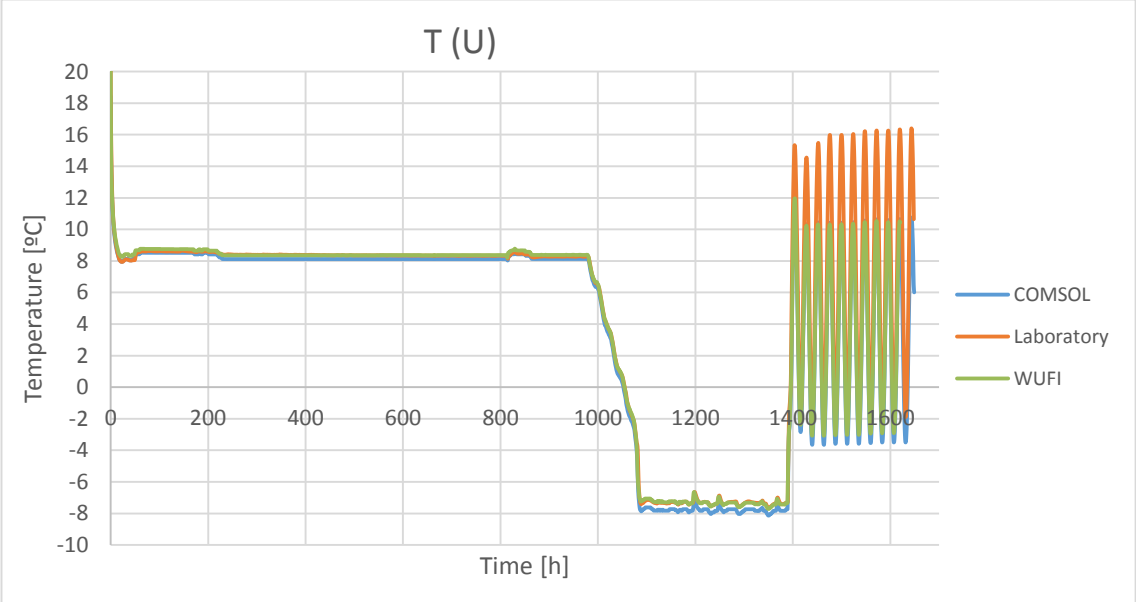

Figure 68: Comsol, WUFI and laboratory temperature at point U of the structure 8.

3.3.9 Results structure 9

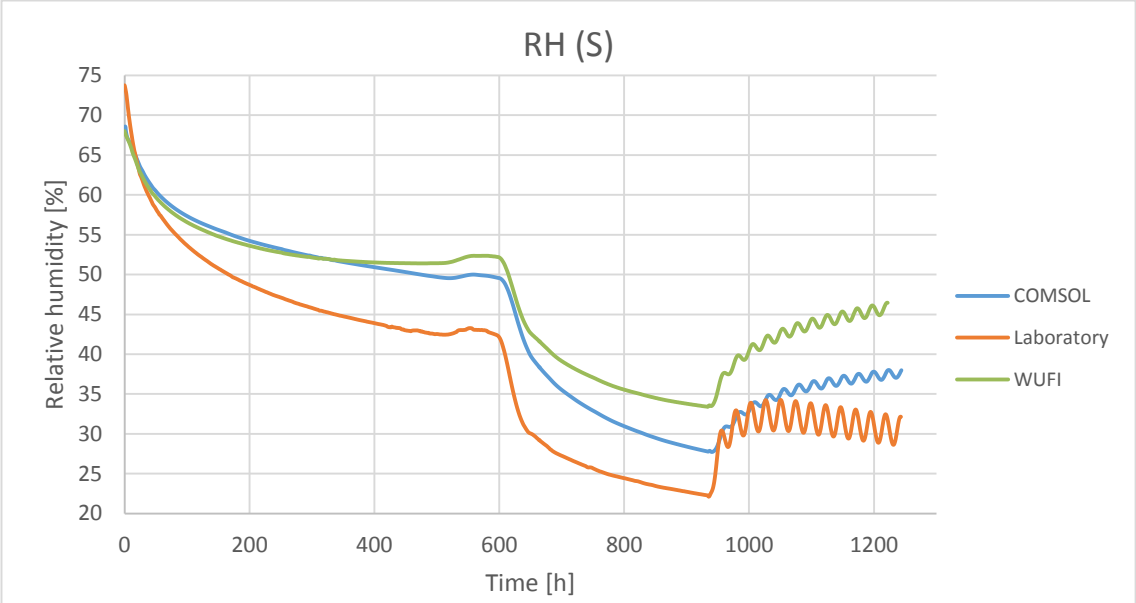

Figure 69: Comsol, WUFI and laboratory relative humidity at point S of the structure 9.

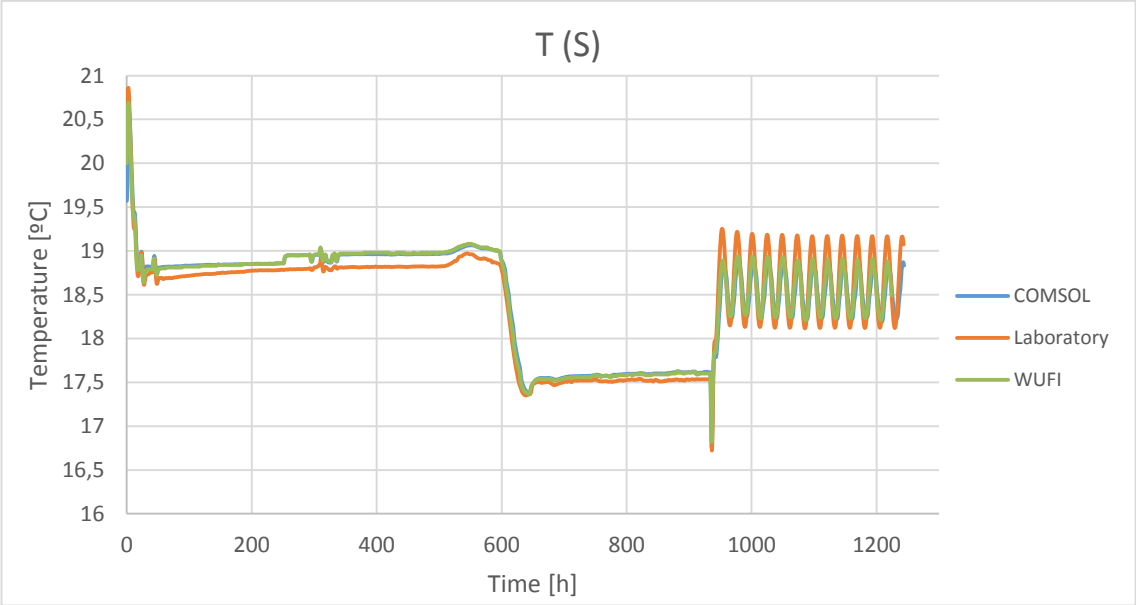

Figure 70: Comsol, WUFI and laboratory temperature at point S of the structure 9.

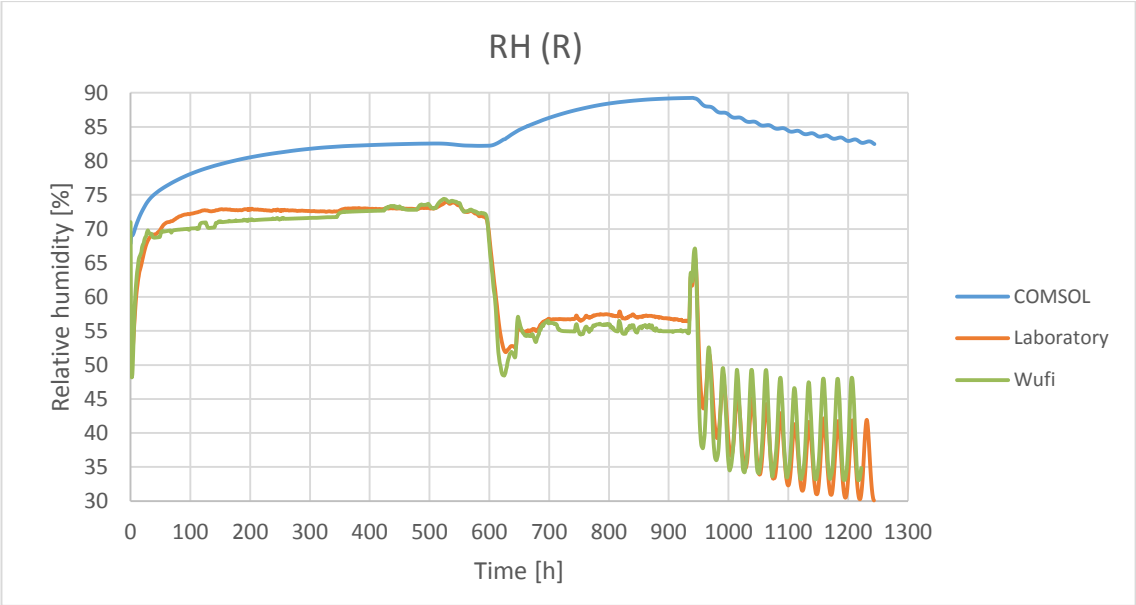

Figure 71: Comsol, WUFI and laboratory relative humidity at point R of the structure 9.

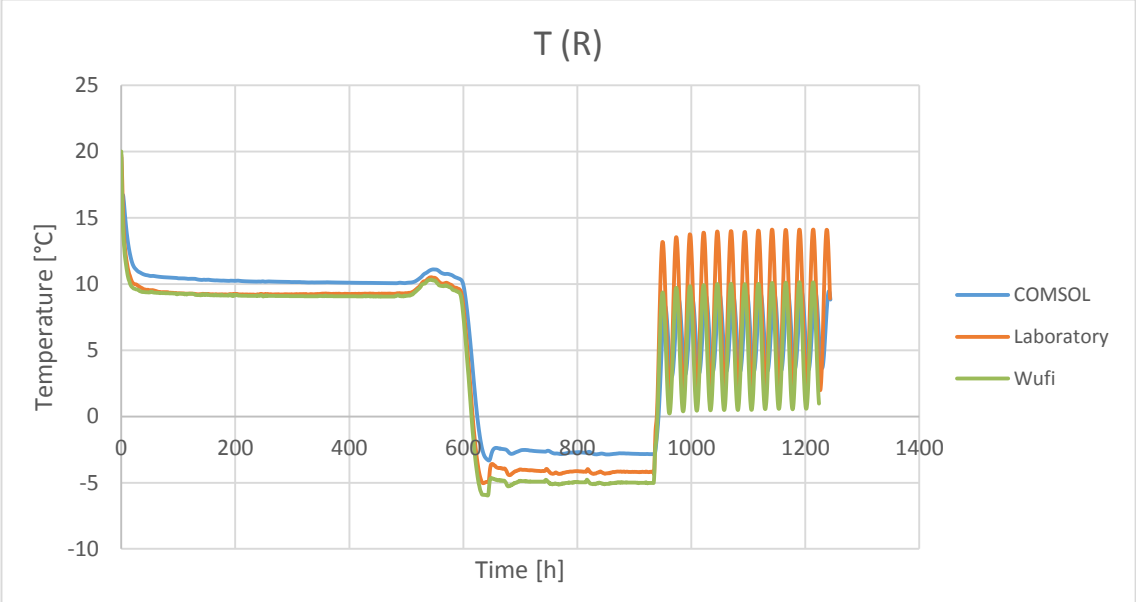

Figure 72: Comsol, WUFI and laboratory temperature at point R of the structure 9.

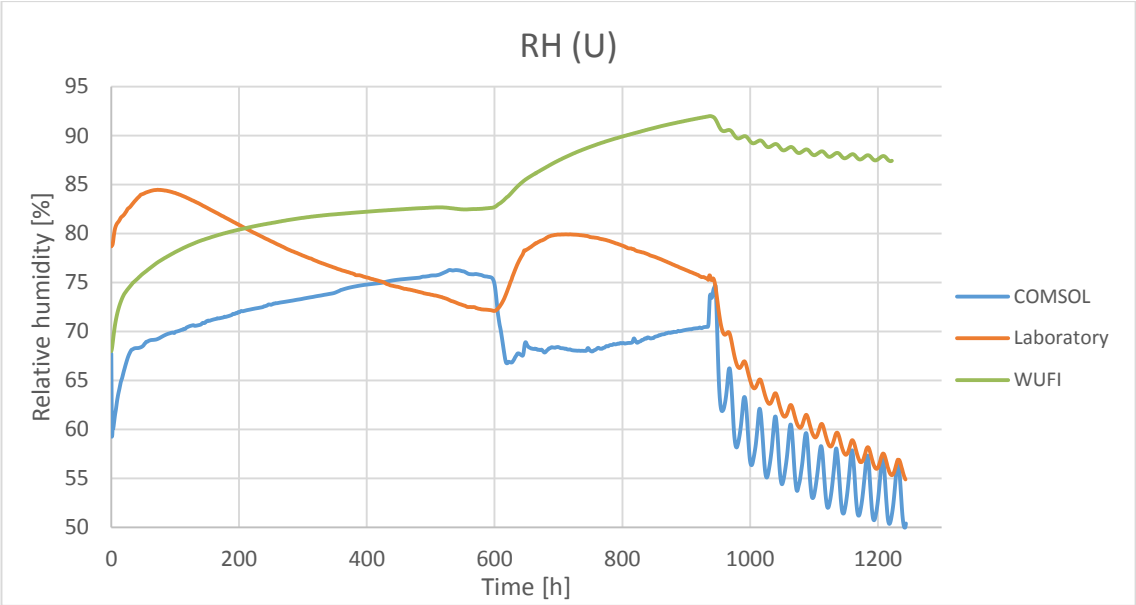

Figure 73: Comsol, WUFI and laboratory relative humidity at point U of the structure 9.

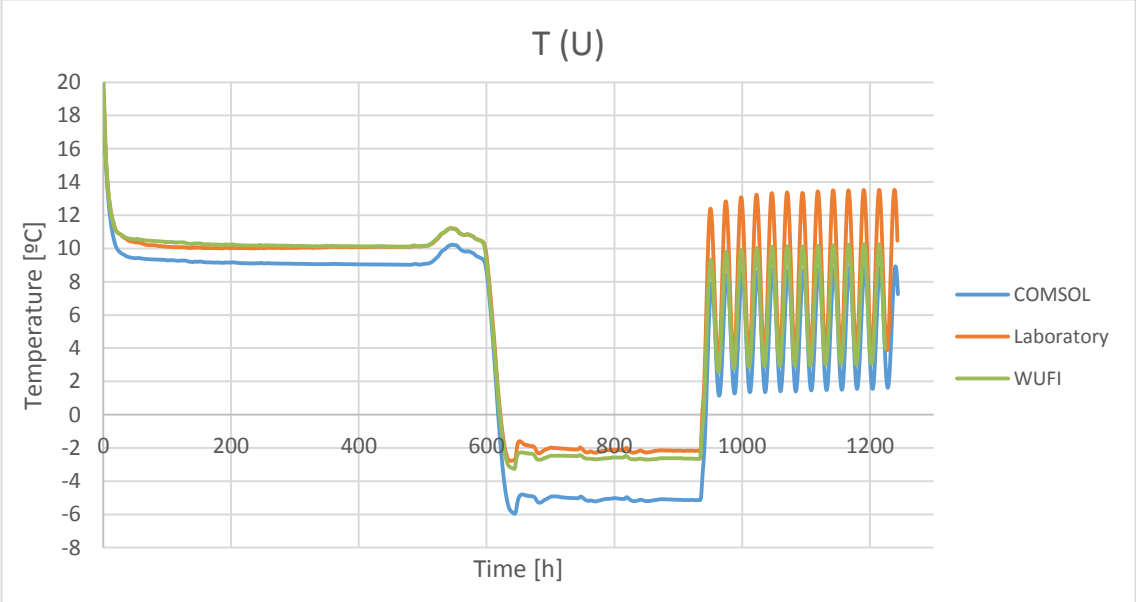

Figure 74: Comsol, WUFI and laboratory temperature at point U of the structure 9.

3.3.10 Results structure 10

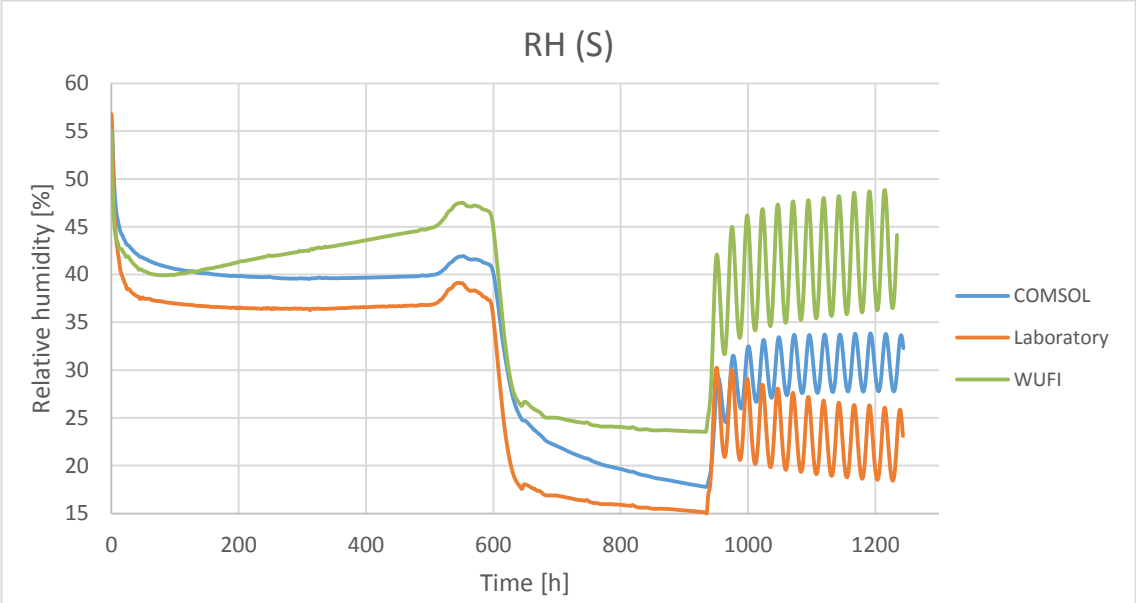

Figure 75: Comsol, WUFI and laboratory relative humidity at point S of the structure 10.

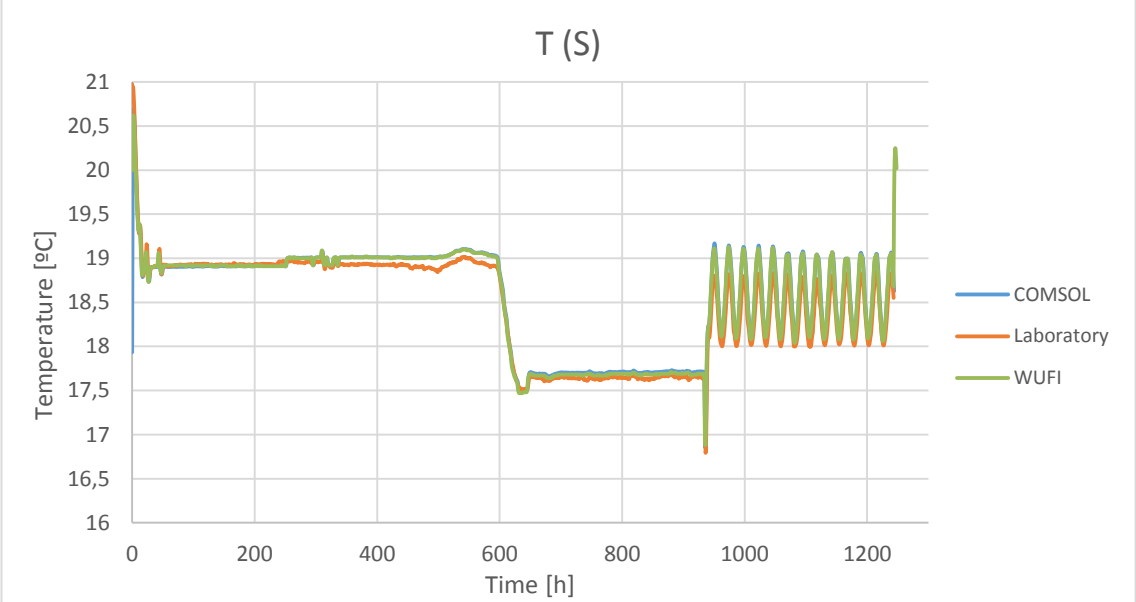

Figure 76: Comsol, WUFI and laboratory temperature at point S of the structure 10.

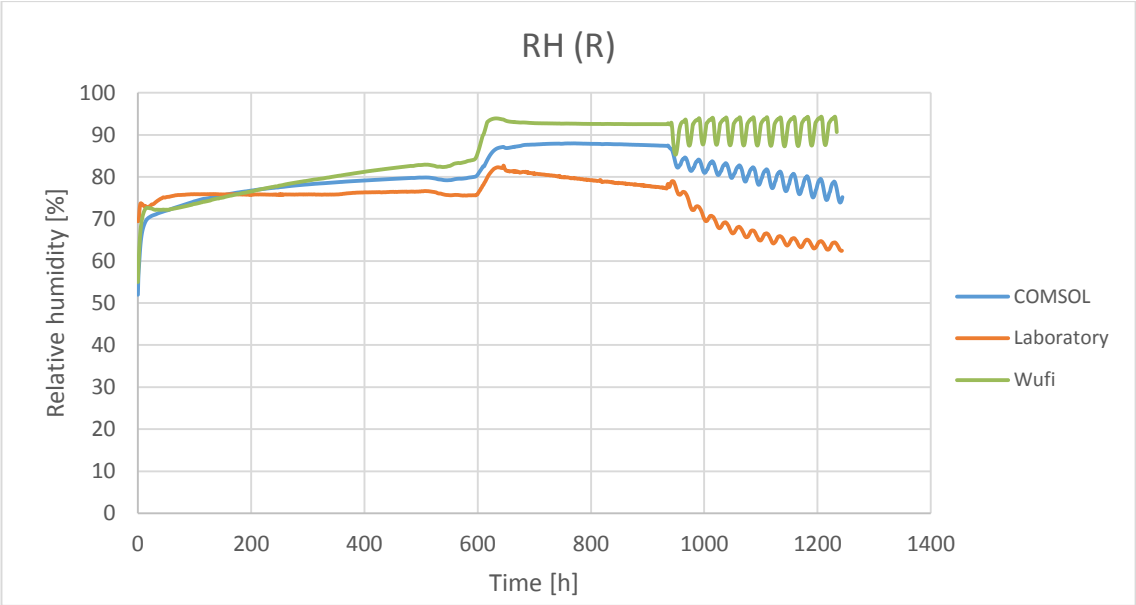

Figure 77: Comsol, WUFI and laboratory relative humidity at point R of the structure 10.

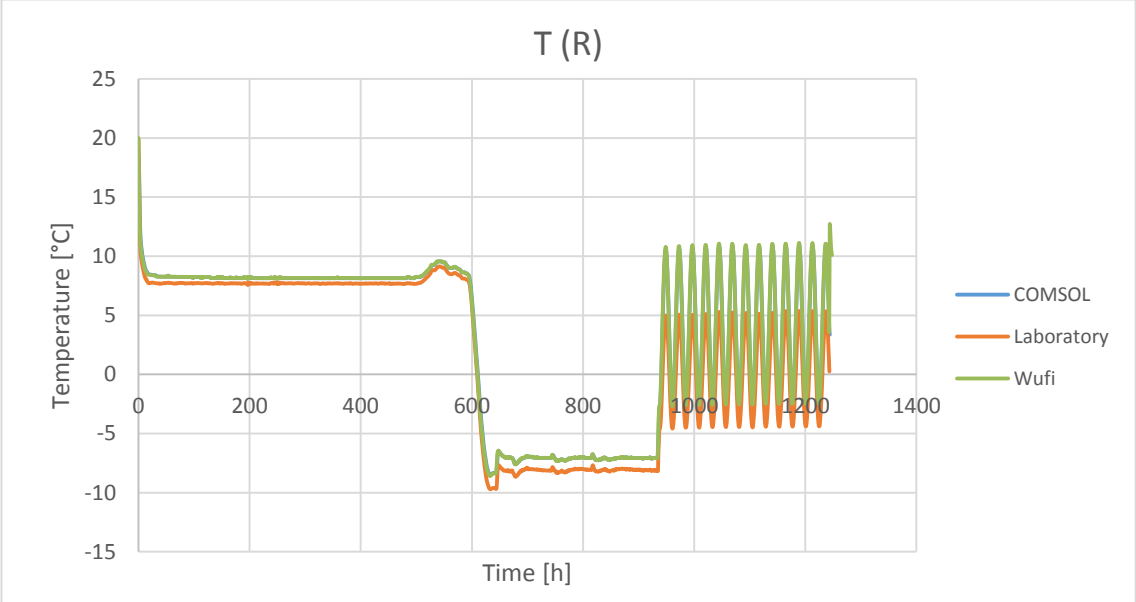

Figure 78: Comsol, WUFI and laboratory temperature at point R of the structure 10.

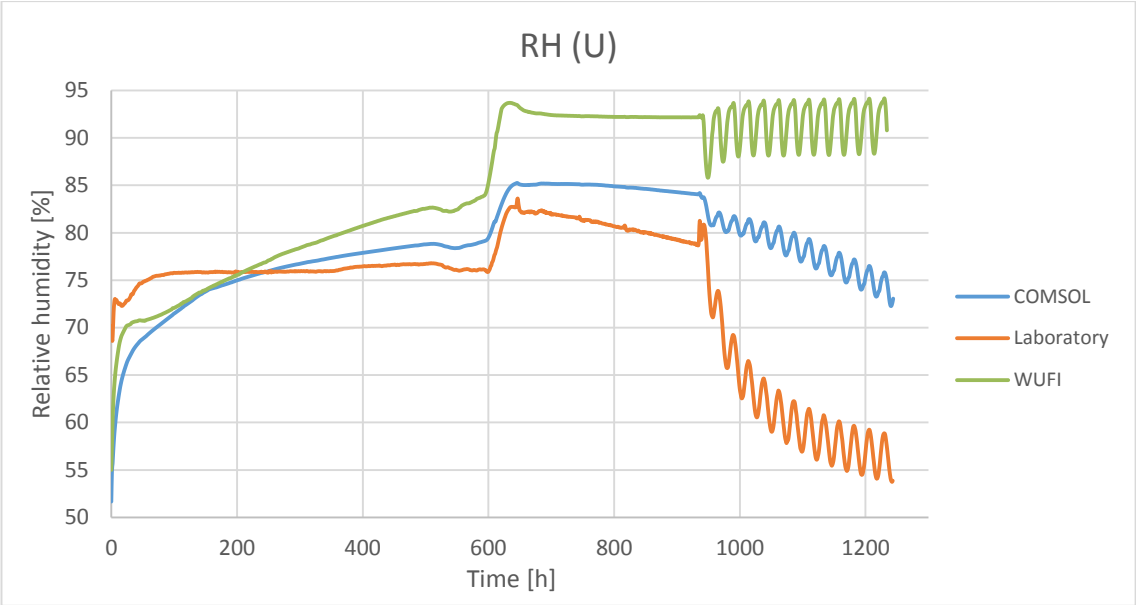

Figure 79: Comsol, WUFI and laboratory relative humidity at point U of the structure 10.

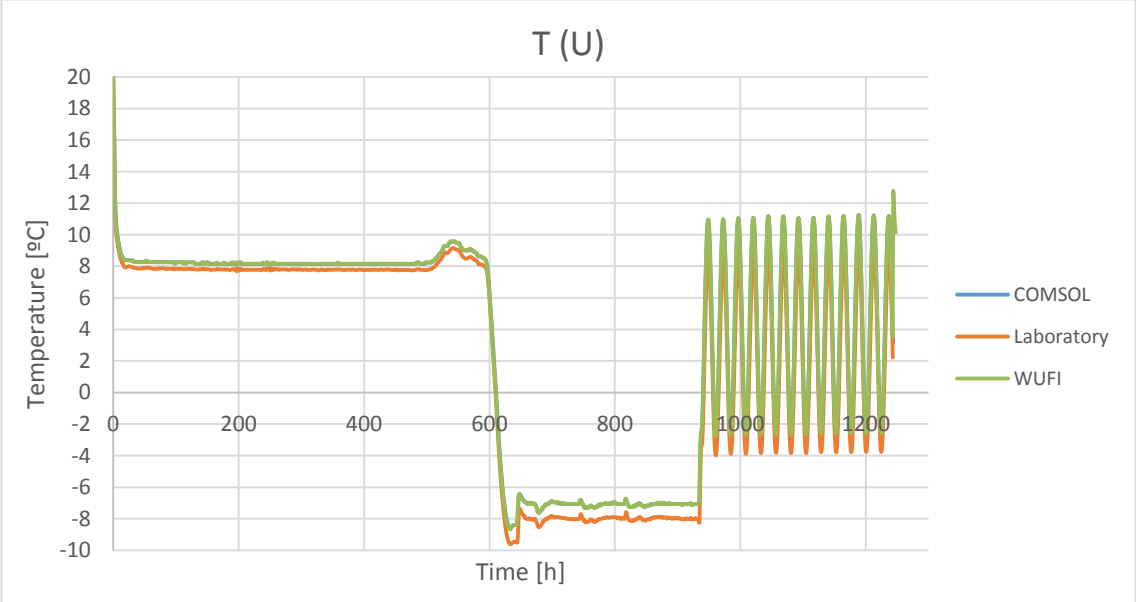

Figure 80: Comsol, WUFI and laboratory temperature at point U of the structure 10.

3.3.11 Results observations

The comparison graphs show differences between the curves from the three methods and the three sensors. By a general analysis of each graph, it is possible to observe that in the three sensors the temperature from Comsol matches with the WUFI's temperature and they have the same curve that the laboratory results in every structure. Nonetheless, the

relative humidities determined in the simulations from Comsol and WUFI do not share even the curve in most of the structures. In general, the relative humidity in Comsol's simulations is just better or equal than WUFI's.

The results of both temperature and relative humidity from Comsol and WUFI at sensor S match almost perfectly in every structure except for the numbers 7, 9 and 10. Moreover, the sensor whose results are closest to the laboratory results in both temperature and relative humidity is the point S.

The structures with closest results are the structures 1 and 6. The temperatures from Comsol and WUFI of these structures at the three sensors match and they almost match with the experimental results. The relative humidities from the three methods have the same curve and they are really close at every sensor. The structures with worst results are the structures 9 and 10. The temperatures from Comsol and WUFI match and they are close to the laboratory results, but the relative humidites from every method and at every sensor are different, they do not share the curve and they are not even close.

4. CONVECTION AND DIFFUSION MODELLING IN COMSOL

The second step consists of the simulation of heat, air and moisture transfer through Comsol. Therefore, another module will be included in order to simulate the air transfer. The structure changes and there are a singularity, a series of perforations.

4.1 Model description

The geometry utilised in this simulations represents a wall tested in the laboratory. The real wall is a composed wall containing several layers of different materials and it has a wooden frame which encloses the wall. The figure 81 contains the front and lateral views of the wall. Its dimensions are 1185 mm of height, 1185 mm of width and 224 mm of depth including the external wooden frame.

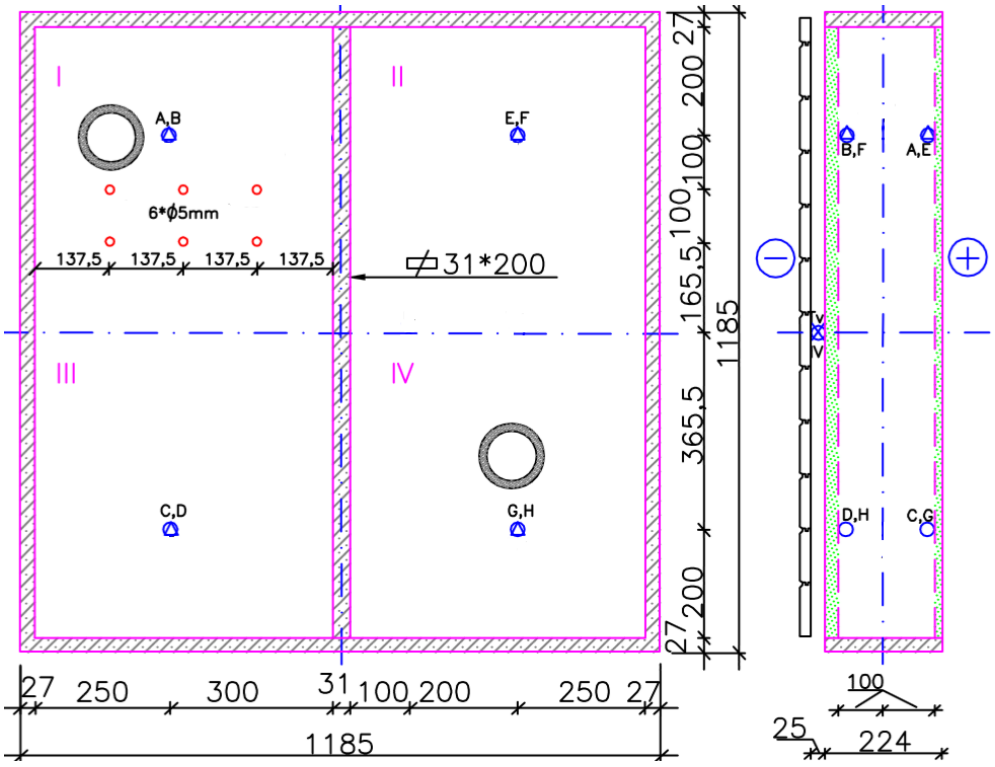

Figure 81: Views of the real test wall with the real measures. The sensors positions (A, B, C, D, E, F, G, H) can be appreciated.

It is possible to observe the layers arrangement and identify them:

1. Inner lining. Material: porous fibreboard (12 mm).
2. Insulation. Material: fiberglass (200 mm).
3. Sheathing. Material: porous fibreboard (12 mm).
4. Central frame. Material: pine (200 mm).

The model used in COMSOL is a 2D model which has some modifications regarding the real geometry. The right part of the wall has been skipped in the simulations in order to simplify as the aim is to analyse a perforated wall and the perforations appear only in the left part. Also, due to the complex calculations needed for this case, three more simplifications have been adopted. Firstly, the transferred flow will be studied in two dimensions instead of three. Secondly, due to the previous reason, the area which the air flow rate goes through changes from the six perforations to a couple of perforation rows whose height matches with the holes height (5 mm) and the width is a half wall (550 mm). Therefore, the geometry employed in the Comsol's simulation corresponds with the view side of the structure of the figure 81. The dimensions are 1131 mm of height and 224 mm of width.

The laboratory test was performed inside a box where the temperature and humidity were almost the same so in these simulations they will be considered constant. Those conditions stood for the interior and exterior of a building envelope, so in the COMSOL model the conditions were already established as well as the material properties in order to simulate the test. All of the constant properties are summarized in the table 6, where the surface relative humidities have been calculated in the same way that they were in the section 3.2. The necessary variables in each module, such as the vapour pressure or the vapour permeability, and the material properties needed are detailed in the appendix 1.

Table 6

Name		Expression	Description
General	COMSOL		
T_i	T_in	292.13 [K]	Interior surface temperature
T_e	T_out	264.56 [K]	Exterior surface temperature
h_i	hi	7 [W/(m^2*K)]	Interior heat transfer coefficient
h_e	he	25 [W/(m^2*K)]	Exterior heat transfer coefficient
H_v	hv	2260000 [J/kg]	Heat of vaporization
RH_i	RH_in	0.5	Interior relative humidity
RH_e	RH_out	0.9	Exterior relative humidity
R_w	R	8.314 [J/(mol*K)]	Universal gas constant
M_w	Mw	0.018 [kg/mol]	Molar mass of water

4.2 Heat, air and moisture transfer

The aim of this section is to inspect the suitability and accuracy of COMSOL in modelling combined heat, air and moisture transfer in building physical applications. Therefore, the model simulates a laboratory test. In this test, the wall was subjected to a three different phases where the conditions were different:

I. The first phase is the depressurization phase and it elapses in the first 298 hours. The pressure in the interior side (-10 Pa) is lower than the pressure outside (0 Pa), so the air flow rate throughout the perforation area is negative, $R_a = -5.84\ \left(\frac{\text{l}}{\text{min}}\right) = -9.73 \cdot 10^{-5}\ \left(\frac{m^3}{\text{s}}\right)$ which means that the flow rate direction is from the exterior to the interior.

II. The second phase is the no pressurized phase which covers the range from 298 hours to 555 hours. Therefore, there is only heat and moisture transfer, the air transfer is neglected.

III. The third phase is the overpressure phase which elapses from 555 hours until 786 hours, the end. In this period, the inside pressure (10 Pa) is greater than the outside one (0 Pa). Hence, the air flow rate is positive, $R_a = 6.77\ \left(\frac{\text{l}}{\text{min}}\right) = 1.13 \cdot 10^{-4}\left(\frac{m^3}{\text{s}}\right)$ regarding the direction from inside to outside.

4.2.1 Air transfer

The air flow was simulated with the "Fluid Flow" module and particularly using the domain setting "Free and Porous Media Flow". This represents the best option within the interface "Porous Media and Surface Flow" for this type of wall due to the materials used and the boundary conditions taken into account.

The domains included in this module are only the insulation and the sheathing. The interior lining is not included because the flow leaks into the wall through the perforations and it crosses the insulation and sheathing but it does not affect the interior lining.

The porous media flow is usually controlled by Darcy's law but in this case there are perforations, so Brinkman equations are applied in the porous media, as a transition between N-S equations and Darcy's law, due to the necessity of including the viscous effects:

$$\frac{\rho}{\epsilon_p}\left((\boldsymbol{u}\cdot\nabla)\frac{\boldsymbol{u}}{\epsilon_p}\right) = \nabla\cdot\left[-p\boldsymbol{I} + \frac{\mu}{\epsilon_p}(\nabla\mathbf{u} + (\nabla\mathbf{u})^T) - \frac{2\mu}{3\epsilon_p}(\nabla\mathbf{u})\boldsymbol{I}\right] - \left(\frac{\mu}{\kappa_{br}}\right)\boldsymbol{u} + \boldsymbol{F} \qquad (4.1)$$

$$\rho\nabla\cdot\boldsymbol{u} = 0$$

- κ_{br}: permeability of the material [m^2].
- $\epsilon_{p:}$ porosity of the material [-].

Four dependent variables are calculated in this interface: the three components of the velocity field (**u**): *u*, *v* and *w* and the pressure (p). The equation (4.1) is in vector form, where transpose has been used.

The default domain setting in this interface is "Fluid properties", where it is employed the equation (4.1) due to the utilisation of the porous matrix properties. In its setting window, the model data and the fluid properties are established; the temperature required is the result of the other module calculations, the pressure need to be input and the fluid properties (density and dynamic viscosity) are defined by the material already selected in Comsol (the air).

It is needed to define the properties of layer materials, as done in the previous section with the Mathemathics module. The node for that is called "Porous Matrix Properties" and it is governed by the equation (4.1). This node will be added as many times as different materials there are and the features which need to be input are the porosity (ϵ_p) and the permeability (κ_{br}).

Regarding the boundary conditions, the "Wall" and "Initial values" are default conditions. In the case studied, the option chosen is **no slip**, which means that the fluid at the selected surface does not move (**u**=0), and it is applied to all the geometry elements except the perforations area and the outside surface.

The pressure and the velocity field at the beginning of the simulation are considered the initial values in this occasion. Both conditions are constant in the whole domain at the beginning: the initial velocity field are u=0, v=0 and w=0, and the pressure is 0 atm.

Two more boundary conditions are needed in order to describe the restrictions at the interior and exterior sides of the wall, the perforation area and at the inside surface. That function is fulfilled by "Inlet" and "Outlet" options (COMSOL 2012). Both settings have different ways through which setting the restrictions: velocity, pressure, laminar inflow, normal stress or mass flow. The boundary conditions will depend on the phase of the test which is being simulated.

In the first phase, according to its specifications which have been previously set, the option chosen to set the "Inlet" condition is the pressure (0 Pa) at the outside surface. The

"Outlet" condition is defined by the velocity at the perforation area. This velocity follows from the air flow rate by this equation:

$$R_a = \boldsymbol{u} \cdot A \tag{4.2}$$

- R_a: air flow rate [m^3/s].
- **u:** velocity [m/s].
- A: area through which the air flows [m^2].

In this case, taking into account the air flow rate in the depressurization phase and the perforation area of each row (2 x 5 x 550 mm), the input velocity is **u** = $1.77 \cdot 10^{-2}$ m/s.

Moreover, the "Inlet" option, according to the direction of the third phase flow, is the velocity whose value is u = $2.05 \cdot 10^{-2}$ m/s, by the equation (4.2), applied at the perforation area. The "Outlet" option is established by the pressure (0 Pa) at the outside surface.

4.2.2 Heat and moisture transfer

This transfer is simulated by the PDE interface and particularly the "Coefficient form PDE" node, as have been explained in the section 3.2. The equation which controls this transfer is the equation (3.1). The addition of capillarity was considered but it took a great amount of memory which slowed the computation and it did not have a significant effect so it was neglected finally. There is a new term, the convection coefficient β, which relates the heat and moisture transfer with the air transfer. Therefore, the equation in this case is the following:

$$d_a \frac{\partial \boldsymbol{u}}{\partial t} + \nabla \cdot (-c\nabla \boldsymbol{u}) + \beta \cdot \nabla \boldsymbol{u} = 0 \tag{4.3}$$

where **u** is the field vector whose components are the temperature and the relative humidity. The damp or mass coefficient and the diffusion coefficient have been exposed in the equations (3.3) and (3.4) and the convective term is expressed as:

$$\beta \nabla \boldsymbol{u} = \begin{bmatrix} \beta_{T,T} & \beta_{T,RH} \\ \beta_{RH,T} & \beta_{RH,RH} \end{bmatrix} \cdot \begin{bmatrix} \nabla T \\ \nabla RH \end{bmatrix} = \begin{bmatrix} \begin{bmatrix} u \cdot \dfrac{R_{air}}{C_{p,air}\, T} p_{atm} \\ v \cdot \dfrac{R_{air}}{C_{p,air}\, T} p_{atm} \end{bmatrix} & \begin{bmatrix} 0 \\ 0 \end{bmatrix} \\ \begin{bmatrix} u \cdot \dfrac{RH \cdot M_w}{RT} \dfrac{dp_{vsat}}{dt} \\ v \cdot \dfrac{RH \cdot M_w}{RT} \dfrac{dp_{vsat}}{dt} \end{bmatrix} & \begin{bmatrix} u \cdot \dfrac{M_w p_{vsat}}{RT} \\ v \cdot \dfrac{M_w p_{vsat}}{RT} \end{bmatrix} \end{bmatrix} \cdot \begin{bmatrix} \nabla T \\ \nabla RH \end{bmatrix} \tag{4.4}$$

where p_{atm} is atmospheric pressure (101325 Pa), R_{air} (R/M_{air}) is the specific gas constant for air (287.058 J/(mol·K)) and $C_{p,air}$ is the specific heat capacity of air at constant pressure (1003.5 J/m^3·K). Thus, the equation (4.3) turns into:

$$\begin{bmatrix} \rho C_p + cw & 0 \\ 0 & \xi \end{bmatrix} \cdot \begin{bmatrix} \frac{\mathrm{dT}}{\mathrm{dt}} \\ \frac{\mathrm{dRH}}{\mathrm{dt}} \end{bmatrix} - \begin{bmatrix} \lambda + H_v \delta_p RH \cdot \frac{dp_{vsat}}{dT} & H_v \delta_p p_{vsat} \\ \delta_p RH \cdot \frac{dp_{vsat}}{dT} & \delta_p p_{vsat} \end{bmatrix} \cdot \nabla \begin{bmatrix} \nabla T \\ \nabla RH \end{bmatrix} + \\ + \begin{bmatrix} \begin{bmatrix} u \cdot \frac{R_{air}}{C_{p,air}\, T} p_{atm} \\ v \cdot \frac{R_{air}}{C_{p,air}\, T} p_{atm} \end{bmatrix} & \begin{bmatrix} 0 \\ 0 \end{bmatrix} \\ \begin{bmatrix} u \cdot \frac{RH \cdot M_w}{RT} \frac{dp_{vsat}}{dt} \\ v \cdot \frac{RH \cdot M_w}{RT} \frac{dp_{vsat}}{dt} \end{bmatrix} & \begin{bmatrix} u \cdot \frac{M_w p_{vsat}}{RT} \\ v \cdot \frac{M_w p_{vsat}}{RT} \end{bmatrix} \end{bmatrix} \cdot \begin{bmatrix} \nabla T \\ \nabla RH \end{bmatrix} = 0 \tag{4.5}$$

where, the components of all the coefficients have been developed in the section 2.4. The solving of this equation provides the temperature and relative humidity behaviour.

The default nodes are "Zero flux" and "Initial values" which have been explained before. In this case, there are two different initial values and one extra zero flux node. The interior lining and the insulation layer have the same initial temperature and relative humidity, which change according to the phase of the test. The sheathing has different initial values. The extra zero flux condition is added in the perforation area since all the boundary conditions in that area are set by the fluid flow module. The initial values have been input just in the depressurization phase; the initial values in the next two phases were the final values of the previous phase respectively.

Three different nodes are added: two "Flux/Source" and one "Dirichlet Boundary Condition". In every phase, the Dirichlet condition is applied to the outer surface, since the air flow through the perforation area is set by the fluid flow interface and the rest of the inner surface is defined by a flux condition.

The flux condition stands for the interior environmental conditions. The equation applied in this node is the same than the "Zero flux" one but with adding the source term:

$$-\boldsymbol{n} \cdot (-c\nabla \mathbf{u} - \alpha \mathbf{u} + \gamma) = g - q\boldsymbol{u} \tag{4.6}$$

$$\boldsymbol{u} = [T, RH]^T$$

$$\nabla = \left[\frac{\partial}{\partial x}, \frac{\partial}{\partial y}, \frac{\partial}{\partial z}\right]$$

- *q*: boundary absorption/impedance term [1/m], which in this modelling is zero.
- *g:* the boundary flux/source [1/m].

The last condition added is called “Outflow”. It is applied to the outlets, where g was defined as null. The temperature and relative humidity derivate are zero so the flux at the outlet is purely due to convection.

4.2.3 Mesh

The interfaces needs different meshes since them and the physics involved are clearly different. In the fluid flow interface, the option chosen is the default mesh which is created by the program. It is called “Physics-controlled mesh” and Comsol adapts it in function of the physic used. The only parameter which needs to be decided is the size of the mesh. It is necessary accuracy for the mesh so the size selected is extra fine. In figure 82, the mesh in the region of the perforation rows.

The hygrothermal mesh has been built as in the diffusion model, with the free triangular option, as can be seen in figure 83. In this geometry, both lining boards are meshed selecting the fluid dynamics option and the size “fine”. The insulation layer is meshed also with the triangular mesh but the element size is normal. The perforation area needs a special treatment because the flow goes through it. There is an option called “Distribution” and it allows choosing the number of elements (100) and the element ratio (1.5) by selecting “Predefined distribution type”. As said before, the building order has a great importance in order to avoid computation errors.

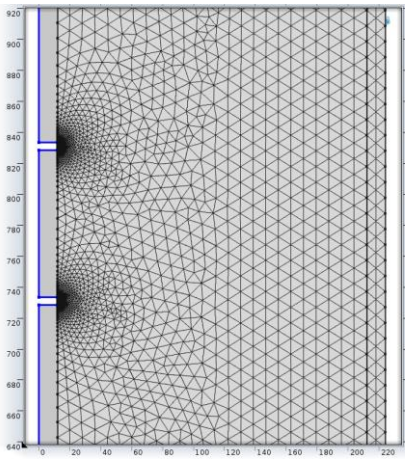

Figure 82: Air flow mesh. Picture from Comsol.

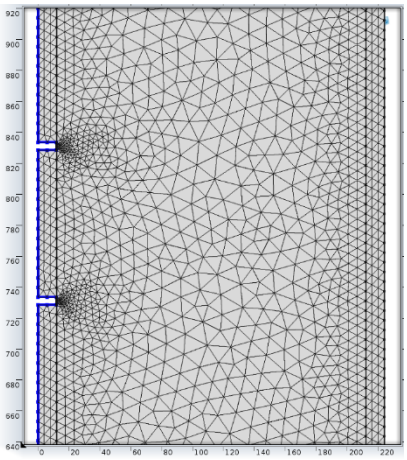

Figure 83: Hygrothermal mesh. Picture from Comsol.

4.2.4 Study

The selected kind of study is “Stationary” for the fluid-flow module because the analysis of this physic can be done without taking into account the time dimension and “Time-dependent” for moisture and heat coupled transfer as was established in the diffusion case. The range of time in this simulation is (0, 300, 168*3600). Therefore, the maximum step of the time stepping should be modified (300 s). Moreover, as have been already mentioned, it is necessary the selection of the “Iterative” and “Segregated” nodes instead of the default nodes for memory efficiency reasons.

4.3 Results and comparison with the laboratory tests

The temperature and relative humidity were measured in the laboratory test through several sensors. In this case, the comparisons have been performed taking the results of temperature and relative humidity from the points of four of the eight sensors: A, B, C and D whose positions can be observed in the figure 81.

This chapter is divided in three sections corresponding to the three phases: depressurization, no pressure and overpressurization. Each section contain two kinds of figures. Firstly, there are the Comsol distributions of pressure, temperature, relative humidity and velocity at the final of the simulation inside the wall in each phase (figures 84-87, 91-92 and 96-99 respectively, all of them taken from Comsol). The following figures in each section show the graphs with the comparisons between the Comsol results and the laboratory results at the mentioned points (figures 88-90, 93-95 and 100-102 respectively).

4.3.1 Results of the depressurization phase

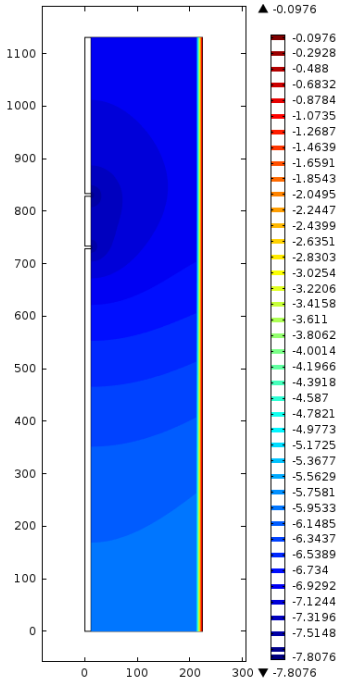

Figure 84: Pressure.

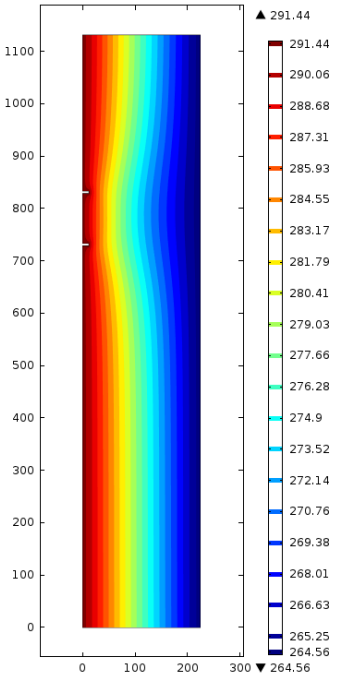

Figure 85: Temperature.

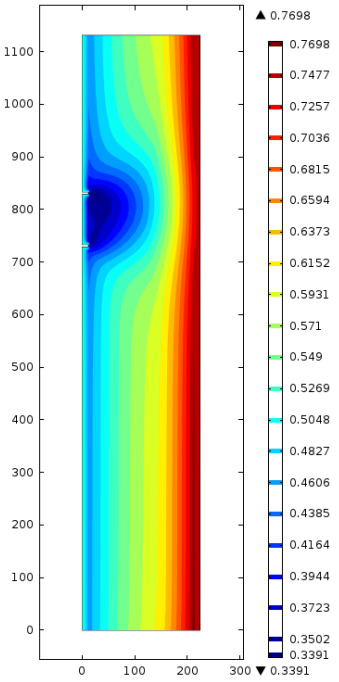

Figure 86: Relative humidity.

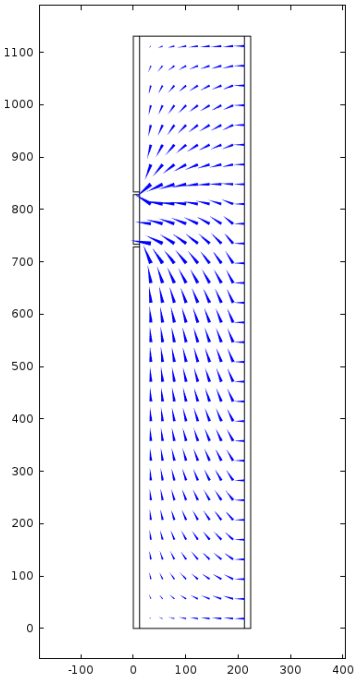

Figure 87: Velocity flow (logarithmic).

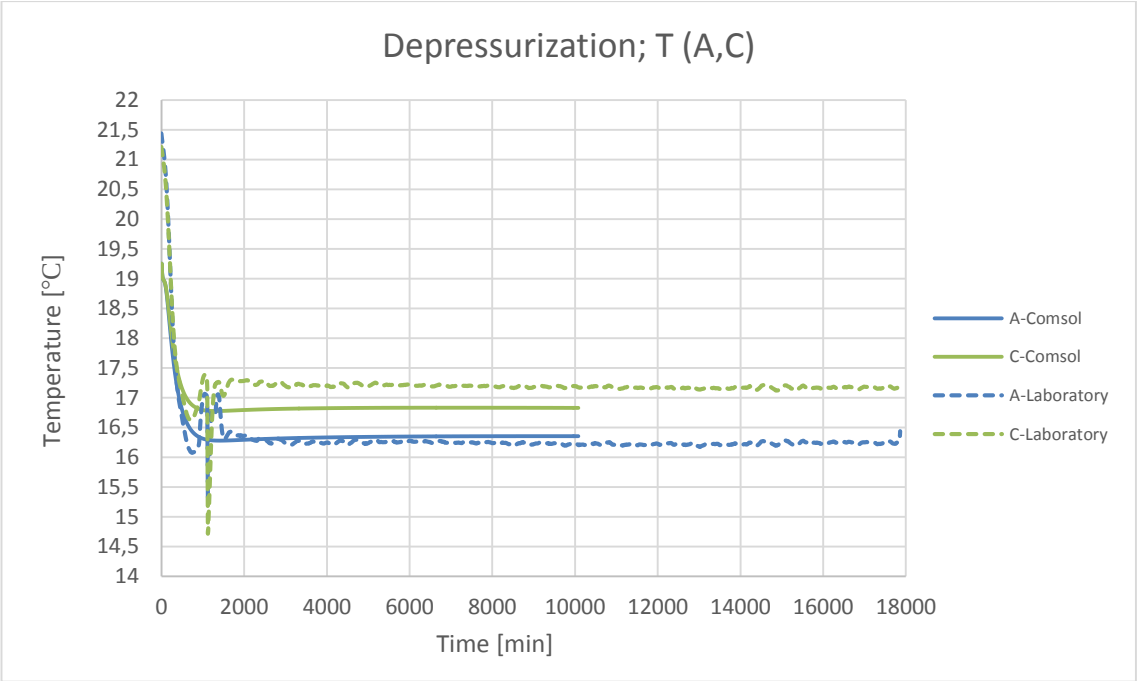

Figure 88: Temperatures from Comsol and the laboratory tests at points A and C in the depressurization phase.

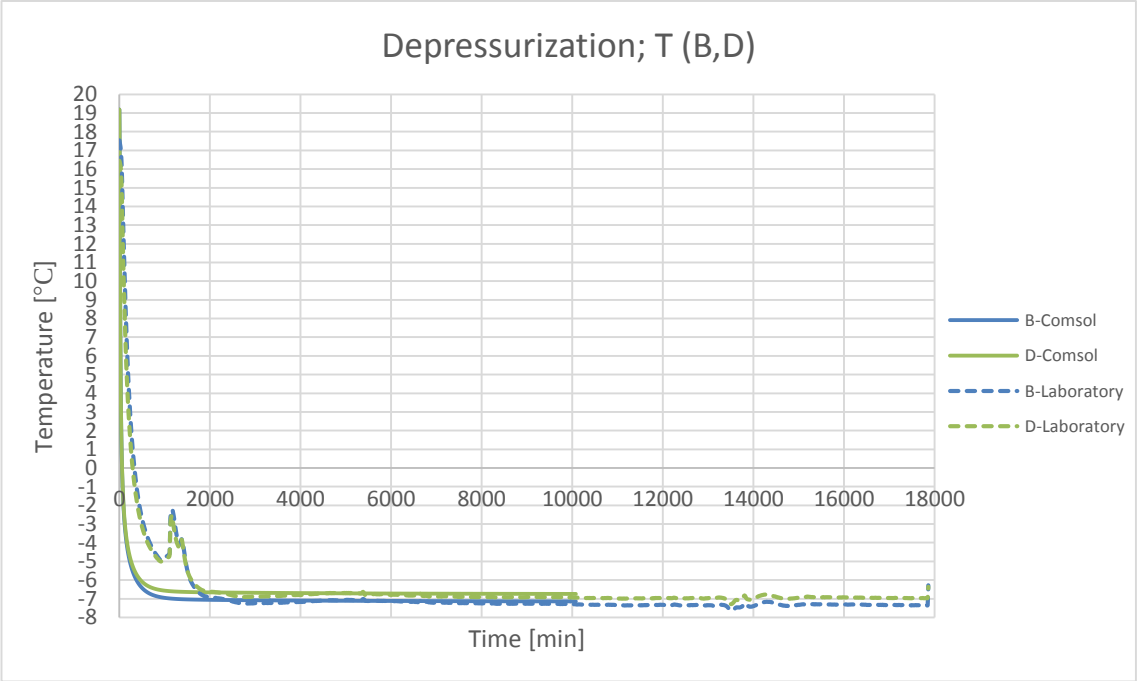

Figure 89: Temperatures from Comsol and the laboratory tests at points B and D in the depressurization phase.

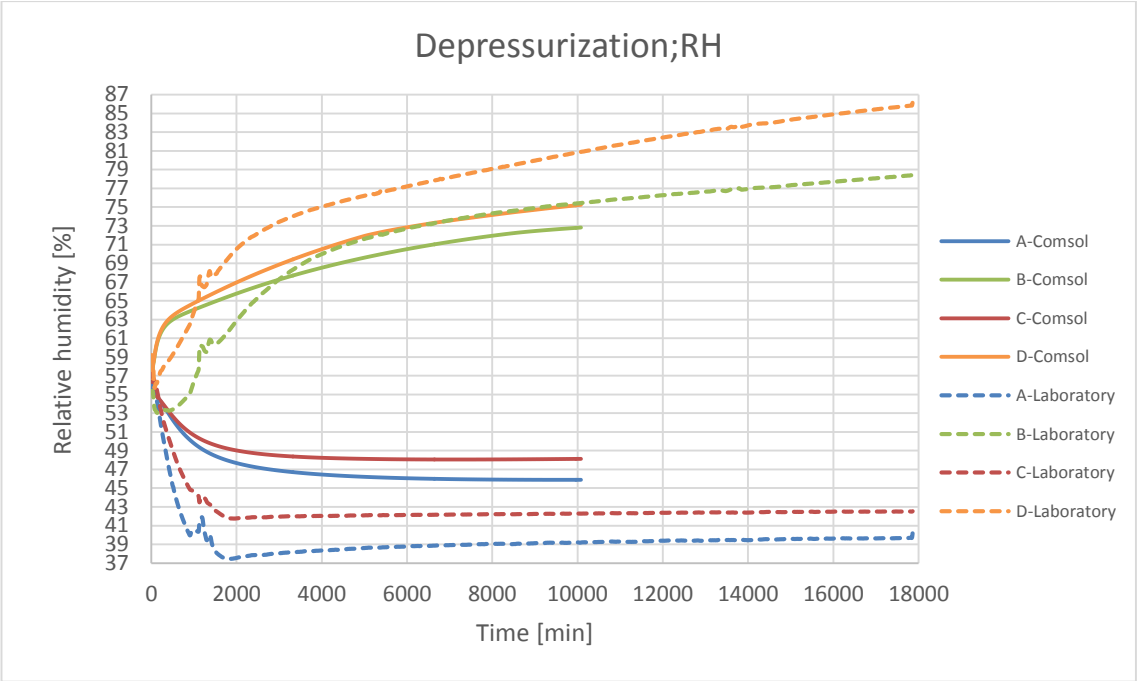

Figure 90: Relative humidity from Comsol and the laboratory tests at every point in the depressurization phase.

4.3.2 Results of the no pressure phase

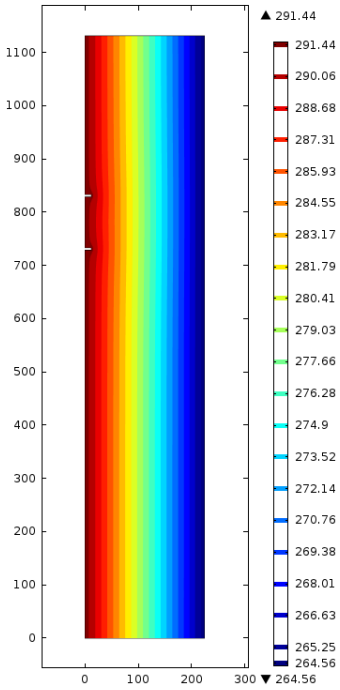

Figure 91: Temperature.

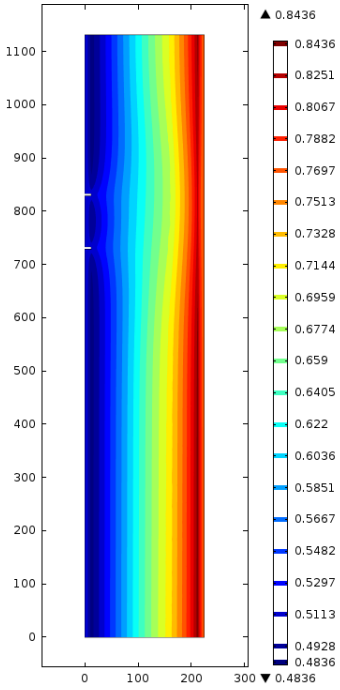

Figure 92: Relative humidity.

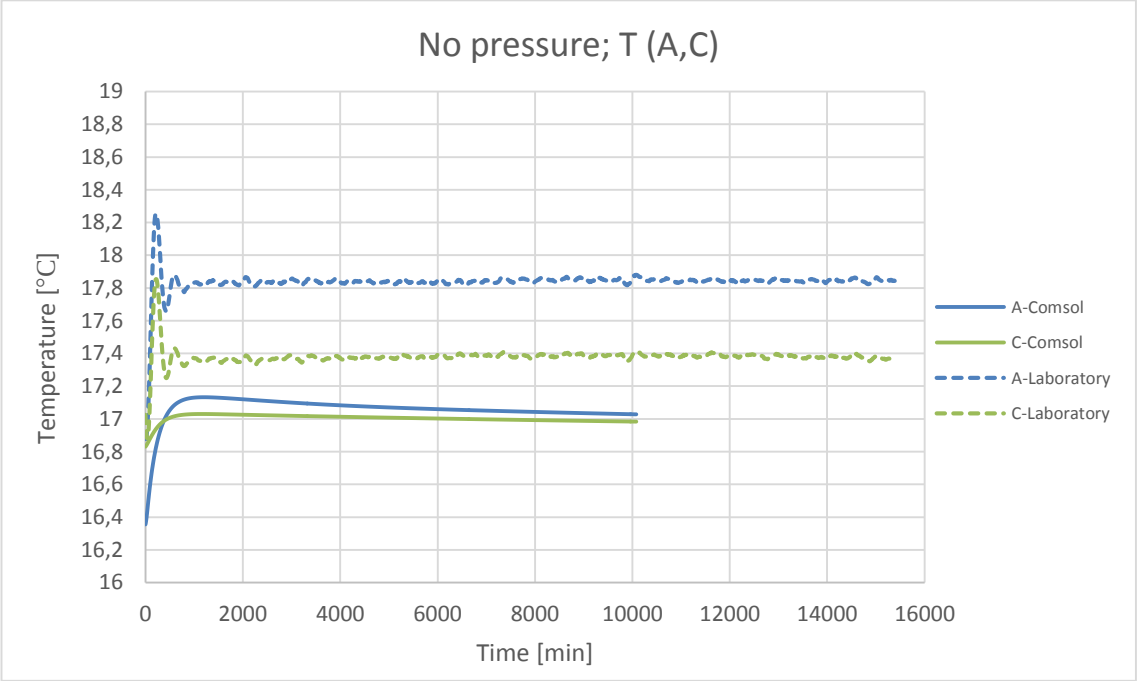

Figure 93: Temperatures from Comsol and the laboratory tests at points A and C in the no pressure phase.

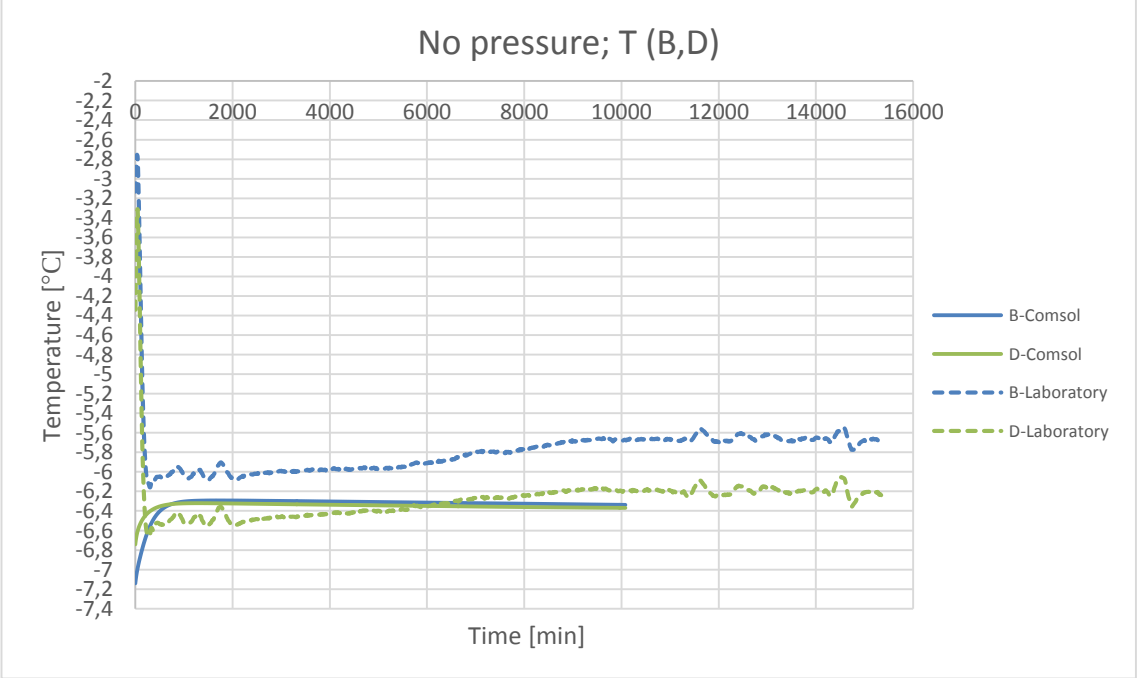

Figure 94: Temperatures from Comsol and the laboratory tests at points B and D in the no pressure phase.

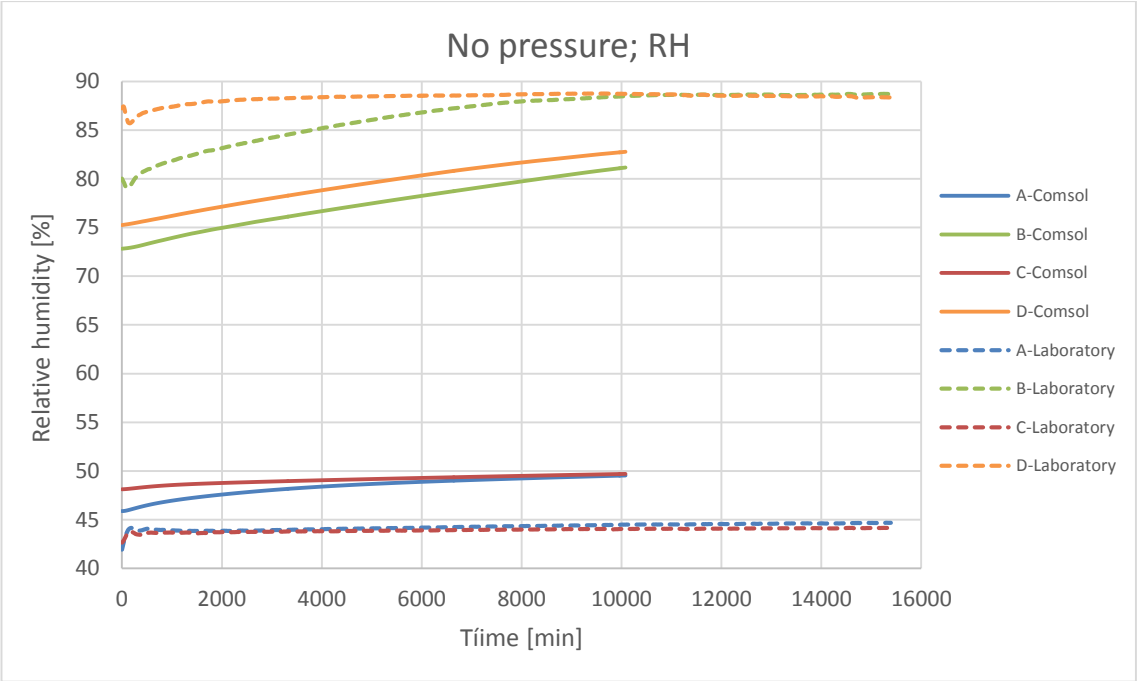

Figure 95: Relative humidity from Comsol and the laboratory tests at every point in the no pressure phase.

4.3.3 Results of the overpressurization phase

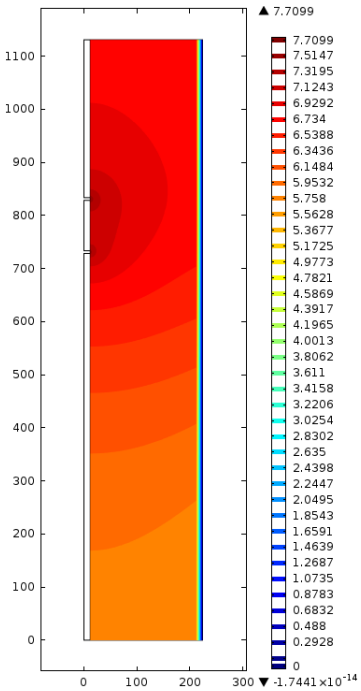

Figure 96: Pressure.

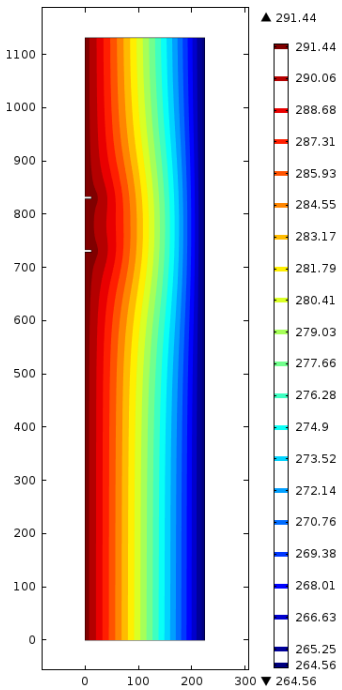

Figure 97: Temperature.

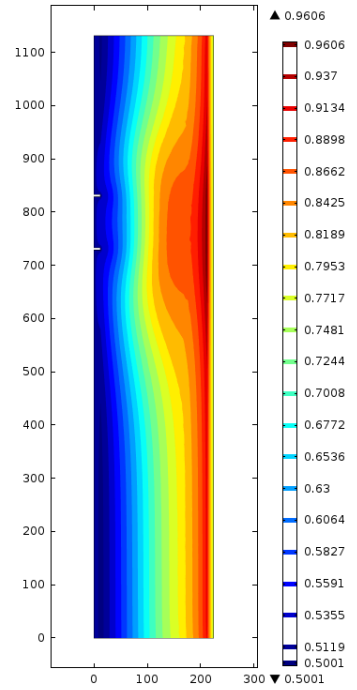

Figure 98: Relative humidity.

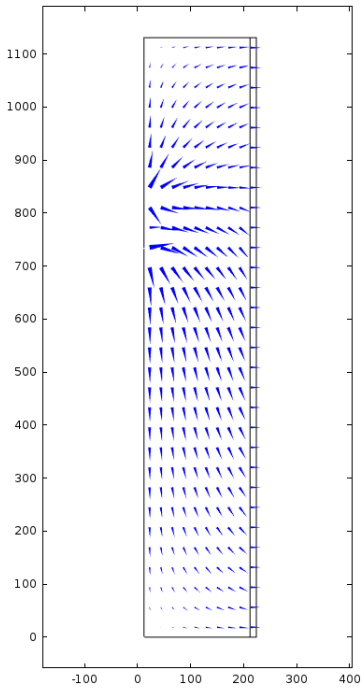

Figure 99: Velocity flow (logarithmic).

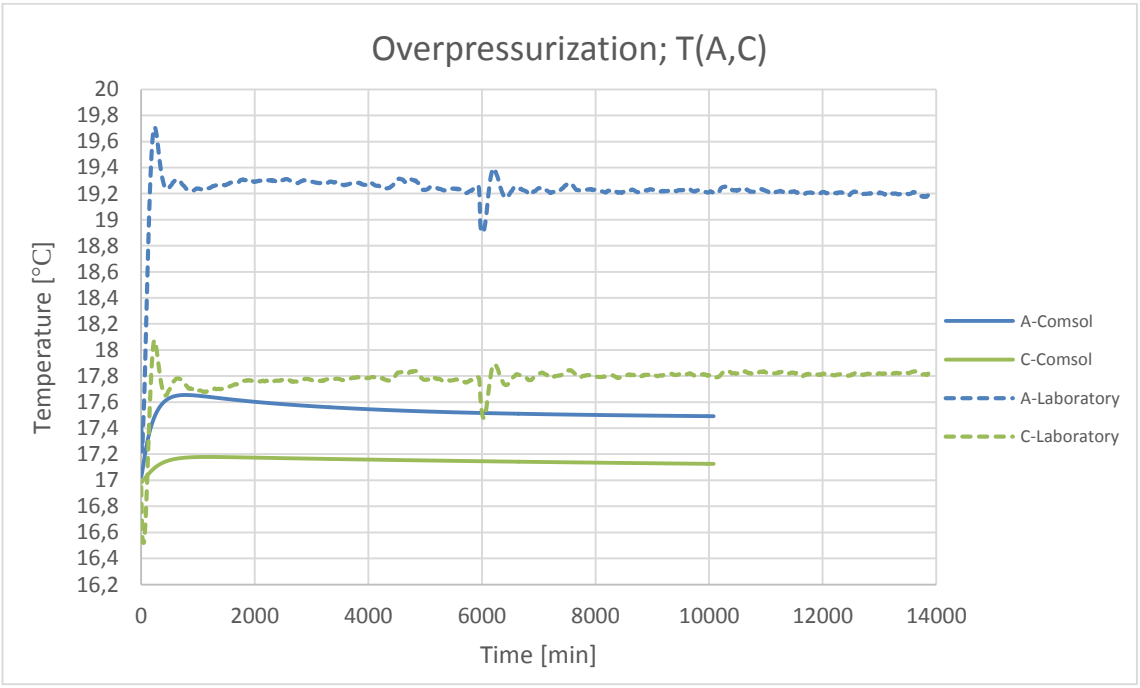

Figure 100: Temperatures from Comsol and the laboratory tests at points A and C in the overpressurization phase.

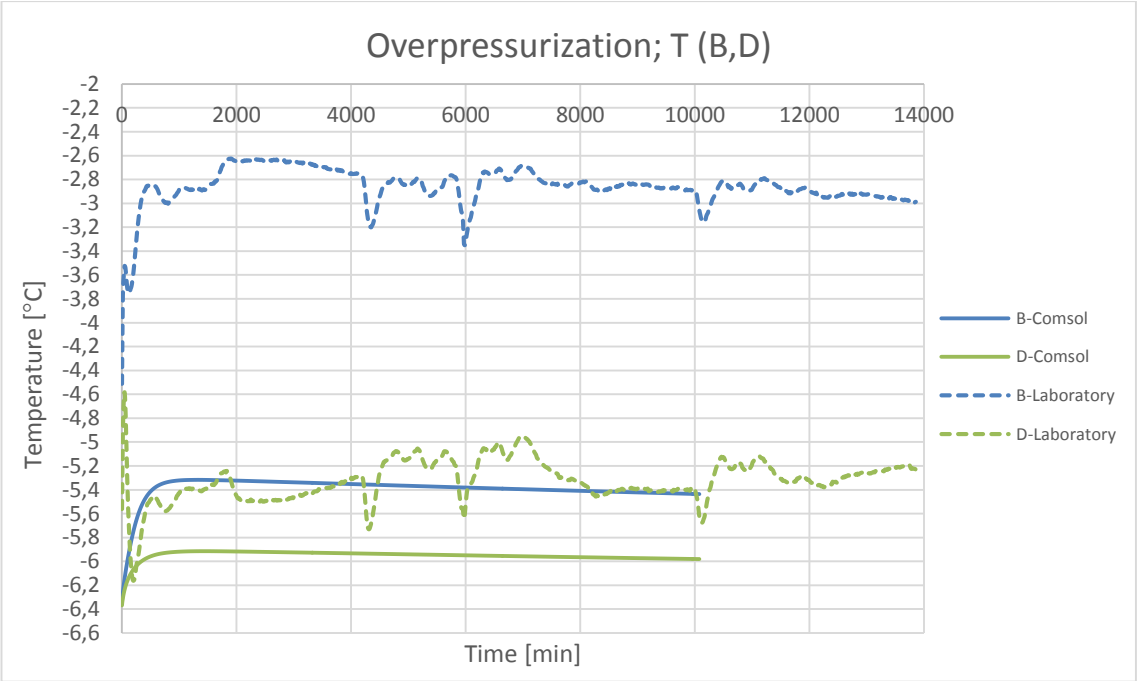

Figure 101: Temperatures from Comsol and the laboratory tests at points B and D in the depressurization phase.

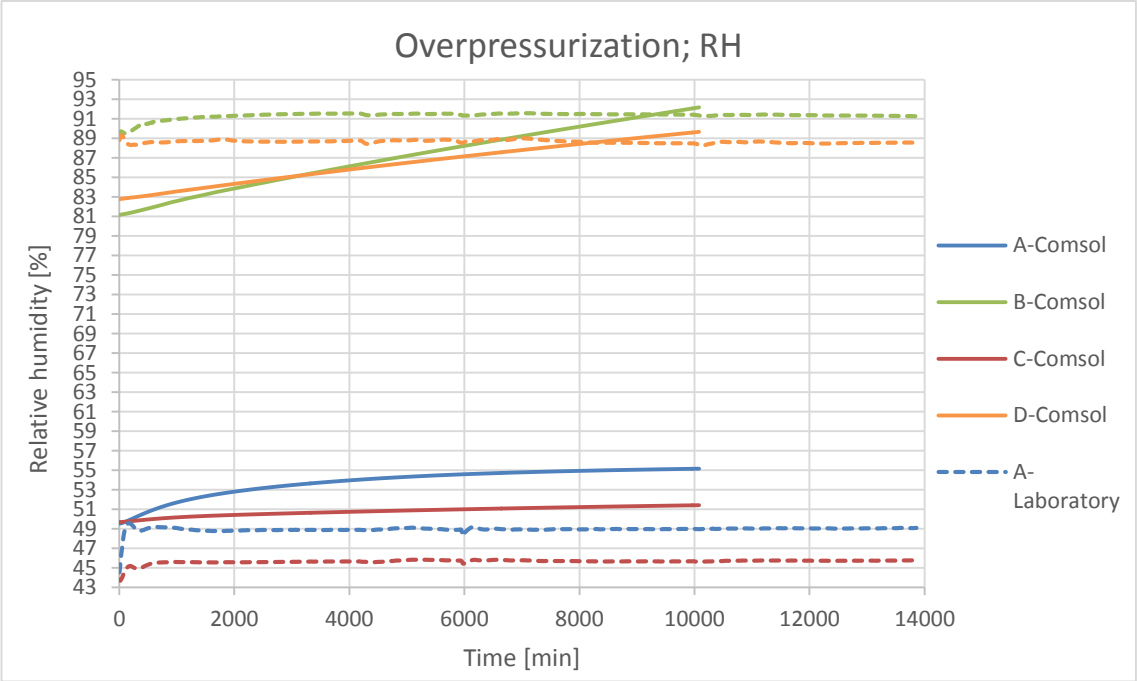

Figure 102: Relative humidity from Comsol and the laboratory tests at every point in the overpressurization phase.

4.3.4 Results observations

The temperature at every point (A, B, C and D) of the depressurization phase matches very well and all of them seem to have reached the stationary state (figures 88 and 89). The temperature at points A, B and D is almost the same from both methods, but the difference between Comsol's simulation and the laboratory test at point D is 0.5 °C. Otherwise as can be observed in figure 90, the relative humidity of one method is not enough close to the other in the last time step of the Comsol's simulation (around 7% at A and C and 2-4% at B and D). Moreover, the points B and D have not reached the stationary state in the simulation nor even in the laboratory tests, which last around 133 more hours, while the points A and C seem to have reached it in both methods.

The temperatures in the no pressure phase match quite well at every point: the points A and B have a difference over 0.7-0.8°C and the difference at the points C and D is about 0.2-0.4°C (figures 93 and 94). I think they need some more hours to reach the stationary state, thought they have almost reached it. Regarding the relative humidity (figure 95), the situation in this case is similar to the previous phase: the differences between the simulation and the laboratory test are around 6% at the points A and C which seem to almost be in a stationary phase. The relative humidity at points B and D has already reached that state in the laboratory results, but the Comsol's simulations need more time to get it.

The overpressurization phase have the biggest difference between temperatures (figures 100 and 101). The greater differences are at points B (2.4 °C) and A (1.7 °C), while the difference at points C and D is similar to the previous phase (both around 0.6 °C). The simulations at the four points need to be extended in some hours. Once again, the relative humidity is almost stationary in the laboratory tests and in the simulations at points A and C, but not in the simulations at the points B and D (figure 102). The difference at points A and C is around 5% of RH.

From the figures 84 and 96, which represent the pressure distribution in the depressurization and overpressurization phases respectively, it can be observed that the pressure difference between both sides is near 8 Pa. The real difference, established as boundary condition at the beginning of the simulations, is 10 Pa. Therefore, the pressure difference after the simulation is not far from which it should be.

5. DISCUSSION

5.1 Diffusion simulations

The first comment is focused on the different curves followed by the laboratory tests results and the programs results in both the temperature and the relative humidity graphs. Especially in the relative humidity representations, the laboratory test curves was usually different than the result graphs of the two programs which maybe did not have exactly the same curve but they used to be similar, especially in the temperature results. This happens because the programs apply a regular and reasonable behavior but the reality is that the variables behavior in each material, more significantly the relative humidity, can vary according with specific materials so they do not follow the prediction of the models.

There is other two reasons that may explain that the results from Comsol and WUFI are similar between them but so different from the laboratory results. The first cause consists on the poor accuracy of the material properties. If the properties described in tables 2 and 3 and used in both programs were not precise enough, it would be understandable the results difference. The second reason is the fact that the hygrothermal balance as well as its equations input in the Mathematical module are not suitable enough to describe the hygrothermal process.

The origin of these hygrothermal problems can be an error in the basis of the transference model. The transference process presented in this thesis is bases on the Fickian moisture transfer. This Fickian model is based on two assumptions, called “Fickian assumptions” (Krabbenhoft & Damkilde 2004): the first one is that the moisture transfer is ruled over an equation within the Fickian type gradient law, which means that the moisture flux is proportional to a scalar coefficient and a gradient, for instance the equation (2.25). The second one says that the water inside the material pores and the vapor water are in equilibrium in every moment. (Krabbenhoft & Damkilde 2004).

The first assumption is acceptable but the consideration of the second one might be the key for the relative humidity differences. If the non-Fickian model is taken into consideration then the moisture balance applied in this thesis would be wrong. This fact would explain why the differences between the behaviour of the relative humidity form the real structures and the computer simulations. The modification of the moisture balanced would be based on the addition of the vapour pressure as a third variable within the **u** field. Even if the research of Krabbenhoft and Damkilde was performed in wood, this theory could be applicable to other materials.

5.2 Convection and diffusion simulation

This section include the previous one so the previous comments should be taken into account. The materials properties should be reviewed in order to dismiss any problem related. The equations may have an important role in the relative humidity differences. Finally, the Fickian approach should not be taken as a right assumption.

In general, the temperatures match quite well, especially in the two first phases, and the relative humidities are more similar at points A and C in every phase but they did not reach the stationary state in most of the cases.

The clearest conclusions of this section are that the simulations need some more hours, particularly due to the RH-simulations and the overpressurization phase. This is a critical issue because most of the relative humidity results from Comsol have not reached a stationary state and it is not possible to compare the results if they are not stable.

6. CONCLUSION

The aim of this survey was to check the accuracy of the program Comsol Multyphisics as a heat, air and moisture transfer simulator compared with WUFI, another computer simulator. It has been tested by the comparisons of the Comsol's results with the results of WUFI because the same equations have been used. Both programs have been also compared with the laboratory tests results.

After the analysis of the first results, it is clear that the Comsol simulations are similar to the WUFI's simulations because the equations are the same, but they are not enough close to the laboratory tests. The comparisions have shown that Comsol is better and heavier in numerical computing but even if it is better, both programs are not enough accurate. This can be due to a poor accuracy of the material properties input in both programs or to the equations employed, although in some cases the results match pretty well so the material properties may not be the greatest problem. Moreover, the structures modelled have a membrane layer within its geometry which hinder the process, because it needs a special treatment. The membranes have been modelled applying "Fickian assumptions" and they are not justified. A third cause of errors can be the omission of the hysteresis in the moisture storage.

The second part, which insert the perforation area and the three different phases of the test, deepens in the fluid transference due to the addition of the air transfer. This addition allows to analyse the pressure and velocity distribution as well as the behaviour of the same structure affected by different boundary conditions. Although some curves are quite close in both the Comsol and the laboratory test, they are not similar at every point, with both variables and in every phase. Therefore, the equations have to be reviewed because the results from the stationary values do not match well and the settling of the variables is very slow compared with the measurements.

For futures research about this topic, the first step would be to review the equations and try to find where they can be improved. Also, the material properties should be checked in order to ensure its veracity and it is necessary to take into account the Non-Fickian approach since it could be the key for bringing closer the simulations to the reality. Also, the convection and diffusion simulation should have more enduring simulations because some curves are not stable yet, so they cannot be properly evaluated.

7. REFERENCES

Bruneau, C-H & Mortazavi, I. 2006. *Numerical modelling and passive flow control using porous media.* Université de Bordeaux, INRIA Team MC2. [WWW]. [Accessed on 11.01.2014]. Available at: http://www.math.u-bordeaux1.fr/~chabrune/publi/BM-CF.pdf.

COMSOL. 2008. *Coupled Free and Porous Media Flow. Solved with Comsol Multiphysics 3.5.* [WWW]. [Accessed on 11.02.2014]. Available at: http://www.comsol.com/model/download/39648/porous_free.pdf.

COMSOL. 2012. *COMSOL Multiphysics User's Guide. Version 4.3.* pp 1238-1245.

Frei, W. 2013. *Improving Convergence of Multiphysics Problems.* COMSOL Blog. [WWW]. [Accessed on 24.05.2014]. Available at: http://www.comsol.pt/blogs/improving-convergence-multiphysics-problems/

Frei, W. 2013. *Solving Multiphysics Problems*. COMSOL Blog. [WWW]. [Accessed on 24.05.2014]. Available at: http://www.comsol.com/blogs/solving-multiphysics-problems/.

Hagentoft, C. 2001. *Introduction to Building Physics*. Studentlitteratur. United States of America. pp 4-89.

Hens, H. 2007. *Building Physics-Heat, Air and Moisture. Fundamentals and Engineering methods with Examples and Exercises*. Ernst & Sohn. Berlin. pp 11-191.

Krabbenhoft, K. & Damkilde, L. 2004. *A model for non-Fickian moisture transfer in wood*. Department of Civil Engineering, Technical University of Denmark. Lyngby.

Krus, M. 1996. *Moisture Transport and Storage Coefficients of Porous Mineral Building Materials. Theoretical Principles and New Test Methods.* Fraunhofer IRB Verlag. Stuttgart. pp 11-23.

Künzel, H. 1995. *Simultaneous Heat and Moisture Transport in Building Components. One- and two-dimensional calculation using simple parameters.* Fraunhofer Institute of Building Physics. Stuttgart. pp 6-29.

Palacios, F. 2008. *Resolución aproximada de ecuaciones: Método de Newton-Raphson*. Escuela Politécnica Superior de Ingeniería de Manresa. Manresa.

Shi, Z & Wang, X. 2007. *Comparison of Darcy's Law, the Brinkman Equation, the Modified N-S Equation and the Pure Diffusion Equation in PEM Fuel Cell Modeling*. (Excerpt from the Proceedings of the COMSOL Conference 2007, Boston). Oakland University. [WWW]. [Accessed on 13.3.2014]. Available at: http://www.comsol.com/paper/download/98313/Wang_Xia.pdf.

Straube, J. 2006. *Moisture and materials.* Building Science Digest 138. Building Science Corporation. [WWW]. [Accessed on 20.6.2014]. Available at: http://www.buildingscience.com/documents/digests/bsd-138-moisture-and-materials.

APPENDIX I: CONVECTION-DIFUSSION MATERIAL PROPERTIES

- Fibreboard

Name	**Expression**	**Description**
λ	0.05	Thermal conductivity
ρ_p	270	Density
$C_{p,p}$	1500	Specific heat capacity
μ	5.5	Dynamic viscosity
ϵ_p	0.85	Porosity
κ_{br}	5 10-12	Permeability

- Fiberglass

Name	Expression	Description
λ	0.039	Thermal conductivity
ρ_p	37	Density
$C_{p,p}$	2000	Specific heat capacity
μ	1.3	Dynamic viscosity
ϵ_p	0.98	Porosity
κ_{br}	2 10-9	Permeability

- Air

Name	Expression	Description
ρ	1.2	Density
μ	1.7 10-5	Dynamic viscosity

- Sorption curve **w (RH)** (kg/m3)

	Fibreboard	Fiberglass
RH	**w**	**w**
0	0	0
0.33	12.4	1.9
0.55	19.6	3.1
0.65	22.4	4

0.75	25.2	4.8
0.80	33.6	6.1
0.83	38.7	6.8
0.86	45.9	8.6
0.93	62.7	12.9
0.97	71.3	15.2
1	240	440

- Thermal conductivity **λ(w)** (W/(mK))

Fibre-board	**w**	0	12.4	22.4	45.9	71.3	850
	λ	0.0465	0.0494	0.512	0.0529	0.0543	0.6
Fiberglass	**w**	0	1.9	4	8.6	15.2	970
	λ	0.038	0.038	0.038	0.039	0.4	0.6

- Moisture diffusion coefficient $\mathbf{D_w}$ **(w)** (m^2/s)

Fibreboard	
w	$\mathbf{D_w}$
0	0
30	0
33.6	4.17E-12
34	4.23E-12
35	4.37E-12
36	4.51E-12
37	4.66E-12
38	4.82E-12
39	4.98E-12
40	5.15E-12
41	5.32E-12
42	5.50E-12
43	5.68E-12
44	5.87E-12
45	6.07E-12
46	6.27E-12
47	6.48E-12
48	6.70E-12
49	6.92E-12
50	7.15E-12

Fiberglass	
w	$\mathbf{D_w}$
0	0
4	0
6.1	1.18E-10
7	1.19804E-10
8	1.21841E-10
9	1.23913E-10
10	1.2602E-10
11	1.28163E-10
12	1.30342E-10
13	1.32558E-10
14	1.34812E-10
15	1.37104E-10
16	1.39436E-10
17	1.41806E-10
18	1.44218E-10
19	1.4667E-10
20	1.49164E-10
25	1.62284E-10
30	1.76558E-10
35	1.92087E-10

51	7.39E-12
52	7.64E-12
53	7.89E-12
54	8.16E-12
55	8.43E-12
56	8.71E-12
57	9.00E-12
58	9.30E-12
59	9.62E-12
60	9.94E-12
61	1.03E-11
62	1.06E-11
63	1.10E-11
64	1.13E-11
65	1.17E-11
66	1.21E-11
67	1.25E-11
68	1.29E-11
69	1.34E-11
70	1.38E-11
71	1.43E-11
72	1.47E-11
73	1.52E-11
74	1.57E-11
75	1.63E-11
76	1.68E-11
77	1.74E-11
78	1.80E-11
79	1.86E-11
80	1.92E-11
81	1.98E-11
82	2.05E-11
83	2.12E-11
84	2.19E-11
85	2.26E-11
86	2.34E-11
87	2.41E-11
88	2.50E-11
89	2.58E-11
90	2.67E-11
91	2.75E-11

40	2.08983E-10
45	2.27364E-10
50	2.47362E-10
55	2.6912E-10
60	2.92791E-10
65	3.18544E-10
70	3.46562E-10
75	3.77045E-10
80	4.10208E-10
85	4.46289E-10
90	4.85543E-10
95	5.28251E-10
100	5.74714E-10
110	6.80261E-10
120	8.05191E-10
130	9.53065E-10
140	1.1281E-09
150	1.33527E-09
160	1.5805E-09
170	1.87076E-09
180	2.21432E-09
190	2.62098E-09
200	3.10233E-09
210	3.67207E-09
220	4.34645E-09
230	5.14468E-09
240	6.08951E-09
250	7.20785E-09
260	8.53158E-09
270	1.00984E-08
280	1.1953E-08
290	1.41482E-08
300	1.67465E-08
310	1.9822E-08
320	2.34623E-08
330	2.77712E-08
340	3.28714E-08
350	3.89083E-08
355	4.23305E-08
360	4.60538E-08
365	5.01046E-08

92	2.85E-11
93	2.94E-11
94	3.04E-11
95	3.14E-11
96	3.25E-11
97	3.36E-11
98	3.47E-11
99	3.58E-11
100	3.70E-11
105	4.37E-11
110	5.15E-11
115	6.07E-11
120	7.15E-11
125	8.43E-11
130	9.93E-11
135	1.17E-10
140	1.38E-10
145	1.63E-10
150	1.92E-10
156	2.34E-10
157	2.41E-10
158	2.50E-10
159	2.58E-10
160	2.66E-10
161	2.75E-10
162	2.85E-10
163	2.94E-10
164	3.04E-10
165	3.14E-10
166	3.25E-10
167	3.35E-10
168	3.47E-10
169	3.58E-10
170	3.70E-10
171	3.83E-10
172	3.95E-10
173	4.09E-10
174	4.22E-10
175	4.36E-10
176	4.51E-10
177	4.66E-10

370	5.45116E-08
375	5.93063E-08
380	6.45228E-08
385	7.0198E-08
390	7.63724E-08
395	8.30899E-08
400	9.03983E-08
401	9.19353E-08
402	9.34986E-08
403	9.50883E-08
404	9.67052E-08
405	9.83495E-08
406	1.00022E-07
407	1.01722E-07
408	1.03452E-07
409	1.05211E-07
410	1.07E-07
0	0
4	0
6.1	1.18E-10
7	1.19804E-10
8	1.21841E-10
9	1.23913E-10
10	1.2602E-10
11	1.28163E-10
12	1.30342E-10
13	1.32558E-10
14	1.34812E-10
15	1.37104E-10
16	1.39436E-10
17	1.41806E-10
18	1.44218E-10
19	1.4667E-10
20	1.49164E-10
25	1.62284E-10
30	1.76558E-10
35	1.92087E-10
40	2.08983E-10
45	2.27364E-10
50	2.47362E-10
55	2.6912E-10

178	4.82E-10
179	4.98E-10
180	5.14E-10
181	5.32E-10
182	5.49E-10
183	5.68E-10
184	5.87E-10
185	6.06E-10
186	6.27E-10
187	6.48E-10
188	6.69E-10
189	6.92E-10
190	7.15E-10
191	7.39E-10
192	7.63E-10
193	7.89E-10
194	8.15E-10
195	8.43E-10
196	8.71E-10
197	9.00E-10
198	9.30E-10
199	9.61E-10
200	9.93E-10
201	1.03E-09
202	1.06E-09
203	1.10E-09
204	1.13E-09
205	1.17E-09
206	1.21E-09
207	1.25E-09
208	1.29E-09
209	1.34E-09
210	1.38E-09

60	2.92791E-10
65	3.18544E-10
70	3.46562E-10
75	3.77045E-10
80	4.10208E-10
85	4.46289E-10
90	4.85543E-10
95	5.28251E-10
100	5.74714E-10
110	6.80261E-10
120	8.05191E-10
130	9.53065E-10
140	1.1281E-09
150	1.33527E-09
160	1.5805E-09
170	1.87076E-09
180	2.21432E-09
190	2.62098E-09
200	3.10233E-09
210	3.67207E-09
220	4.34645E-09
230	5.14468E-09
240	6.08951E-09
250	7.20785E-09
260	8.53158E-09
270	1.00984E-08
280	1.1953E-08
290	1.41482E-08
300	1.67465E-08
310	1.9822E-08
320	2.34623E-08
330	2.77712E-08
340	3.28714E-08
380	6.45228E-08
400	9.03983E-08
410	1.07E-07